ФИЗИКА ЭЛЕМЕНТАРНЫХ ЧАСТИЦ И АТОМНОГО ЯДРА
2002. Т. 33. ВЫП. 1

УДК 539.12.01

EFFECTS OF HIGHER ORDERS IN LARGE ANGLE BHABHA SCATTERING

A. Arbuzov

Avadh Bhatia Phys. Lab., Edmonton, AB, Canada T6G 2J1

E. Kuraev, B. Shaikhatdenov

Joint Institute for Nuclear Research, Dubna

ФИЗИКА ЭЛЕМЕНТАРНЫХ ЧАСТИЦ И АТОМНОГО ЯДРА
2002. Т. 33. ВЫП. 1

УДК 539.12.01

EFFECTS OF HIGHER ORDERS IN LARGE ANGLE BHABHA SCATTERING

A. Arbuzov

Avadh Bhatia Phys. Lab., Edmonton, AB, Canada T6G 2J1

E. Kuraev, B. Shaikhatdenov

Joint Institute for Nuclear Research, Dubna

The present status of theoretical description of large angle Bhabha scattering with the account for radiative corrections (RC) in the leading and next-to-leading approximations is reviewed. Besides RC coming from emission of virtual, soft and additional hard photons, there has been considered a e^+e^- pair production. The goal of all this activity is to reach the accuracy level of $0.1\,\%$. In addition, some numeric MC estimates for LEP2 conditions are presented. Details of calculations are given in appendices.

Дан обзор современного состояния теоретического описания процесса электрон-позитронного рассеяния с учетом радиационных поправок (РП) в лидирующем и следующем за лидирующим приближениях. Наряду с РП от излучения виртуального, мягкого и жесткого дополнительного фотона также рассмотрено образование дополнительной e^+e^--пары. Требуемая точность вычисления сечений — на уровне $0{,}1\,\%$. Обсуждаются результаты численных расчетов для LEP2, проведенных с помощью МК-генератора событий, основанного на аналитических выражениях, приведенных в обзоре. В приложениях даются детали вычислений.

1. LARGE ANGLE BHABHA SCATTERING

The process of electron-positron scattering is commonly used for luminosity measurements at e^+e^- colliders. It has almost pure electrodynamical nature and could therefore be described to any desired precision within a framework of perturbative QED. Nevertheless, the accuracy of modern experiments is ahead of that provided by theory. A lot of work has recently been done to uplift the theoretical uncertainty to about one per mille under conditions of small angle Bhabha scattering at LEP1 [1] and afterwards up to $0.05-0.06\,\%$ [2].

The large angle kinematics of Bhabha scattering (LABS) process is extensively used for calibration purposes at e^+e^- colliders of moderately high energies, such as ϕ, J/ψ, B and c/τ factories and LEP2 [3,4]. At the Born and one-loop levels the process was investigated in detail in [5–9], taking into account both QED and electroweak effects.

Small scattering angle kinematics of Bhabha scattering is used for high-energy colliders such as LEP I [10, 11]. As far as $0.1\,\%$ accuracy is desirable in the determination of $\mathcal{L}$, the corresponding requirement

$$\left|\frac{\delta\sigma}{\sigma}\right| \leq 10^{-3} \tag{1.1}$$

on the Bhabha cross section theoretical description appears. The quantity $\Delta\sigma$ is an unknown uncertainty in the cross section due to higher order RC. A great attention was paid to this process during the last decades (see review [5] and references therein).

In paper [12] we considered Bhabha scattering to $\mathcal{O}(\alpha)$ order exactly improved by the structure function method. The latter, based on the renormalization group approach, allows one to evaluate the leading radiative corrections to higher orders, including all the terms $\sim (\alpha L_s)^n$, $n = 2, 3, \ldots$, where $L_s = \ln(s/m^2)$ is a large logarithm; s is the total centre-of-mass (c.m.s) energy of incoming particles squared and m is the mass of fermion.

To reach the one per mille accuracy it is required to take into account radiative corrections (RC) up to third order within the leading logarithmic approximation (LLA) and up to second order in the next-to-leading approximation (NLA). In a series of papers several sources of these corrections were considered in detail [13–16].

Let's sketch what we are going to present in this review. In Chapter 1.1 the emission of two hard photons [13] in LABS is revised followed by a pair production [14] in Chapter 1.2. We further proceed with the consideration of the radiative LABS in different kinematical settings, namely, the most general one with all particles outgoing at large angles [16], and another one with an emitted photon radiated within a narrow cone about a beam direction [17]. In the last Chapter the numerical implication of the analytical results presented is reviewed in some detail. We start with outlining the MC generator for LABS at LEP2 and then pass on to the comparison with other existing codes. Concluding remarks are given in the Outlook.

1.1. Emission of Two Hard Photons. The Born cross section with weak interactions taken into account and the first order QED radiative corrections to it were studied in detail [18]. Both contributions, the one enhanced by *the large* logarithmic multiplier $L = \ln(s/m^2)$ (where $s = (p_+ + p_-)^2 = 4\varepsilon^2$ is the total c.m.s. energy squared; m is the electron mass), and the one without L, are to be kept in the limits 1.1: $\alpha L/\pi$, α/π. As for the corrections in the second order of the perturbation theory, they are necessary in the leading and next-to-leading approximations and take the following orders, respectively:

$$(\alpha/\pi)^2 L^2, \quad (\alpha/\pi)^2 L. \tag{1.2}$$

The total two-loop ($\sim (\alpha/\pi)^2$) correction could be constructed from:

1. two-loop corrections arising from the emission of two virtual photons;
2. one-loop corrections to a single real (soft and hard) photon emission;
3. those arising from the emission of two real photons;
4. virtual and real e^+e^--pair production [14].

As for the corrections in the third order of perturbation theory, only the leading ones proportional to $(\alpha L/\pi)^3$ should be taken into account.

In this section we consider the emission of two real hard photons:

$$e^+(p_+) + e^-(p_-) \to e^+(q_+) + e^-(q_-) + \gamma(k_1) + \gamma(k_2). \tag{1.3}$$

The relevant contribution to the *experimental* cross section has the following form

$$\sigma_{\rm exp} = \int {\rm d}\sigma \; \Theta_+\Theta_-, \tag{1.4}$$

where Θ_+ and Θ_- are the experimental restrictions providing the simultaneous detection of both the scattered electron and positron. First, this means that their energy fractions should be larger than a certain (small) quantity $\varepsilon_{\rm th}/\varepsilon$, $\varepsilon_{\rm th}$ is the energy threshold of the detectors. The second condition restricts their angles with respect to the beam axes. They should be larger than a certain finite value ψ_0 ($\psi_0 \sim 35^\circ$ in the experimental conditions accepted in [3]):

$$\pi - \psi_0 > \theta_-,\, \theta_+ > \psi_0, \qquad \theta_\pm = \widehat{\mathbf{q}_\pm \mathbf{p}_-}\,, \tag{1.5}$$

where $\theta_\pm$ are the polar angles of the scattered leptons with respect to the beam axes ($\mathbf{p}_-$). We accept the condition on the energy threshold of the charged-particle registration $q_\pm^0 > \varepsilon_{\rm th}$. Both photons are assumed to be hard. Their minimal energy

$$\omega_{\rm min} = \Delta\varepsilon, \qquad \Delta \ll 1, \tag{1.6}$$

could be considered as the threshold of the photon registration.

The main ($\sim (\alpha L/\pi)^2$) contribution to the total cross section (5) comes from the collinear region: when both the emitted photons move within narrow cones along the charged particle momenta (they may go along the same particle). So we will distinguish 16 kinematical regions:

$$\begin{array}{l} \widehat{\mathbf{a}\mathbf{k}_1} \;\text{ and }\; \widehat{\mathbf{a}\mathbf{k}_2} < \theta_0, \qquad \widehat{\mathbf{a}\mathbf{k}_1} \;\text{ and }\; \widehat{\mathbf{b}\mathbf{k}_2} < \theta_0, \\ \dfrac{m}{\varepsilon} \ll \theta_0 \ll 1, \qquad a \neq b, \quad a,\, b = p_-, p_+, q_-, q_+\,. \end{array} \tag{1.7}$$

The matrix element module square summed over spin states in the regions (1.7) is of the form of the Born matrix element multiplied by the so-called collinear

factors. The contribution to the cross section of each region has also the form of $2 \to 2$ Bhabha cross sections in the Born approximation multiplied by factors of the form

$$\mathrm{d}\sigma_i^{\mathrm{coll}} = \mathrm{d}\sigma_{0i}\left[a_i(x_j,y_j)\ln^2\left(\frac{\varepsilon^2\theta_0^2}{m^2}\right) + b_i(x_j,y_j)\ln\left(\frac{\varepsilon^2\theta_0^2}{m^2}\right)\right], \tag{1.8}$$

where $x_j = \omega_j/\varepsilon$, $y_1 = q_-^0/\varepsilon$, $y_2 = q_+^0/\varepsilon$ are the energy fractions of the photons and of the scattered electron and positron. The dependence on the auxiliary parameter θ_0 will be cancelled in the sum of the contributions of the collinear and semicollinear regions. The last region corresponds to the kinematics, when only one photon is emitted inside the narrow cone $\theta_1 < \theta_0$ along one of the charged particle momenta. And the second photon is emitted outside any cone of that sort along charged particles ($\theta_2 > \theta_0$):

$$\mathrm{d}\sigma_i^{\mathrm{sc}} = \frac{\alpha}{\pi}\ln\left(\frac{4\varepsilon^2}{m^2}\right)\mathrm{d}\sigma_{0i}^{\gamma}(k_2), \tag{1.9}$$

where $\mathrm{d}\sigma_{0i}^{\gamma}$ has the known form of the single hard bremsstrahlung cross section in the Born approximation [19].

Below we show explicitly that the result of the integration over the single hard photon emission in Eq. (1.9) in the kinematical region $\theta_2^i > \theta_0$ (θ_2^i is the emission angle of the second hard photon with respect to the direction of one of the four charged particles) has the following form

$$\int \mathrm{d}\sigma_{0i}^{\gamma}(k_2) = -2\ln\left(\frac{\theta_0^2}{4}\right)a_i(x,y)\mathrm{d}\sigma_0^i + \mathrm{d}\tilde{\sigma}^i. \tag{1.10}$$

The collinear factors in the double bremsstrahlung process were first considered in papers of the CALCUL collaboration [20]. Unfortunately they have a rather complicated form which is less convenient for further analytical integration in comparison with the expressions given below. The method of calculation of the collinear factors may be considered as a generalization of the quasireal electron method [21] to the case of multiple bremsstrahlung. Another generalization is required for the calculations of the cross section of process $e^+e^- \to 2e^+2e^-$ [14].

It is interesting that the collinear factors for the kinematical region of the two hard photon emission along the projectile and the scattered electron are found the same as for the electron-proton scattering process considered in paper [22].

There are 40 Feynman diagrams of the tree type which describe the double bremsstrahlung process in e^+e^- collisions. The differential cross section in terms of helicity amplitudes was computed about ten years ago [20, 23]. It has a very complicated form. We note that the contribution from the kinematical region in which the angles (in the CM system) between any two final particles are large

compared with m/ε is of the order

$$\frac{\alpha^2 r_0^2 m^2}{\pi^2 \varepsilon^2} \sim 10^{-36}\ \mathrm{cm}^2, \tag{1.11}$$

where r_0 is the classical electron radius. Thus the corresponding events will possess rather poor statistics at colliders with luminosity $\mathcal{L} \sim 10^{31}$–$10^{32}\ \mathrm{cm}^{-2}\cdot\mathrm{s}^{-1}$. More probable are the cases of double bremsstrahlung imitating the processes $e^+e^- \to e^+e^-$ or $e^+e^- \to e^+e^-\gamma$, which corresponds to the emission of one or two photons along charged-particle momenta.

1.1.1. Collinear Kinematics. It is convenient to introduce, in the collinear region, new variables and transform the phase volume of the final state in the following way (from now on we will work in the CM system):

$$\begin{aligned}
\int \mathrm{d}\Gamma &= \int \frac{\mathrm{d}^3q_-\mathrm{d}^3q_+\mathrm{d}^3k_1\mathrm{d}^3k_2}{16q_-^0 q_+^0\omega_1\omega_2(2\pi)^8}\delta^{(4)}(\eta_1 p_- + \eta_2 p_+ - \lambda_1 q_- - \lambda_2 q_+) = \\
&= \frac{m^4\pi^2}{4(2\pi)^6}\int\limits_\Delta^1 \mathrm{d}x_1 \int\limits_\Delta^1 \mathrm{d}x_2\ x_1x_2 \int\limits_0^{2\pi}\frac{\mathrm{d}\phi}{2\pi}\int\limits_0^{z_0}\mathrm{d}z_1\int\limits_0^{z_0}\mathrm{d}z_2\int \mathrm{d}\Gamma_q, \\
\int \mathrm{d}\Gamma_q &= \int \frac{\mathrm{d}^3q_-\mathrm{d}^3q_+}{4q_-^0 q_+^0(2\pi)^2}\delta^{(4)}(\eta_1 p_- + \eta_2 p_+ - \lambda_1 q_- - \lambda_2 q_+), \\
z_{1,2} &= \left(\frac{\theta_{1,2}\varepsilon}{m}\right)^2, \quad \phi = \widehat{\mathbf{k}_{1\perp}\mathbf{k}_{2\perp}}, \quad x_i = \frac{\omega_i}{\varepsilon}, \\
z_0 &= \left(\frac{\theta_0\varepsilon}{m}\right)^2 \gg 1, \quad \Delta = \frac{\omega_{\min}}{\varepsilon},
\end{aligned} \tag{1.12}$$

where θ_i $(i = 1, 2)$ is the polar angle of the i-photon emission with respect to the momentum of the charged particle that emits the photon; $\eta_\pm$ and $\lambda_\pm$ depend on the specific emission kinematics, they are given in Table 1.

Table 1. **The values of η_i and λ_i for different collinear kinematics**

	p_-p_-	q_-q_-	p_+p_+	q_+q_+	p_-p_+	q_-q_+	p_-q_-	p_+q_+	p_-q_+	p_+q_-
η_1	y	1	1	1	$1-x_1$	1	$1-x_1$	1	$1-x_1$	1
η_2	1	1	y	1	$1-x_2$	1	1	$1-x_1$	1	$1-x_1$
λ_1	1	$\frac{1}{y}$	1	1	1	$\frac{1}{1-x_1}$	$1+\frac{x_2}{y_1}$	1	1	$1+\frac{x_2}{y_1}$
λ_2	1	1	1	$\frac{1}{y}$	1	$\frac{1}{1-x_2}$	1	$1+\frac{x_2}{y_2}$	$1+\frac{x_2}{y_2}$	1

The columns of Table 1 correspond to a certain choice of the kinematics in the following way: p_-p_- means the emission of both photons along the projectile

electron, p_+q_- means that the first of the photons goes along the projectile positron; the second, along the scattered electron and so forth. The contributions from 6 remaining kinematical regions (when the photons in the last 6 columns are interchanged) could be found by the simple substitution $x_1 \leftrightarrow x_2$. We will use the momentum conservation law

$$\eta_1 p_- + \eta_2 p_+ = \lambda_1 q_- + \lambda_2 q_+ \,, \tag{1.13}$$

and the following relations coming from it:

$$\eta_1 + \eta_2 = \lambda_1 y_1 + \lambda_2 y_2, \qquad \lambda_1 y_1 \sin\,\theta_- = \lambda_2 y_2 \sin\,\theta_+, \qquad y_{1,2} = \frac{q^0_{1,2}}{\varepsilon}\,,$$
$$\lambda_2 y_2 = \frac{\eta_1^2 + \eta_2^2 + (\eta_2^2 - \eta_1^2)c}{\eta_1 + \eta_2 + (\eta_2 - \eta_1)c}\,. \tag{1.14}$$

Each of 16 contributions to the cross section of process (1.3) can be expressed in terms of the corresponding Born-like cross section multiplied by its collinear factor:

$$\begin{aligned}
\mathrm{d}\sigma_{\mathrm{coll}} &= \frac{1}{2!}\left(\frac{\alpha}{2\pi}\right)^2 \frac{x_1 x_2}{2} \sum_{(\eta,\lambda)} \overline{K}(\eta,\lambda)\mathrm{d}\tilde{\sigma}_0(\eta,\lambda)\mathrm{d}x_1\mathrm{d}x_2,\\
\mathrm{d}\tilde{\sigma}_0(\eta,\lambda) &= \frac{2\alpha^2}{s}\,B(\eta,\lambda)\,\mathrm{d}I(\eta,\lambda), \qquad B(\eta,\lambda) = \left(\frac{\tilde{s}^{\,2} + \tilde{t}^{\,2} + \tilde{s}\tilde{t}}{\tilde{s}\tilde{t}}\right)^2,\\
\mathrm{d}I_i(\eta,\lambda) &= \int \frac{\mathrm{d}^3 q_- \mathrm{d}^3 q_+}{q_-^0\, q_+^0}\delta^{(4)}(\eta_1 p_- + \eta_2 p_+ - \lambda_1 q_- - \lambda_2 q_+) =\\
&= \frac{4\pi\eta_1\eta_2 \mathrm{d}c}{\lambda_1^2\lambda_2^2[c(\eta_2 - \eta_1) + \eta_1 + \eta_2]^2}\,,\\
\overline{K}(\eta,\lambda) &= m^4 \int\limits_0^{z_0} \mathrm{d}z_1 \int\limits_0^{z_0} \mathrm{d}z_2 \int\limits_0^{2\pi} \frac{\mathrm{d}\phi}{2\pi}\mathcal{K}(\eta,\lambda),\\
\tilde{t} &= (\eta_1 p_- - \lambda_1 q_-)^2 = -\tilde{s}\frac{\eta_1(1-c)}{\eta_1 + \eta_2 + (\eta_2 - \eta_1)c}\,,\\
\tilde{s} &= (\eta_1 p_- + \eta_2 p_+)^2 = 4\varepsilon^2\eta_1\eta_2 = s\eta_1\eta_2, \quad \tilde{s} + \tilde{t} + \tilde{u} = 0.
\end{aligned} \tag{1.15}$$

The sum over (η,λ) means the sum over 16 collinear kinematical regions. The corresponding (η,λ) could be found in Table 1. The quantities $\mathcal{K}_i(\eta,\lambda)$ are as

follows:

$$\mathcal{K}(p_-p_-) = \frac{2}{y}\mathcal{A}(A_1, A_2, A, x_1, x_2, y),$$
$$\mathcal{K}(q_-q_-) = 2y\mathcal{A}\left(B_1, B_2, B, \frac{-x_1}{y}, \frac{-x_2}{y}, \frac{1}{y}\right),$$
$$\mathcal{K}(p_+p_+) = \frac{2}{y}\mathcal{A}(C_1, C_2, C, x_1, x_2, y),$$
$$\mathcal{K}(q_+q_+) = 2y\mathcal{A}\left(D_1, D_2, D, \frac{-x_1}{y}, \frac{-x_2}{y}, \frac{1}{y}\right), \tag{1.16}$$
$$\mathcal{A}(A_1, A_2, A, x_1, x_2) = -\frac{yA_2}{A^2A_1} - \frac{yA_1}{A^2A_2} + \frac{1+y^2}{x_1x_2A_1A_2} + \frac{r_1^3 + yr_2}{AA_1x_1x_2} +$$
$$+\frac{r_2^3 + yr_1}{AA_2x_1x_2} + \frac{2m^2(y^2+r_1^2)}{AA_1^2x_2} + \frac{2m^2(y^2+r_2^2)}{AA_2^2x_1},$$

$$\mathcal{K}(p_-p_+) = 2K_1K_2, \qquad \mathcal{K}(p_-q_+) = -2K_1K_3,$$
$$\mathcal{K}(p_+q_-) = -2K_4K_5, \qquad \mathcal{K}(q_-q_+) = 2K_6K_7,$$
$$\mathcal{K}(p_-q_-) = -2K_1K_5, \qquad \mathcal{K}(p_+q_+) = -2K_4K_3,$$
$$K_1 = \frac{g_1}{A_1x_1r_1} + \frac{2m^2}{A_1^2}, \quad K_2 = \frac{g_2}{C_2x_2r_2} + \frac{2m^2}{C_2^2}, \quad K_3 = \frac{g_4}{D_2x_2t_2} - \frac{2m^2}{D_2^2},$$
$$K_4 = \frac{g_1}{C_1x_1r_1} + \frac{2m^2}{C_1^2}, \quad K_5 = \frac{g_3}{B_2x_2t_1} - \frac{2m^2}{B_2^2}, \quad K_6 = \frac{g_1}{B_1x_1} - \frac{2m^2}{B_1^2},$$
$$K_7 = \frac{g_2}{D_2x_2} - \frac{2m^2}{D_2^2}, \qquad r_1 = 1 - x_1, \quad r_2 = 1 - x_2, \tag{1.17}$$
$$g_1 = 1 + r_1^2, \quad g_2 = 1 + r_2^2, \quad g_3 = y_1^2 + t_1^2, \quad g_4 = y_2^2 + t_2^2,$$
$$t_1 = y_1 + x_2, \quad t_2 = y_2 + x_2, \quad y = 1 - x_1 - x_2,$$

y_1, y_2 are the energy fractions of the scattered electron and positron defined in Eq. (1.14).

The expressions (1.17) agree with the results of paper [20] except for a simpler form of $\mathcal{K}(q_-q_+)$. As for Eq. (1.16) it has an evident advantage in comparison to the corresponding formulae given in paper [20]. Let us note that the remaining factors $\mathcal{K}(p,q)$ could be obtained from the ones given in Eq. (1.17) using relations of the following type:

$$\mathcal{K}(p_-q_-)(x_1, x_2, A_1, B_2) = \mathcal{K}(q_-p_-)(x_2, x_1, A_2, B_1). \tag{1.18}$$

Note also that terms of the kind $m^4/(B_2^2C_1^2)$ do not give logarithmically enhanced contributions, and we will omit them below. The denominators of the propagators

entering into Eqs. (1.16), (1.17) are:

$$\begin{aligned} A_i &= (p_- - k_i)^2 - m^2, \qquad & A &= (p_- - k_1 - k_2)^2 - m^2, \\ B_i &= (q_- + k_i)^2 - m^2, \qquad & B &= (q_- + k_1 + k_2)^2 - m^2, \\ C_i &= (k_i - p_+)^2 - m^2, \qquad & C &= (k_1 + k_2 - p_+)^2 - m^2, \\ D_i &= (q_+ + k_i)^2 - m^2, \qquad & D &= (q_+ + k_1 + k_2)^2 - m^2. \end{aligned} \tag{1.19}$$

For further integration it is useful to rewrite the denominators in terms of the photon energy fractions $x_{1,2}$ and their emission angles. In the case of the emission of both the photons along p_- we would have

$$\begin{aligned} \frac{A}{m^2} &= -x_1(1+z_1) - x_2(1+z_2) + x_1x_2(z_1+z_2) + 2x_1x_2\sqrt{z_1z_2}\cos\phi, \\ \frac{A_i}{m^2} &= -x_i(1+z_i), \end{aligned} \tag{1.20}$$

where $z_i = (\varepsilon\theta_i/m)^2$, ϕ is the azimuthal angle between the planes containing the space vector pairs $(\mathbf{p}_-\,, \mathbf{k}_1)$ and $(\mathbf{p}_-\,, \mathbf{k}_2)$. In the same way one can obtain in the case $k_1\,, k_2 \| q_-$:

$$\begin{aligned} \frac{B}{m^2} &= \frac{x_1}{y_1}(1+y_1^2z_1) + \frac{x_2}{y_1}(1+y_1^2z_2) + x_1x_2(z_1+z_2) + 2x_1x_2\sqrt{z_1z_2}\cos\phi, \\ \frac{B_i}{m^2} &= \frac{x_i}{y_1}(1+y_1^2z_i). \end{aligned} \tag{1.21}$$

Then we perform the elementary azimuthal angle integration and the integration over $z_1\,, z_2$ within the logarithmical accuracy using the procedure suggested in paper [22]:

$$\overline{a} = m^4 \int\limits_0^{z_0} \mathrm{d}z_1 \int\limits_0^{z_0} \mathrm{d}z_2 \int\limits_0^{2\pi} \frac{\mathrm{d}\phi}{2\pi} a. \tag{1.22}$$

The list of relevant integrals is given in Appendix I. This way we obtain the differential cross section in the collinear region,

$$\mathrm{d}\sigma_{\mathrm{coll}} = \frac{\alpha^4 L}{4\pi^2 s} \frac{\mathrm{d}^3q_+ \mathrm{d}^3q_-}{q_+^0 q_-^0} \frac{\mathrm{d}x_1 \mathrm{d}x_2}{x_1x_2} \big(1 + \mathcal{P}_{1,2}\big) \Bigg\{ \frac{1}{yr_1^2} \Bigg[\frac{1}{2}(L+2l) g_1 g_5 + \\ + (y^2 + r_1^4) \ln\frac{x_2 r_1^2}{x_1 y} + x_1x_2(y - x_1x_2) - 2r_1 g_5 \Bigg] [B_{p_-p_-}\delta_{p_-p_-} + B_{p_+p_+}\delta_{p_+p_+}] +$$

$$+\frac{1}{yr_1^2}\left[\frac{1}{2}(L+2l+4\ln y)g_1g_5+(y^2+r_1^4)\ln\frac{x_1r_1^2}{x_2y}+x_1x_2(y-x_1x_2)-2r_1g_1\right]\times$$
$$\times[B_{q_-q_-}\delta_{q_-q_-}+B_{q_+q_+}\delta_{q_+q_+}]+B_{p_-p_+}\delta_{p_-p_+}\left[(L+2l)\frac{g_1g_2}{r_1r_2}-2\frac{g_1}{r_1}-2\frac{g_2}{r_2}\right]+$$
$$+B_{q_-q_+}\delta_{q_-q_+}\left[(L+2l+2\ln(r_1r_2))\frac{g_1g_2}{r_1r_2}-2\frac{g_1}{r_1}-2\frac{g_2}{r_2}\right]+$$
$$+[B_{p_-q_-}\delta_{p_-q_-}+B_{p_+q_-}\delta_{p_+q_-}]\left[(L+2l+2\ln y_1)\frac{g_1g_3}{r_1y_1t_1}-2\frac{g_1}{r_1}-2\frac{g_3}{y_1t_1}\right]+$$
$$+[B_{p_+q_+}\delta_{p_+q_+}+B_{p_-q_+}\delta_{p_-q_+}]\left[(L+2l+2\ln y_2)\frac{g_1g_4}{r_1y_2t_2}-2\frac{g_1}{r_1}-2\frac{g_4}{y_2t_2}\right]\Bigg\}. \tag{1.23}$$

The permutation operator $\mathcal{P}_{1,2}$ acts as follows

$$\mathcal{P}_{1,2}f(x_1,x_2)=f(x_2,x_1).$$

We used the notation (see also Eq. (1.17)):

$$l=\ln\left(\frac{\theta_0^2}{4}\right),\qquad g_5=y^2+r_1^2, \tag{1.24}$$

where θ_0 is the collinear parameter. Delta function $\delta_{p,q}$ corresponds to the specific conservation law of the kinematical situation defined by the pair p,q (see Table 1): $\delta_{p,q}=\delta^{(4)}(\eta_2p_+{+}\eta_1p_-{-}\lambda_1q_-{-}\lambda_2q_+)$. Besides, we imply that the first photon is emitted along the momentum p; and the second, along the momentum $q(p,\, q=p_-,\, p_+,\, q_-,\, q_+)$. These δ functions could be taken into account in the integration as is made in the expression for $\mathrm{d}I(\eta,\lambda)$ (see Eq. (1.15)). Finally, we define

$$B_{p,q}=\left(\frac{\eta_2 s}{\lambda_1 t}+\frac{\lambda_1 t}{\eta_2 s}+1\right)^2,\qquad t=(p_--q_-)^2. \tag{1.25}$$

1.1.2. Semicollinear Kinematics. We will suggest for definiteness that the photon with momentum k_2 moves inside a narrow cone along the momentum direction of one of the charged particles, while the other photon moves in any direction outside that cone along any charged particle. This choice allows us to omit the statistical factor $1/2!$. The quasireal electron method [21] may be used to obtain the cross section:

$$\begin{aligned}\mathrm{d}\sigma^{\mathrm{sc}} &= \frac{\alpha^4}{32s\pi^4}\frac{\mathrm{d}^3q_-\mathrm{d}^3q_+\mathrm{d}^3k_1}{q_-^0q_+^0k_1^0}V\frac{\mathrm{d}^3k_2}{k_2^0}\left\{\frac{\mathcal{K}_{p_-}}{p_-k_2}\delta_{p_-}R_{p_-}+\right.\\ &+ \left.\frac{\mathcal{K}_{p_+}}{p_+k_2}\delta_{p_+}R_{p_+}+\frac{\mathcal{K}_{q_-}}{q_-k_2}\delta_{q_-}R_{q_-}+\frac{\mathcal{K}_{q_+}}{q_+k_2}\delta_{q_+}R_{q_+}\right\}.\end{aligned} \tag{1.26}$$

We omitted the terms of the kind $m^2/(p_-k_2)^2$ in Eq. (1.26) because their contribution does not contain the large logarithm L. The quantities entering into Eq. (1.26) are given by:

$$\begin{aligned} V &= \frac{s}{k_1p_+k_1p_-}+\frac{s'}{k_1q_+k_1q_-}-\frac{t'}{k_1p_+k_1q_+}-\frac{t}{k_1p_-k_1q_-}+ \\ &+ \frac{u'}{k_1p_+k_1q_-}+\frac{u}{k_1q_+k_1p_-}, \end{aligned} \tag{1.27}$$

V is the known accompanying radiation factor; $\mathcal{K}_i$ are the single photon emission collinear factors:

$$\mathcal{K}_{p_-}=\mathcal{K}_{p_+}=\frac{g_2}{x_2r_2},\ \mathcal{K}_{q_-}=\frac{y_1^2+(y_1+x_2)^2}{x_2(y_1+x_2)},\ \mathcal{K}_{q_+}=\frac{y_2^2+(y_2+x_2)^2}{x_2(y_2+x_2)}. \tag{1.28}$$

The quantities R_i read,

$$\begin{aligned} &R_{p_-}=R[sr_2,tr_2,ur_2,s',t',u'], \quad R_{p_+}=R[sr_2,t,u,s',t'r_2,u'r_2], \\ &R_{q_-}=R\left[s,t\frac{t_1}{y_1},u,s'\frac{t_1}{y_1},t',u'\frac{t_1}{y_1}\right], \\ &R_{q_+}=R\left[s,t,u\frac{t_2}{y_2},s'\frac{t_2}{y_2},t'\frac{t_2}{y_2},u'\right], \end{aligned} \tag{1.29}$$

where the function R has the form [6]:

$$\begin{aligned} &R[s,t,u,s',t',u']=\frac{1}{ss'tt'}\left[ss'(s^2+s'^2)+tt'(t^2+t'^2)+uu'(u^2+u'^2)\right], \\ &s=(p_++p_-)^2, \quad s'=(q_++q_-)^2, \quad t=(p_--q_-)^2, \\ &t'=(p_+-q_+)^2, \quad u=(p_--q_+)^2, \quad u'=(p_+-q_-)^2. \end{aligned} \tag{1.30}$$

Finally, we define

$$\begin{aligned} \delta_{p_-} &= \delta^{(4)}(p_-r_2+p_+-q_+-q_--k_1), \\ \delta_{p_+} &= \delta^{(4)}(p_-+p_+r_2-q_+-q_--k_1), \\ \delta_{q_-} &= \delta^{(4)}(p_-+p_+-q_+-q_-\frac{y_1+x_2}{y_1}-k_1), \\ \delta_{q_+} &= \delta^{(4)}(p_-+p_+-q_+\frac{y_2+x_2}{y_2}-q_--k_1). \end{aligned} \tag{1.31}$$

Performing the integration over angular variables of the collinear photon we obtain

$$\begin{aligned} \mathrm{d}\sigma^{\mathrm{sc}} &= \frac{\alpha^4L}{16s\pi^3}\frac{\mathrm{d}^3q_-\mathrm{d}^3q_+\mathrm{d}^3k_1}{q_-^0q_+^0k_1^0}\mathrm{d}x_2V\Big\{\mathcal{K}_{p_-}[R_{p_-}\delta_{p_-}+R_{p_+}\delta_{p_+}]+ \\ &+ \frac{1}{y_2}\mathcal{K}_{q_+}R_{q_+}\delta_{q_+}+\frac{1}{y_1}\mathcal{K}_{q_-}R_{q_-}\delta_{q_-}\Big\}. \end{aligned} \tag{1.32}$$

To see that the sum of cross sections (1.23) and (1.32)

$$\mathrm{d}\sigma^{\gamma\gamma} = \mathrm{d}\sigma^{\mathrm{coll}} + \int \mathrm{d}O_1 \left(\frac{\mathrm{d}\sigma^{\mathrm{sc}}}{\mathrm{d}O_1} \right) \tag{1.33}$$

does not depend on the auxiliary parameter θ_0. We verify that terms Ll from Eq. (1.23) cancel out with the terms

$$L \frac{k_1^0 q_i^0}{2\pi} \int \frac{\mathrm{d}O_1}{k_1 q_i} \;\approx\; -Ll, \tag{1.34}$$

which arise from 16 regions in the semicollinear kinematics.

1.1.3. Numerical Results and Discussion. We separated the contribution of the collinear and semicollinear regions using the auxiliary parameter θ_0. By direct numerical integration according to the presented formulae we had convinced ourselves that the total result is independent of the choice of θ_0.

It is convenient to compare the cross section of double hard photon emission with the Born cross section

$$\sigma^{\mathrm{Born}} = \frac{\alpha^2 \pi}{2s} \int\limits_{-\cos\psi_0}^{\cos\psi_0} \left(\frac{3 + c^2}{1 - c} \right)^2 \mathrm{d}c. \tag{1.35}$$

For illustrations we integrated over some typical experimental angular acceptance and chose the following values of the parameters:

$$\begin{gathered} \psi_0 = \pi/4, \quad \sqrt{s} = 0.9 \text{ GeV}, \quad \Delta_1 = 0.4, \quad \Delta = 0.05, \\ \theta_0 = 0.05, \quad L = 15.0, \quad l = -7.38\,, \end{gathered} \tag{1.36}$$

where Δ_1 defines the energy threshold for the registration of the final electron and positron: $q_\pm^0 > \varepsilon_{\mathrm{th}} = \varepsilon\Delta_1$. Note that restrictions on θ_0 (1.7) and (1.12) $(z_0 = \exp\{L + l\} \gg 1)$ are fulfilled.

For the parameters chosen we get

$$\begin{aligned} &\sigma^{\mathrm{Born}} = 1.2 \text{ mkb}, \qquad \frac{\sigma^{\mathrm{coll}}}{\sigma^{\mathrm{Born}}} \cdot 100\,\% = -0.25\,\%, \\ &\frac{\sigma^{\mathrm{sc}}}{\sigma^{\mathrm{Born}}} \cdot 100\,\% = 0.81\,\%, \qquad \delta\sigma^{\mathrm{tot}} = \frac{\sigma^{\mathrm{sc}} + \sigma^{\mathrm{coll}}}{\sigma^{\mathrm{Born}}} \cdot 100\,\% = 0.56\,\%. \end{aligned} \tag{1.37}$$

The *phenomenon* of negative contribution to the cross section from the collinear kinematics is an artifact of our approach. Namely, we systematically omitted positive terms without large logarithms, among them we dropped terms proportional to l^2. The cancellation of l^2 terms can be seen only after adding the contribution of the noncollinear kinematics (when both photons are emitted outside narrow

cones along charged-particle momenta). The noncollinear kinematics does not provide any large logarithm L.

Both quantities $\sigma^{\rm coll}$ and $\sigma^{\rm sc}$ depend on auxiliary parameter θ_0. We eliminated by hands from Eq. (1.23) the terms proportional to l and obtained the following quantity:

$$\frac{\sigma^{\rm bare}_{\rm coll}}{\sigma^{\rm Born}}\cdot 100\,\% = 1.43\,\%. \tag{1.38}$$

This quantity corresponds to an approximation for the correction under consideration in which one considers only the collinear regions and takes into account only terms proportional to L^2 and L (all terms dependent on θ_0 are to be omitted). Having in mind the cancellation of θ_0 dependence in the sum of the collinear and semicollinear contributions, we may subtract from the value of the semicollinear contribution the part which is associated with l:

$$\sigma^{\rm bare}_{\rm sc} = \sigma_{\rm sc} + (\sigma_{\rm coll} - \sigma^{\rm bare}_{\rm coll}), \qquad \frac{\sigma^{\rm bare}_{\rm sc}}{\sigma^{\rm Born}}\cdot 100\,\% = -0.87\,\%.$$

Looking at *bare* quantities one can get an idea of relative impact of two considered regions. We see that at the precision level of $0.1\,\%$ the next-to-leading contributions of semicollinear regions are important.

1.2. Hard Pair Production. In this chapter we consider the process of the $2\to 4$ type:

$$e^-(p_1)+e^+(p_2)\to e^-(q_1)+e^+(q_2)+e^-(p_-)+e^+(p_+)\,. \tag{1.39}$$

We assume for definiteness that two final particles $e^-(q_1)$ and $e^+(q_2)$ hit the detectors, allowing the following angular aperture and energy thresholds:

$$\Psi_0<\theta_1,\ \theta_2<\pi-\Psi_0,\ \theta_{1,2}=\widehat{\mathbf{q}_{1,2}\mathbf{p}_1},\ y_{\rm th}<y_{1,2}<1,\ y_{1,2}=\frac{q^0_{1,2}}{\varepsilon}, \tag{1.40}$$

where the *dead* angle Ψ_0 depends on the detector ($\Psi_0\sim 20^\circ$ for DAΦNE [4] and $\Psi_0\sim 35^\circ$ for CMD-1 [3]); $y_{\rm th}\gtrsim 0.1$, ε is the beam energy (a c.m.s. reference frame of the initial particles is implied).

In our recent paper [10] similar problems were considered for the case of small angle Bhabha scattering (SABS). We had there at least three simplifications: i) the generalized eikonal form of the amplitude allowed to omit all scattering-type Feynman diagrams with more than one exchanged photons in the t channel; ii) at the $\mathcal{O}(\alpha^2)$ level it was possible to omit all annihilation-type Feynman diagrams and contributions connected with heavy Z, W and H bosons; iii) the interference of the *emission from the positron line* with *the emission from the electron line* was suppressed for real photon or pair production. Calculations for the LABS case are considerably more complicated. Only the possibility of omitting heavy-boson contributions in the $\mathcal{O}(\alpha^2)$ order remains here.

1.2.1. Definitions of Kinematical Regions. There are 36 tree level Feynman diagrams (Fig. 9) which describe a e^+e^- pair production in LABS. Quite a lot was paid to this process in the literature [5, 24], where different cross sections were obtained in terms of chiral amplitudes. It was found that in the general kinematics the cross section has a rather complicated form. Fortunately in the general case, when the angles between each two final particles are not small, the correspondent RC contribution to the Born cross section will have the value $(\alpha/\pi)^2 \sim 10^{-5}$:

$$\mathrm{d}\sigma^{e\bar{e}\to 2e2\bar{e}} \sim \mathrm{d}\sigma_0^{e\bar{e}\to e\bar{e}} \left(1 + \mathcal{O}\left(\frac{\alpha^2}{\pi^2}\right)\right). \tag{1.41}$$

It can be safely omitted working within an accuracy of $0.1\,\%$. In RC contributions due to pair production some enhancements appear in the cases when one or two final particles move within a small angle $\theta_i \sim m_e/\varepsilon$ to the direction of one of the tagged (initial or final registered) particles. In these cases one will have logarithmically enhanced contributions of the orders $(\alpha L/\pi)^2$ and $(\alpha/\pi)^2 L$, where $L = \ln s/m_e^2$ is the *large logarithm,* $s = 4\varepsilon^2$ ($L \sim 15$ for $\sqrt{s} \sim 1$ GeV). The aim of this chapter is to extract contributions of that sort because of their importance at the $0.1\,\%$ accuracy level.

Our method of calculating is to separate the contributions of the collinear and semicollinear kinematical regions. In the collinear kinematics (CK) two of the final particles (which are not registered) go within the narrow cone about the direction of one of the initial particles or about the direction of one of the registered final particles:

$$\theta_i < \theta_0, \qquad \frac{m_e^2}{\varepsilon^2} \ll \theta_0 \ll 1, \tag{1.42}$$

where $\theta_i,\ i = 1, 2$ are the polar angles of the two particles with respect to the chosen direction. As the semicollinear case we define the kinematics when only one of the nonregistered final particles move within this cone and the second one does not (with respect to all tagged directions). The contribution of the collinear kinematics has the form

$$a\left(\frac{\alpha}{\pi}(L + \ln\,\theta_0^2)\right)^2 + b\left(\frac{\alpha}{\pi}\right)^2 (L + \ln\,\theta_0^2), \tag{1.43}$$

while the semicollinear one reads

$$\left(\frac{\alpha}{\pi}\right)^2 f(\theta_0) L, \qquad f(\theta_0) = -2a \ln\theta_0^2 + C, \tag{1.44}$$

where C is finite for $\theta_0 \to 0$. The sum of the contributions does not depend on the auxiliary parameter θ_0 within the logarithmic accuracy (we omit the terms

$(\alpha/\pi)^2 \ln^2 \theta_0^2$ and $(\alpha/\pi)^2 \ln \theta_0^2$). The cancellation of the dependence provides a test of our calculations.

Consider now the structure of the collinear region contribution to the cross section. It could be presented as a sum of the cross sections of hard subprocesses multiplied by the so-called collinear factors. In the case of the emission of one or two hard collinear photons, the hard subprocess is just the Bhabha scattering. This is the manifestation of the well-known factorization theorem in its simplest form [6]. In the case of pair production, besides Bhabha scattering there appear three other types of hard subprocesses: Compton scattering, two-quantum annihilation of the initial particles, and the subprocess of the creation of the final registered particles by two photons moving close to the directions of the initial beams. Note that this rather complicated form of the factorization theorem appears first in the process under consideration.

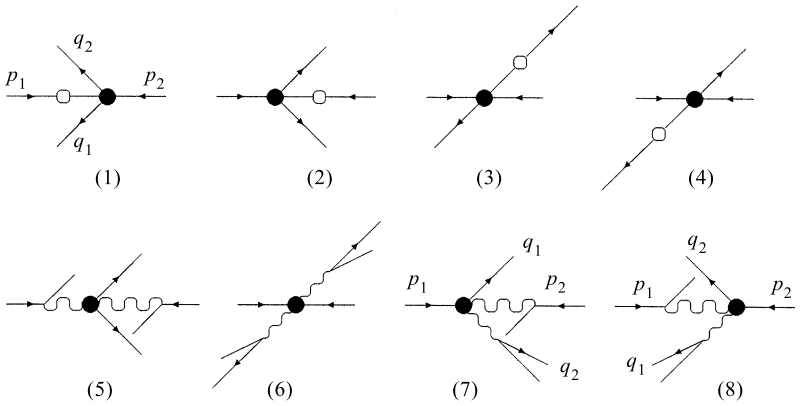

Fig. 1. Kinematical diagrams for collinear pair production

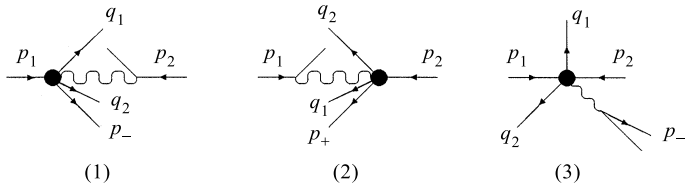

Fig. 2. Kinematical diagrams for semicollinear pair production

The contributions of semicollinear regions could as well be expressed in terms of hard subprocesses of the $2 \to 3$ type [6]: a single photon emission in e^+e^- scattering, and the process of pair creation in a photon-electron (-positron)

scattering. In Figs. 1, 2 we show the kinematical schemes for the collinear and semicollinear regions (empty circles denote the production of a collinear undetected pair; the full ones, hard subprocesses).

Our method, we believe, saves a lot of computation work. Indeed instead of 8-fold integration of very complicated expressions with sharp singularities it provides 2(3)-fold integrals of smooth functions within the same accuracy.

1.2.2. Collinear Regions. Consider first a set of collinear kinematics. We will see that there are 8 different cases. As we've underlined above, the experimental criterion for an event to be chosen is a kinematics in which at least one outgoing lepton moves at large angles to the beam direction in the opposite hemispheres. In the case of the emission of a particle with momentum k, moving along the direction of its parent particle with momentum p, a small quantity $2pk$ appears in the denominator of the matrix element. Evidently, at least, two such small denominators are necessary to obtain a nonzero contribution integrating over the small phase volume of the two emitted particles in the collinear kinematics ($\mathrm{d}\Gamma_2 \sim \theta_0^4$). Our criterion of the Feynman-diagram selection out of the total 36 ones (or out of 18 gauge invariant pairs of diagrams) (see Fig. 9 in Appendix III) is to choose such gauge invariant sets which have one diagram with two small denominators. The list of the collinear kinematics regions and the relevant Feynman diagrams from Fig. 9 (in parentheses we put their numbers) reads

$$
\begin{aligned}
&1)\ \ \mathbf{p}_+, \mathbf{p}_- \parallel \mathbf{p}_1: \quad (1,2),\ (7,8),\ (25,26),\ (23,24);\\
&2)\ \ \mathbf{p}_+, \mathbf{p}_- \parallel \mathbf{q}_1: \quad (1,2),\ (3,4),\ (27,28),\ (31,32);\\
&3)\ \ \mathbf{p}_+, \mathbf{p}_- \parallel \mathbf{p}_2: \quad (9,10),\ (17,18),\ (25,26),\ (15,16);\\
&4)\ \ \mathbf{p}_+, \mathbf{p}_- \parallel \mathbf{q}_2: \quad (9,10),\ (21,22),\ (27,28),\ (33,34);\\
&5)\ \ \mathbf{p}_- \parallel \mathbf{p}_1,\quad \mathbf{p}_+ \parallel \mathbf{p}_2: \quad (19,20);\\
&6)\ \ \mathbf{p}_- \parallel \mathbf{p}_1,\quad \mathbf{p}_+ \parallel \mathbf{q}_1: \quad (11,12);\\
&7)\ \ \mathbf{p}_- \parallel \mathbf{q}_2,\quad \mathbf{p}_+ \parallel \mathbf{p}_2: \quad (13,14);\\
&8)\ \ \mathbf{p}_- \parallel \mathbf{q}_2,\quad \mathbf{p}_+ \parallel \mathbf{q}_1: \quad (29,30).
\end{aligned}
\tag{1.45}
$$

We verified explicitly the validity of the criterion for the first kinematics considering the full set of 36 diagrams. Note that collinear regions 5–8 are specific for the pair production process and arise due to the presence of identical particles in the final state.

The calculation of the collinear factors for the region 1–4 was described in detail in papers [20, 25], therefore here we concern with only the main points of the derivations. Let's start with the general form of the cross section for the region 1:

$$
\mathrm{d}\sigma^{(1)}_{\mathrm{coll}} = \frac{\alpha^4}{8\pi^4 s} \sum_{\mathrm{spin}} |M^{(1)}|^2 \frac{\mathrm{d}^3 q_1 \mathrm{d}^3 q_2}{4 q_1^0 q_2^0} \frac{\mathrm{d}^3 p_- \mathrm{d}^3 p_+}{4 p_-^0 p_+^0} \delta^4(y p_1 + p_2 - q_1 - q_2), \tag{1.46}
$$

$$y = 1 - x_- - x_+, \qquad x_\pm = \frac{p_\pm^0}{\varepsilon},$$

where

$$\sum_{\text{spin}} |M^{(1)}|^2 = \frac{4}{y}\frac{I^{(1)}}{m_e^4} 16 \left(\frac{s_1}{t_1} + \frac{t_1}{s_1} + 1 \right)^2,$$
$$s_1 = ys = 4y\varepsilon^2, \quad t_1 = yt = -2yy_1\varepsilon^2(1 - c_-), \tag{1.47}$$
$$c_- = \cos \widehat{\mathbf{q_1 p_1}}, \quad y_{1,2} = \frac{q_{1,2}^0}{\varepsilon},$$

and quantity $I^{(1)}$ is a rather complicated function of $z_\pm = \varepsilon^2\theta_\pm^2/m_e^2$ and $x_\pm$, it is given explicitly in [25, 26].

Transforming the phase volume of the created pair into the form

$$\int \mathrm{d}\Phi = \int \frac{\mathrm{d}^3p_- \mathrm{d}^3p_+}{4p_-^0 p_+^0} = \frac{\pi^2}{4} m_e^4 \int_0^{2\pi} \frac{\mathrm{d}\phi}{2\pi} \int_0^{z_0} \mathrm{d}z_+ \int_0^{z_0} \mathrm{d}z_- \int_0^{1-y} \mathrm{d}x_+ \int_0^{1-y-x_-} x_- x_+ \mathrm{d}x_- ,$$
$$z_0 = \left(\frac{\varepsilon\theta_0}{m_e} \right)^2 \gg 1, \tag{1.48}$$

and performing all integrations over variables of pair components except its total energy fraction $(1 - y)$, one obtains

$$\mathrm{d}\sigma_{\text{coll}}^{(1)} = \frac{2\alpha^4}{\pi^2 s} \frac{\mathrm{d}y}{y} F^{(1)}(y) \left(\frac{s_1}{t_1} + \frac{t_1}{s_1} + 1 \right)^2 \frac{\mathrm{d}^3q_1 \mathrm{d}^3q_2}{4q_1^0 q_2^0} \times$$
$$\times \ \delta^4(yp_1 + p_2 - q_1 - q_2). \tag{1.49}$$

The next step is to rewrite the contribution in terms of the scattered electron observable variables c_- and y_1.

The conservation law gives

$$1 + y = y_1 + y_2, \qquad -1 + y = y_1 c_- + y_2 c_+,$$
$$y_1 \sin\theta_- = y_2 \sin\theta_+, \qquad c_+ = \cos \widehat{\mathbf{q_2 p_1}} = \cos\theta_+. \tag{1.50}$$

The final result for the contribution of the first collinear kinematics region reads

$$\frac{\mathrm{d}\sigma^{(1)}}{\mathrm{d}y_1 \mathrm{d}c_-} = \frac{\alpha^4}{s\pi} \frac{F^{(1)}(y, z_0)}{y} \frac{y_1}{[2 - y_1(1 - c_-)]} \left(1 - y_1 \frac{1 - c_-}{2} - \frac{2}{y_1(1 - c_-)} \right)^2,$$
$$y = \frac{y_1(1 + c_-)}{2 - y_1(1 - c_-)}. \tag{1.51}$$

The quantity $F^{(1)}(y,z_0)$ can be found in papers [25,26] and it has the following form

$$\begin{aligned}
F^{(1)}(y,z_0) &= L\biggl(\frac{1}{2}R(y)L+f(y)\biggr), \qquad L=\ln z_0,\\
R(y) &= \frac{2}{3}\,\frac{1+y^2}{1-y}+\frac{1-y}{3y}(4+7y+4y^2)+2(1+y)\ln y,\\
f(y) &= \frac{1}{9}\biggl(-107+136y-6y^2-\frac{12}{y}-\frac{20}{1-y}\biggr)+\frac{2}{3}\biggl(-4y^2-5y+1+\\
&+ \frac{4}{y(1-y)}\biggr)\ln(1-y)+\frac{1}{3}\biggl(8y^2+5y-7-\frac{13}{1-y}\biggr)\ln y- \qquad (1.52)\\
&- \frac{2}{1-y}\ln^2 y+4(1+y)\ln y\ln(1-y)+\\
&+ \frac{2(1-3y^2)}{1-y}\mathrm{Li}_2(1-y), \qquad \mathrm{Li}_2(x)=-\int\limits_0^x\frac{\mathrm{d}t\ln(1-t)}{t}\,.
\end{aligned}$$

We remember the way in which this differential cross section enters into the experimentally observable one:

$$\Delta\sigma^{(1)}_{\text{exp}}=\int\limits_{-c_0}^{c_0}\mathrm{d}c_-\int\limits_{y_{\text{th}}}^{1}\mathrm{d}y_1\Theta(c_0^2-c_+^2)\Theta(y_2-y_{\text{th}})\Theta(1-y_2)\frac{\mathrm{d}\sigma^{(1)}_{\text{coll}}}{\mathrm{d}y_1\mathrm{d}c_-}, \qquad (1.53)$$

where

$$\begin{aligned}
y_2&=\frac{1+(1-y_1)^2+y_1(2-y_1)c_-}{2-y_1(1-c_-)},\\
c_+&=\frac{-1+y-y_1c_-}{y_2}, \quad c_0=\cos\Psi_0.
\end{aligned} \qquad (1.54)$$

Let us consider as a check that our formula for $\mathrm{d}\sigma_c^{(1)}$ agrees with the corresponding contribution to the SABS cross section. Really, the correspondence would take place if we took the small angle limit:

$$c_-=1-\frac{\theta_-^2}{2}, \quad \theta_+=y\theta_-, \quad z=\frac{\theta_+^2}{\theta_1^2}, \quad Q_1^2=\varepsilon^2\theta_1^2. \qquad (1.55)$$

In this way we obtain

$$\mathrm{d}\sigma^{(1)}=\frac{\alpha^2}{4\pi^2}\frac{4\pi\alpha^2}{Q_1^2}F^{(1)}(y,z_0)\mathrm{d}y\frac{\mathrm{d}z}{z^2}. \qquad (1.56)$$

This formula agrees with Eq. (39) from [10], where two directions were taken into account (we have to note that the expression for $f(y)$ in [10] contains some misprints, they are corrected above).

The third collinear region gives the same contribution:

$$\Delta\sigma_{\rm exp}^{(3)} = \Delta\sigma_{\rm exp}^{(1)}. \tag{1.57}$$

Also, the contributions of the collinear regions 2 and 4 are equal:

$$\Delta\sigma_{\rm exp}^{(2)} = \Delta\sigma_{\rm exp}^{(4)},$$

$$\Delta\sigma_{\rm exp}^{(2)} = \int\limits_{-c_0}^{c_0} {\rm d}c_- \int\limits_{y_{\rm th}}^{1} {\rm d}y_1 \frac{{\rm d}\sigma_{\rm coll}^{(2)}}{{\rm d}y_1 {\rm d}c_-}, \qquad y_2 = 1, \quad c_+ = -c_-, \quad y_1 = y,$$

$$\frac{{\rm d}\sigma^{(2)}}{{\rm d}y_1 {\rm d}c_-} = \frac{\alpha^4}{2s\pi} F^{(2)}(y, z_0)\left(1 - \frac{1-c_-}{2} - \frac{2}{1-c_-}\right)^2, \tag{1.58}$$

$$F^{(2)}(y, z_0) = -yF^{(1)}\left(\frac{1}{y}, z_0 y^2\right) = L\left(\frac{1}{2}R(y)L + 2R(y)\ln y + f_1(y)\right),$$

$$f_1(y) = \frac{1}{9}\left(-116 + 127y + 12y^2 + \frac{6}{y} - \frac{20}{1-y}\right) + \frac{2}{3}\left(-4y^2 - 5y + 1 + \right.$$

$$\left. + \frac{4}{y(1-y)}\right)\ln(1-y) + \frac{1}{3}\left(8y^2 - 10y - 10 + \frac{5}{1-y}\right) \times$$

$$\times \quad \ln y - (1+y)\ln^2 y + 4(1+y)\ln y \ln(1-y) + \frac{2(3-y^2)}{1-y}{\rm Li}_2(1-y).$$

Again one can check the correspondence of this result with the case of SABS (see Eq. (39) in [10]).

(1) (2)

Fig. 3. Diagrams for collinear factors in a space-like kinematics (1) and in a time-like one (2)

We underline that neglecting terms of order α^2/π^2 permits us within the accuracy of $0.1\,\%$ to express the contribution to $\sigma_{\rm exp}$ in terms of two-fold integrals of smooth functions.

Consider now the collinear region 5 (see Fig. 1 (5)) in which two of the final particles move close to the directions of the initial beams and the registered pair is created by two almost real photons moving also very close to the initial particle directions. The method of the collinear-factor calculations in this case can be considered as an essential generalization of the Weizsäcker–Williams approximation [21, 27]. Let us consider the block of the kinematical diagram, Fig. 1 (5), that describes the emission of an undetected fermion and an almost real photon (both close to the initial direction). The photon enters then into a

hard block (see Fig. 3 (1)). The corresponding matrix element reads

$$M = \frac{1}{q^2} J_\nu g^{\mu\nu} I_\mu, \qquad J_\nu = \bar{u}(p_1')\gamma_\nu u(p_1), \tag{1.59}$$

where I_μ is the current corresponding to the hard block. Let's decompose following Sudakov [28] the 4-momentum of the emitted fermion,

$$\begin{aligned} p_1' &= \alpha\tilde{p}_2 + \beta\tilde{p}_1 + p_{1\perp}', \qquad p_{1\perp}' p_1 = p_{1\perp}' p_2 = 0, \\ \tilde{p}_{1,2} &= p_{1,2} - p_{2,1}\frac{m^2}{s}, \qquad s = 2p_1p_2 \gg m^2. \end{aligned} \tag{1.60}$$

The 4-momenta $\tilde{p}_{1,2}$ are almost light-like. The parameter β here amounts about unity. It has the meaning of energy fraction of the scattered electron; $1-\beta$ is the energy faction of our almost real photon; $p_{1\perp}'$ is the two-dimensional vector describing the components of the scattered electron momentum transverse with respect to the initial direction (and further we denote transverse momentum components by symbol $\perp$). Parameter $\alpha = ((\mathbf{p}_1)^2+m^2)/(s\beta)$ is small: $\alpha \ll 1$. It could be found from the mass shell condition for the scattered electron: ${p_1'}^2 = m^2$. In that way we obtain also the useful equation

$$q^2 = -\frac{((p_{1\perp}')^2 + m^2(1-\beta)^2)}{\beta} < 0. \tag{1.61}$$

Representing identically the metric tensor, entering into the photon Green function, in the form

$$g^{\mu\nu} = g_\perp^{\mu\nu} + \frac{2}{s}(p_1^\mu p_2^\nu + p_1^\nu p_2^\mu), \tag{1.62}$$

we note that it could be effectively written in the form

$$g^{\mu\nu} \approx g_\perp^{\mu\nu} + \frac{2}{s}\, p_1^\mu p_2^\nu, \tag{1.63}$$

since the contribution of the omitted term is suppressed by an additional factor of order q^2/s. Taking that into account, one obtains

$$M = \frac{1}{q^2}\left\{(JI)_\perp + \frac{2}{s}(Jp_2)\left(-\frac{Ip_{1\perp}'}{1-\beta}\right)\right\}, \tag{1.64}$$

where the current conservation condition

$$Iq = I(\alpha_1 p_2 + (1-\beta)p_1 + q_\perp) \approx I((1-\beta)p_1 + q_\perp) = 0 \tag{1.65}$$

was used. Now we sum up over fermion spin states:

$$\begin{aligned}&\sum_{\text{spin}}|(JI)_\perp|^2=\mathrm{Tr}\,(\hat{p}_1'+m)I_\perp(\hat{p}_1+m)I_\perp=-2q^2I_\perp^2>0,\\&\sum_{\text{spin}}|Jp_2|^2=2s^2\beta,\quad\sum_{\text{spin}}(Jp_2)(JI)_\perp^*=2s(q_\perp I_\perp),\quad q_\perp=-p_{1\perp}'.\end{aligned}\tag{1.66}$$

And we obtain

$$\sum_{\text{spin}}|M|^2=\frac{1}{(q^2)^2}\left[-2q^2I_\perp^2+\frac{8}{(1-\beta)^2}(p_{1\perp}'I_\perp)^2\right],\tag{1.67}$$

where q^2 are to be taken from Eq. (1.61). The phase volume of the scattered electron could be presented in the form

$$\int\frac{\mathrm{d}^3p_1'}{2\varepsilon_1'}=\int\frac{\mathrm{d}\beta}{2\beta}\int\frac{\mathrm{d}\phi}{2\pi}\,2\pi\int\limits_0^{(\varepsilon\beta\theta_0)^2}\frac{\mathrm{d}(p_{1\perp}')^2}{2}\,.\tag{1.68}$$

Then we carry out a simple integration and obtain

$$\int\sum_{\text{spin}}|M|^2\frac{\mathrm{d}^3p_1'}{2\varepsilon_1'}=\pi(I_\perp)^2Q(\beta,z_0)\mathrm{d}\beta,\tag{1.69}$$

where the collinear factor $Q(\beta,z_0)$ for a space-like virtual photon has the form

$$Q(\beta,z_0)=\frac{1+\beta^2}{1-\beta}\left[L+2\ln\frac{\beta}{1-\beta}\right]-\frac{2\beta}{(1-\beta)^2}\,.\tag{1.70}$$

Now we are ready to calculate the cross section in the collinear region 5, where we have two collinear factors $Q(\beta,z_0)$. We need also the matrix element squared of the hard block describing hard e^+e^- pair creation by two photons:

$$\gamma((1-\beta_1)p_1)+\gamma((1-\beta_2)p_2)\to e_+(q_2)+e_-(q_1).\tag{1.71}$$

Taking the phase volume in terms of the detected electron as follows:

$$\begin{aligned}\mathrm{d}\beta_2\frac{\mathrm{d}^3q_1\mathrm{d}^3q_2}{2q_1^02q_2^0}\delta^4(q_1+q_2-p_1(1-\beta_1)-p_2(1-\beta_2))=\\=\frac{(\pi/2)y_1\mathrm{d}y_1\mathrm{d}c_-}{2\beta_1-y_1(1+c_-)}\,,\end{aligned}\tag{1.72}$$

we obtain for the cross section

$$\begin{aligned}\frac{\mathrm{d}\sigma^{(5)}_{\mathrm{coll}}}{\mathrm{d}y_1\mathrm{d}c_-} &= \frac{\alpha^4}{2\pi s}\int\limits_0^1 \frac{\mathrm{d}\beta_1 2y_2(1-c_-c_+)}{\beta_1^2\beta_2^2(2\beta_1-y_1(1+c_-))y_1(1-c_-^2)}\times\\ &\times \left\{(1+(1-\beta_1)^2)\left(L+2\ln\frac{1-\beta_1}{\beta_1}\right)-2(1-\beta_1)\right\}\times\\ &\times \left\{(1+(1-\beta_2)^2)\left(L+2\ln\frac{1-\beta_2}{\beta_2}\right)-2(1-\beta_2)\right\}, \quad (1.73)\end{aligned}$$

where

$$\begin{aligned}&2\beta_1-y_1(1+c_-)>0, \quad \beta_2=\frac{y_1\beta_1(1-c_-)}{2\beta_1-y_1(1+c_-)},\\ &y_2=\frac{2\beta_1^2+y_1(y_1-2\beta_1)(1+c_-)}{2\beta_1-y_1(1+c_-)}, \quad c_+=\frac{1}{y_2}(\beta_1-\beta_2-y_1c_-).\end{aligned} \quad (1.74)$$

For the hard block we used the following expression:

$$\begin{aligned}\sum_{\mathrm{spin}}|M^{\gamma\gamma\to e^+e^-}|^2 &\sim \frac{t_1}{u_1}+\frac{u_1}{t_1}=\frac{y_1(1-c_-)}{y_2(1-c_+)}+\frac{y_2(1-c_+)}{y_1(1-c_-)}=\\ &= \frac{2y_2(1-c_+c_-)}{y_1(1-c_-^2)}. \quad (1.75)\end{aligned}$$

And for the contribution to the *experimental* cross section we get

$$\Delta\sigma^{(5)}=\int\limits_{y_{\mathrm{th}}}^1\mathrm{d}y_1\int\limits_{-c_0}^{c_0}\mathrm{d}c_-\frac{\mathrm{d}\sigma^{(5)}_{\mathrm{coll}}}{\mathrm{d}y_1\mathrm{d}c_-}\Theta(y_2-y_{\mathrm{th}})\Theta(1-y_2)\Theta(c_0^2-c_+^2). \quad (1.76)$$

A similar situation takes place for the collinear kinematics 6, when the initial electron and positron annihilate into two almost real photons, that convert then into two electron-positron pairs.

The matrix element describing the emission of a time-like almost real photon with its subsequent conversion into a pair (see Fig. 3 (2)) has the form

$$M=\frac{g^{\mu\nu}}{k^2}I_\mu J_\nu, \qquad J_\nu=\bar v(p_-)\gamma_\nu u(q_+). \quad (1.77)$$

We use again the Sudakov representation for the momenta of the pair components and the photon:

$$\begin{aligned}&g^{\mu\nu}\approx g_\perp^{\mu\nu}+\frac{2}{s_1}q^\nu q_+^\mu, \qquad q^2=0, \quad 2qq_+=s_1,\\ &p_-=\alpha_1 q+\beta_1\tilde q_++(p_-)_\perp, \qquad \tilde q_+=q_+-q\frac{m^2}{s_1},\\ &k=q_++p_-=\alpha_2 q+\beta_2\tilde q_++k_\perp, \qquad \beta_1=\beta_2-1>0.\end{aligned} \quad (1.78)$$

The current conservation condition here reads

$$kI \approx (\beta_1 \tilde{q}_+ + p_-^\perp) I = 0. \tag{1.79}$$

Using the above definitions we get the matrix element squared summed over spin states in the following form

$$\begin{gathered}\sum_{\text{spin}} |M|^2 = 2\frac{(I^\perp)^2}{(k^2)^2}\,\frac{[(1+(\beta_2-1)^2)(k^\perp)^2 + m^2\beta_2^4]}{\beta_2^2(\beta_2-1)}, \\ k^2 = \frac{(k^\perp)^2 + m^2\beta_2^2}{\beta_2 - 1} > 0.\end{gathered} \tag{1.80}$$

Integrating over the transverse momentum components $(p_-)_\perp$ of the electron from the created pair, we obtain

$$\int \frac{\mathrm{d}^2 p_-^\perp}{2p_-^0} \sum_{\text{spin}} |M|^2 = \frac{\pi (I_\perp)^2 \mathrm{d}\beta_2}{\beta_2^2} \Bigg\{ (1+(\beta_2-1)^2) \left(L + 2\ln\left(y_2 \left(1 - \frac{1}{\beta_2} \right) \right) \right) + \\ + 2(\beta_2 - 1) \Bigg\}. \tag{1.81}$$

Note that due to the character of the hard $e^+e^- \to \gamma\gamma$ block we have $k_1^0 = k_2^0 = \varepsilon$ and the relation between the detected positron energy fraction $y_2 = q_+^0/\varepsilon$ and parameter β_2 reads:

$$\beta_2 = \frac{1}{y_2}\,. \tag{1.82}$$

The cross section for the collinear region 6 takes the form

$$\begin{gathered}\frac{\mathrm{d}\sigma_{\text{coll}}^{(6)}}{\mathrm{d}y_1 \mathrm{d}c_- \mathrm{d}y_2} = \frac{\alpha^4}{4\pi s}\,\frac{1+c_-^2}{1-c_-} \times \\ \times \Big\{ (y_1^2 + (1-y_1)^2) \big(L + 2\ln\big(y_1(1-y_1)\big) \big) + 2y_1(1-y_1) \Big\} \times \\ \times \Big\{ (y_2^2 + (1-y_2)^2) \big(L + 2\ln\big(y_2(1-y_2)\big) \big) + 2y_2(1-y_2) \Big\}.\end{gathered} \tag{1.83}$$

The corresponding contribution to the experimentally observable cross section has the following form:

$$\Delta\sigma^{(6)} = N \int\limits_{y_{\text{th}}}^{1} \mathrm{d}y_1 \int\limits_{y_{\text{th}}}^{1} \mathrm{d}y_2 \int\limits_{-c_0}^{c_0} \mathrm{d}c_- \frac{\mathrm{d}\sigma_{\text{coll}}^{(6)}}{\mathrm{d}y_1 \mathrm{d}c_- \mathrm{d}y_2}\,, \qquad c_+ = -c_-. \tag{1.84}$$

The quantity N depends on a concrete experimental set-up. Namely, $N = 1/2$ when one requires registering two leptons with opposite charges going back-to-back. In a charge-blind set-up one would have $N = 1$.

Consider now two remaining collinear regions Fig. 1 ((7), (8)). They contain, as a hard block, the Compton scattering amplitude. Combining the expressions for the collinear factors for time-like and space-like photons one obtains

$$\Delta\sigma^{(7)} = \Delta\sigma^{(8)} = \int\limits_{y_{\rm th}}^{1} {\rm d}y_1 \int\limits_{-c_0}^{c_0} {\rm d}c_- \, \frac{\sigma^{(8)}}{{\rm d}y_1 {\rm d}c_-} \Theta(1-y_2)\Theta(y_2-y_{\rm th})\Theta(c_0^2-c_+^2),$$

$$\frac{\sigma^{(8)}}{{\rm d}y_1{\rm d}c_-} = \frac{\alpha^4}{2\pi s} \int\limits_{\beta_{1\rm min}}^{1} \frac{{\rm d}\beta_1}{\beta_1^2\beta_2^2(1+\beta_1+c_-(1-\beta_1))} \left(\frac{y_2(1-c_+)}{2} + \frac{2}{y_2(1-c_+)} \right) \times$$

$$\times \left\{ (1+(1-\beta_1)^2) \left(L + 2\ln\frac{1-\beta_1}{\beta_1} \right) - 2(1-\beta_1) \right\} \times$$

$$\times \left\{ (1+(\beta_2-1)^2) \left(L + 2\ln\left(y_2 \frac{(\beta_2-1)}{\beta_2} \right) \right) + 2(\beta_2-1) \right\}, \tag{1.85}$$

$$\beta_2 = \frac{2\beta_1}{y_1(1+\beta_1+(1-\beta_1)c_-)}\,, \quad y_2 = \frac{1+\beta_1^2+c_-(1-\beta_1^2)}{1+\beta_1+c_-(1-\beta_1)}\,,$$

$$c_+ = \frac{1}{y_2}[\beta_1 - 1 - \beta_2 y_1 c_-], \quad \beta_{1\rm min} = \frac{y_1(1+c_-)}{2-y_1(1-c_-)}\,.$$

1.2.3. Semicollinear Regions. The differential cross section of the pair production process in large angle Bhabha scattering (see Fig. 2) has the following form:

$$\begin{aligned}
\Delta\sigma_{\rm s\text{–}coll} &= 2\frac{\alpha}{2\pi}L \int\limits_0^{1-\beta_0} \frac{{\rm d}\beta(1+\beta^2)}{1-\beta} \Sigma_1(\Omega_1,\Omega_2,\Omega_+,\theta_0) \times \\
&\times \ {\rm d}\sigma(\gamma(p_1(1-\beta)) + e^+(p_2) \to e^+(p_+) + e^+(q_2) + e^-(q_1)) + \\
&+ \ \frac{\alpha}{2\pi}L \int\limits_1^{1/y} \frac{{\rm d}\beta}{\beta^2} (1+(\beta-1)^2) \Sigma_2(\Omega_1,\Omega_2,\theta_0) \times \\
&\times \ {\rm d}\sigma(e^-(p_1) + e^+(p_2) \to e^-(q_1) + e^+(q_2) + \gamma(\beta p_+)),
\end{aligned} \tag{1.86}$$

where we used the collinear factors considered above within the logarithmic accuracy, $y = p_+^0/\varepsilon$, and the hard cross sections [6] are

$$\begin{aligned}
\mathrm{d}\sigma^{\gamma(q)+e^+(p_2)\to e^+(p_+)+e^+(q_2)+e^-(q_1)} = \frac{(4\pi\alpha)^3}{16(2\pi)^5 2qp_2}\,\frac{1}{p_2p_+p_2q_2q_1q_2p_+q_1}\times\\
\times\left(p_2q_2q_1p_+((p_2q_2)^2+(q_1p_+)^2)+p_2p_+q_1q_2((q_1q_2)^2+(p_2p_+)^2)+\right.\\
\left.+\,p_2q_1q_2p_+((p_2q_1)^2+(q_2p_+)^2)\right)\times\\
\times\left(\frac{2p_2p_+}{p_2qp_+q}+\frac{2p_2q_2}{p_2qq_2q}+\frac{2q_1p_+}{q_1qp_+q}+\frac{2q_1q_2}{q_1qq_2q}-\frac{2p_2q_1}{p_2qq_1q}-\frac{2p_+q_2}{p_+qq_2q}\right)\times\\
\times\,\delta^4(q+p_2-p_+-q_1-q_2)\frac{\mathrm{d}^3q_1\mathrm{d}^3q_2\mathrm{d}^3p_+}{q_1^0q_2^0p_+^0}\,, \qquad (1.87)
\end{aligned}$$

$$\begin{aligned}
\mathrm{d}\sigma^{e^-(p_1)+e^+(p_2)\to e^-(q_1)+e^+(q_2)+\gamma(q)} = \frac{(4\pi\alpha)^3}{16(2\pi)^5 2p_1p_2}\,\frac{1}{p_1p_2q_1q_2p_1q_1p_2q_2}\times\\
\times\left(p_1p_2q_1q_2((p_1p_2)^2+(q_1q_2)^2)+p_1q_1p_2q_2((p_1q_1)^2+(p_2q_2)^2)+\right.\\
\left.+\,p_1q_2p_2q_1((p_1q_2)^2+(p_2q_1)^2)\right)\times\\
\times\left(\frac{2p_1p_2}{p_1qp_2q}+\frac{2q_1q_2}{q_1qq_2q}+\frac{2p_1q_1}{p_1qq_1q}+\frac{2p_2q_2}{p_2qq_2q}-\frac{2p_1q_2}{p_1qq_2q}-\frac{2p_2q_1}{p_2qq_1q}\right)\times\\
\times\,\delta^4(p_1+p_2-q-q_1-q_2)\frac{\mathrm{d}^3q_1\mathrm{d}^3q_2\mathrm{d}^3q}{q_1^0q_2^0q^0}\,. \qquad (1.88)
\end{aligned}$$

The quantity $1-\beta_0$ in Eq. (1.86) is the minimum energy fraction of the virtual photon in the pair creation process $\gamma^*\bar{e}\to e\bar{e}\bar{e}$ provided that fermions with momenta q_1 and q_2 are to be detected. Multipliers Σ_1 and Σ_2 provide the emission angles of every final state of a fermion with respect to the beam directions; also with respect to each other in order the angles to be larger than θ_0. Note that because of the integration over the phase space of the final particles the identity of two positrons is taken into account automatically. The numerical integration of $\Delta\sigma_{\text{s-coll}}$ (1.86) and different contributions to $\Delta\sigma_{\text{coll}}$ (see Eqs. (1.53), (1.58), (1.76), (1.84), (1.85)) will show that the total sum does not depend on the auxiliary parameter θ_0.

1.2.4. Conclusions. Above we've considered the process of an additional e^+e^--pair production in large angle Bhabha scattering. The differential cross sections within the logarithmic accuracy are obtained. They could be used in a wide range of experiments. Our approach gives analytical expressions for the leading and next-to-leading contributions. That provides a check of the theoretical accuracy within $0.1\,\%$.

Note that in the leading logarithmic approximation, i. e., for the terms of order $(\alpha L)^2$, the parton picture of the cross section is valid: that could be just seen from the above expressions for different collinear kinematics.

Radiative corrections to the considered process, i. e., terms of the order $(\alpha L)^3$ could be obtained using the renormalization group methods. But their contribution is beyond the required accuracy.

The process of the production of two different fermion-antifermion pairs in e^+e^- collisions is of interest for SM testing. As for the problem of the luminosity measurement, we suggest that the case of a heavy pair production could be detected experimentally.

1.3. Radiative Large Angle Bhabha Scattering in General Kinematics. In what follows we survey a process of radiative large angle electron-positron scattering. Two kinematical regimes are studied. The first one is in which a hard photon is emitted close to directions of motion of one of the charged leptons, i. e., initial or scattered electron/positron in c.m.s. [17]. Another one concerns essentially with the noncollinear kinematics when all the c.m.s. angles between initial or final particles are of order unity [16].

In both regimes we see some deviation from the Drell–Yan form for the cross section: contraction of hard subprocess in Born approximation with structure functions (fragmentation functions) of initial (scattered) leptons. This fact could presumably be attributed to the very $2 \to 3$ nature of hard subprocess.

Large angle Bhabha scattering (LABS) plays an important role in e^+e^- colliding beam physics [3]. First, it is traditionally used for calibration, because it has a large cross section and can be easily recognized. Second, it might provide essential background information in a study of quarkonia physics. The result obtained below can also be used to construct Monte Carlo event generators for Bhabha scattering processes.

In previous parts we considered the following contributions to the large angle Bhabha cross section: a pair production (virtual, soft and hard [14]) and two hard photons [13]. This chapter is devoted to the calculation of radiative corrections (RC) to a single hard-photon emission process. We consider the kinematics essentially of type $2 \to 3$, in which all possible scalar products of 4-momenta of external particles are large compared to the electron mass squared.

Considering virtual corrections, we identify gauge invariant sets of Feynman diagrams (FD). Loop corrections associated with emission and absorption of virtual photons by the same fermionic line are called as Glass-type (G) corrections. The case in which a loop involves exchange of two virtual photons between different fermionic lines is called Box-type (B) FD. The third class includes the vertex function and vacuum polarization contributions ($\Gamma\Pi$-type). We see explicitly that all terms that contain the square of large logarithms $\ln(s/m^2)$, as well as those that contain the infrared singularity parameter (fictitious photon mass λ),

cancel out in the total sum, where the emission of an additional soft photon is also considered.

We note here that part of the general result associated with scattering-type diagrams (see Fig. 4 ((1), (5))) was used to describe radiative deep inelastic scattering (DIS) with RC taken into account in Ref. 29 (we labeled it the Compton tensor with heavy photon). A similar set of FD can be used to describe the annihilation channel [14].

The problem of virtual RC calculations at the 1-loop level is cumbersome for the process

$$e^+(p_2) + e^-(p_1) \longrightarrow e^+(p_2') + e^-(p_1') + \gamma(k_1). \tag{1.89}$$

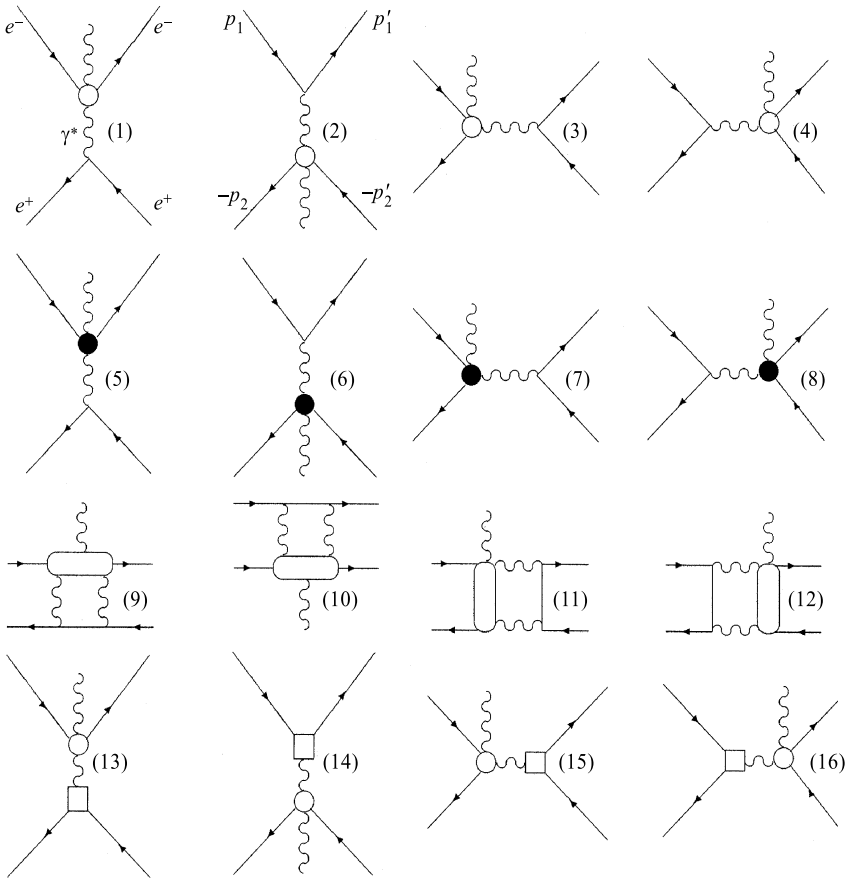

Fig. 4. G- and B-type Feynman diagrams for radiative Bhabha scattering

Specifically, if at the Born level we need to consider eight FD, then at the 1-loop level we have as many as 72. Furthermore, performing loop momentum integration, we introduce scalar, vector, and tensor integrals up to the third rank with 2, 3, 4, and 5 denominators (a set of relevant integrals is given in our preprint [30]). A high degree of topological symmetry of FD for a cross section can be exploited to calculate the matrix element squared. Using them, we can restrict ourselves to the consideration of interferences of the Born-level amplitudes (Fig. 4 ((1)–(4))) with those that contain 1-loop integrals (Fig. 4 ((5)–(16))). Our calculation is simplified since we omit the electron mass m in evaluating the corresponding traces due to the kinematic region under consideration:

$$
\begin{aligned}
&s \sim s_1 \sim -t_1 \sim -t \sim -u \sim -u_1 \sim \chi_{1,2} \sim \chi^{'}_{1,2} \gg m^2,\\
&s = 2p_1p_2, \quad t = -2p_2p_2', \quad u = -2p_1p_2', \quad s_1 = 2p_1'p_2',\\
&t_1 = -2p_1p_1', \quad u_1 = -2p_2p_1', \quad \chi_{1,2} = 2k_1p_{1,2}, \quad \chi'_{1,2} = 2k_1p'_{1,2},\\
&s + s_1 + t + t_1 + u + u_1 = 0, \quad s + t + u = \chi_1',\\
&s_1 + t + u_1 = -\chi_1, \quad t + \chi_1 = t_1 + \chi_1'.
\end{aligned}
\tag{1.90}
$$

We found that some kind of local factorization took place both for the G- and B-type FD: the leading logarithmic contribution to the matrix element squared, summed over spin states, arising from interference of one of the four FD at the Born level (Fig. 4 ((1)–(4))) with some 1-loop-corrected FD (Fig. 4 ((5)–(16))), turns out to be proportional to the interference of the corresponding amplitudes at the Born level. The latter has the form

$$
\begin{aligned}
E_0 &= (4\pi\alpha)^{-3}\sum|M_1|^2 = -\frac{16}{t^2}\,\frac{1}{4}\,\mathrm{Tr}\,(\hat{p}_1'O_{11'}\hat{p}_1\tilde{O}_{11'})\frac{1}{4}\,\mathrm{Tr}\,(\hat{p}_2\gamma_\sigma\hat{p}_2'\gamma_\rho) =\\
&= -\frac{16}{t\chi_1\chi_1'}(u^2+u_1^2+s^2+s_1^2),\\
O_0 &= (4\pi\alpha)^{-3}\sum M_1M_2^* = \frac{8}{tt_1}\left(\frac{s}{\chi_1\chi_2}+\frac{s_1}{\chi_1'\chi_2'}+\frac{u}{\chi_1\chi_2'}+\frac{u_1}{\chi_2\chi_1'}\right)\times\\
&\times\ (u^2+u_1^2+s^2+s_1^2),\\
I_0 &= (4\pi\alpha)^{-3}\sum M_1(M_3^*+M_4^*) = -(1+\hat{Z})\frac{4}{ts_1}\left\{-\frac{4u_1\chi_2'}{\chi_1}+\right.\\
&+\ \frac{4u(s_1+t_1)(s+t)}{\chi_2\chi_1'}-\frac{2}{\chi_1\chi_2}[2suu_1+(u+u_1)(uu_1+ss_1-tt_1)]+\\
&+\ \left.\frac{2}{\chi_1\chi_1'}[2t_1uu_1+(u+u_1)(uu_1+tt_1-ss_1)]\right\},\\
O_{11'} &= \gamma_\rho\frac{\hat{p}_1'+\hat{k}_1}{\chi_1'}\gamma_\mu-\gamma_\mu\frac{\hat{p}_1-\hat{k}_1}{\chi_1}\gamma_\rho, \quad \tilde{O}_{11'} = O_{11'}(\rho\leftrightarrow\mu),
\end{aligned}
\tag{1.91}
$$

where the $\hat{Z}$-operator acts as follows:

$$\hat{Z} = \left| \begin{array}{ll} p_1 \longleftrightarrow p_1' & s \longleftrightarrow s_1 \\ p_2 \longleftrightarrow p_2' & u \longleftrightarrow u_1 \\ k_1 \to -k_1 & t, t_1 \to t, t_1 \end{array} \right|.$$

It can be shown that the total matrix element squared, summed over spin states, can be obtained using symmetry properties realized by means of the permutation operations:

$$\begin{gathered} \sum |M|^2 = (4\pi\alpha)^3 F, \qquad F = (1 + \hat{P} + \hat{Q} + \hat{R})\Phi = \\ = 16\,\frac{ss_1(s^2+s_1^2) + tt_1(t^2+t_1^2) + uu_1(u^2+u_1^2)}{ss_1tt_1} \times \\ \times \left(\frac{s}{\chi_1\chi_2} + \frac{s_1}{\chi_1'\chi_2'} - \frac{t}{\chi_2\chi_2'} - \frac{t_1}{\chi_1\chi_1'} + \frac{u}{\chi_1\chi_2'} + \frac{u_1}{\chi_2\chi_1'} \right), \\ \Phi = E_0 + O_0 - I_0. \end{gathered} \tag{1.92}$$

The explicit form of the $\hat{P}, \hat{Q}, \hat{R}$ operators is

$$\begin{aligned} \hat{P} &= \left| \begin{array}{ll} p_1 \longleftrightarrow -p_2' & s \longleftrightarrow s_1 \\ p_2 \longleftrightarrow -p_1' & t \longleftrightarrow t_1 \\ k_1 \to k_1 & u, u_1 \to u, u_1 \end{array} \right|, \\ \hat{Q} &= \left| \begin{array}{cc} p_2 \longleftrightarrow -p_1' & s \longleftrightarrow t_1 \\ p_2' \to p_2' & s_1 \longleftrightarrow t \\ p_1, k_1 \to p_1, k_1 & u, u_1 \to u, u_1 \end{array} \right|, \\ \hat{R} &= \left| \begin{array}{cc} p_1 \longleftrightarrow -p_2' & s \longleftrightarrow t \\ p_1' \to p_1' & s_1 \longleftrightarrow t_1 \\ p_2, k_1 \to p_2, k_1 & u, u_1 \to u, u_1 \end{array} \right|. \end{aligned} \tag{1.93}$$

The differential cross section at the Born level in the case of large angle kinematics (1.90) was found in Ref. 6:

$$\mathrm{d}\sigma_0(p_1, p_2) = \frac{\alpha^3}{32s\pi^2} F \frac{\mathrm{d}^3p_1'\mathrm{d}^3p_2'\mathrm{d}^3k_1}{\varepsilon_1'\varepsilon_2'\omega_1} \delta^{(4)}(p_1 + p_2 - p_1' - p_2' - k_1), \tag{1.94}$$

where ε_1, ε_2, and ω_1 are the energies of the outgoing fermions and photon, respectively. The collinear kinematic regions (real photon emitted in the direction of one of the charged particles) corresponding to the case in which one of the invariants χ_i, χ_i' is of order m^2 yields the main contribution to the total cross section. These require separate investigation, and will be considered elsewhere.

Here's a brief outline of what's going to be presented. In Sect. 1.3.1 we consider the contribution due to the set of FD (Fig. 4 ((5)–(8))) called *glasses*

here (G-type diagrams). Using crossing symmetry, we construct the whole G-type contribution from the gauge-invariant set of FD in Fig. 4 (5). Moreover, only the set of FD depicted in Fig. 5 (*d*) can be considered in practical calculations, due to an additional mirror symmetry in the diagrams of Fig. 5 (*d, e*). We therefore start by checking the gauge invariance of the Compton tensor described by the FD of Fig. 5 (*d, e*) for all fermions and one of the photons on the mass shell. In Sect. 1.3.2 we consider the contribution of amplitudes containing vertex functions and the virtual photon polarization operator shown in Fig. 4 ((13)–(15)) and Fig. 5 (*f, d*). In Sect. 1.3.3 we take into account the contribution of FD with virtual two–photon exchange, shown in Fig. 4 ((9)–(12)), called *boxes* here (B-type diagrams). Again, using the crossing symmetry of FD, we show how to use only the FD of Fig. 4 (9) in calculations. We show that the terms containing infrared singularities, as well as those containing large logarithms, can be written in simple form, related to certain contributions to the radiative Bhabha cross section in the Born approximation (1.91). We also control terms in the matrix element squared that do not contain large logarithms and are infrared-finite. Thus our considerations permit us to calculate the cross section in the kinematic region (1.90), in principle, to power-law accuracy, i. e., neglecting terms that are

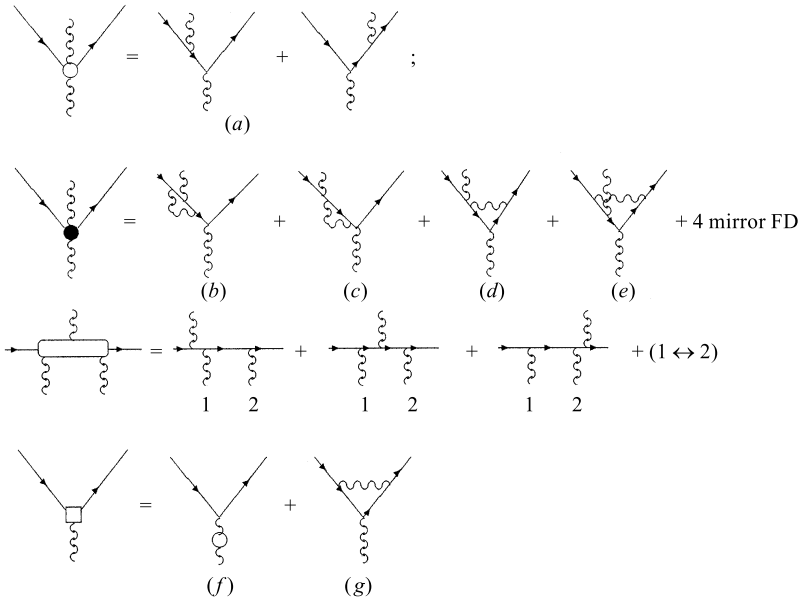

Fig. 5. Deciphering of the notations used in Fig. 4

$$\mathcal{O}\left(\frac{\alpha}{\pi}\frac{m^2}{s}L_s^2\right), \tag{1.95}$$

as compared to $\mathcal{O}(1)$ terms presented in this chapter. Note that the terms in (1.95) are less than 10^{-4} for typical moderately high energy colliders (DAΦNE, VEPP-2M, BEPS). Unfortunately, the nonleading terms are too complicated to be presented analytically, so we have estimated them numerically. In Sect. 1.3.4 we consider emission of an additional soft photon in our radiative Bhabha process. To conclude, we note that the expression for the total correction, taking into account virtual and real soft photon emission in the leading logarithmic approximation, has a very elegant and handy form, although it differs from what one might expect in the approach based on renormalization group ideas. Besides analytic expressions, we also give numerical values, along with the nonleading terms for a few points under typical experimental conditions.

1.3.1. Contribution of G-Type Diagrams. We begin by explicitly checking the gauge invariance of the tensor

$$\bar{u}(p_1^{'})R_{1,1'}^{\sigma\mu}u(p_1). \tag{1.96}$$

This was done indirectly in Ref. 29, where the Compton tensor for a heavy photon was written in terms of explicitly gauge invariant tensor structures. We use the expression

$$R_{1,1'}^{\sigma\mu} = R^{\chi_1} + R^{\chi_1^{'}}, \tag{1.97}$$

$$\begin{aligned} R^{\chi_1} &= A_2\gamma_\sigma\hat{k}_1\gamma_\mu + \int\frac{\mathrm{d}^4k}{\mathrm{i}\pi^2}\left\{\frac{\gamma_\lambda(\hat{p}_1^{'}-\hat{k})\gamma_\sigma(\hat{p}_1-\hat{k}_1-\hat{k})\gamma_\lambda(\hat{p}_1-\hat{k}_1)\gamma_\mu}{-\chi_1(0)(2)(q)}+\right. \\ &+ \left.\frac{\gamma_\lambda(\hat{p}_1^{'}-\hat{k})\gamma_\sigma(\hat{p}_1-\hat{k}_1-\hat{k})\gamma_\mu(\hat{p}_1-\hat{k})\gamma_\lambda}{(0)(1)(2)(q)}\right\}, \end{aligned} \tag{1.98}$$

where

$$\begin{gathered}(0)=k^2-\lambda^2,\quad (2)=(p_1^{'}-k)^2-m^2,\quad (1)=(p_1-k)^2-m^2,\\ (q)=(p_1-k_1-k)^2-m^2,\quad A_2=\frac{2}{\chi_1}\left(L_{\chi_1}-\frac{1}{2}\right),\quad L_{\chi_1}=\ln\frac{\chi_1}{m^2}.\end{gathered}$$

The quantity R^{χ_1} corresponds to the FD depicted in Fig. 5 (*d*), while $R^{\chi_1'}$ corresponds to the FD in Fig. 5 (*e*). The first term on the right-hand side of Eq. (1.98) corresponds to the first two FD of Fig. 5 (*d*) under conditions (1.90).

The gauge invariance condition $R^{\sigma\mu}_{1,1'}k_\mu = 0$ is clearly satisfied. The gauge invariance condition regarding the heavy photon Lorentz index provides some check of the loop momentum integrals, which can be found in Ref. 30:

$$\bar{u}(p_1')R^{\sigma\mu}_{1,1'}u(p_1)q_\sigma e_\mu(k_1) = Ak_1^\mu e_\mu(k_1), \qquad A = -2\frac{L_{\chi_1}-2}{\chi_1} - 6\frac{L_{\chi_1'}-1}{\chi_1'}. \tag{1.99}$$

The gauge invariance thus satisfied due to the Lorentz condition for the on-shell photon, $e(k_1)k_1 = 0$.

As stated above, the use of crossing symmetries of amplitudes permits us to consider only R^{χ_1}. For interference of amplitudes at the Born level (see Fig. 4 ((1)–(4)) and Fig. 4 ((5)–(8))), we obtain in terms of the replacement operators

$$(\Delta|M|^2)_G = 2^5\alpha^4\pi^2(1+\hat{P}+\hat{Q}+\hat{R})(1+\hat{Z})[E_{15}^{\chi_1}+O_{25}^{\chi_1}-I_{35}^{\chi_1}-I_{45}^{\chi_1}], \tag{1.100}$$

with

$$\begin{aligned}
E_{15}^{\chi_1} &= \frac{16}{t^2}\,\frac{1}{4}\,\mathrm{Tr}(\hat{p}_1' R^{\chi_1}\hat{p}_1 O_{11'})\frac{1}{4}\,\mathrm{Tr}\,(\hat{p}_2\gamma_\rho\hat{p}_2'\gamma_\sigma),\\
O_{25}^{\chi_1} &= \frac{16}{tt_1}\,\frac{1}{4}\,\mathrm{Tr}\,(\hat{p}_1' R^{\chi_1}\hat{p}_1\gamma_\rho)\frac{1}{4}\,\mathrm{Tr}\,(\hat{p}_2\gamma_\sigma\hat{p}_2' O_{22'}),\\
I_{35}^{\chi_1} &= \frac{4}{ts_1}\,\frac{1}{4}\,\mathrm{Tr}\,(\hat{p}_1' R^{\chi_1}\hat{p}_1 O_{12}\hat{p}_2\gamma_\sigma\hat{p}_2'\gamma_\rho),\\
I_{45}^{\chi_1} &= \frac{4}{ts}\,\frac{1}{4}\,\mathrm{Tr}\,(\hat{p}_1' R^{\chi_1}\hat{p}_1\gamma_\rho\hat{p}_2\gamma_\sigma\hat{p}_2' O_{1'2'}),\\
O_{11'} &= \gamma_\rho\frac{\hat{p}_1'+\hat{k}_1}{\chi_1'}\gamma_\mu - \gamma_\mu\frac{\hat{p}_1-\hat{k}_1}{\chi_1}\gamma_\rho,\\
O_{22'} &= \gamma_\mu\frac{-\hat{p}_2'-\hat{k}_1}{\chi_2'}\gamma_\rho - \gamma_\rho\frac{-\hat{p}_2+\hat{k}_1}{\chi_2}\gamma_\mu,\\
O_{12} &= -\gamma_\mu\frac{\hat{p}_1-\hat{k}_1}{\chi_1}\gamma_\rho - \gamma_\rho\frac{-\hat{p}_2+\hat{k}_1}{\chi_2}\gamma_\mu,\\
O_{1'2'} &= \gamma_\rho\frac{\hat{p}_1'+\hat{k}_1}{\chi_1'}\gamma_\mu + \gamma_\mu\frac{-\hat{p}_2'-\hat{k}_1}{\chi_2'}\gamma_\rho.
\end{aligned} \tag{1.101}$$

In the logarithmic approximation, the G-type amplitude contribution to the cross section has the form

$$\begin{aligned}
&\mathrm{d}\sigma_{\mathrm{G}} = \frac{\mathrm{d}\sigma_0}{F}\,\frac{\alpha}{\pi}(1+\hat{P}+\hat{Q}+\hat{R})\Phi\left[-\frac{1}{2}L_{t_1}^2+\frac{3}{2}L_{t_1}+2L_{t_1}\ln\frac{\lambda}{m}\right],\\
&L_{t_1} = \ln\frac{-t_1}{m^2}.
\end{aligned} \tag{1.102}$$

1.3.2. Vacuum Polarization and Vertex Insertion Contributions. Let us examine a set of ΓΠ-type FD. The contribution of the Dirac form factor of fermions and vacuum polarization can be parametrized as $(1+\Gamma_t)/(1-\Pi_t)$, while the contribution of the Pauli form factor is proportional to the fermion mass, and is omitted here. We obtain

$$\mathrm{d}\sigma_{\Gamma\Pi} = \frac{\mathrm{d}\sigma_0}{F}\,\frac{\alpha}{\pi} 2(1+\hat{P}+\hat{Q}+\hat{R})(\Gamma_t+\Pi_t)\Phi, \tag{1.103}$$

where

$$\begin{aligned} \Gamma_t &= \frac{\alpha}{\pi}\left\{\left(\ln\frac{m}{\lambda}-1\right)(1-L_t)-\frac{1}{4}L_t-\frac{1}{4}L_t^2+\frac{1}{2}\zeta_2\right\}, \\ \Pi_t &= \frac{\alpha}{\pi}\left(\frac{1}{3}L_t-\frac{5}{9}\right), \quad L_t=\ln\frac{-t}{m^2}. \end{aligned} \tag{1.104}$$

In realistic calculations, the vacuum polarization due to hadrons and muons can be taken into account in a very simple fashion [12], just by adding it to Π_t.

1.3.3. Contribution of B-Type Diagrams. A procedure resembling the one used in the previous section, applied to the B-type set of FD (Fig. 4 ((9)–(12))), enables us to use only certain 1-loop diagrams in practical calculations, specifically three of those in the scattering channel with uncrossed exchanged photon legs:

$$\begin{aligned} (\Delta|M|^2)_B &= 2^5\alpha^4\pi^2\,\mathrm{Re}\,(1+\hat{P}+\hat{Q}+\hat{R})\times \\ &\times\ [(1-\hat{P}_{22'})I_{19}^{\chi_1}+(1+\hat{P}_{22'})I_{29}^{\chi_1}-I], \end{aligned} \tag{1.105}$$

where

$$\hat{P}_{22'} = \left|\begin{array}{cc} p_2\longleftrightarrow -p_2' & s\longleftrightarrow u \\ p_1\longleftrightarrow p_1 & s_1\longleftrightarrow u_1 \\ p_1', k_1\to p_1', k_1 & t, t_1\to t, t_1 \end{array}\right|, \tag{1.106}$$

and

$$\begin{aligned} I_{19}^{\chi_1} &= \int\frac{\mathrm{d}^4k}{\mathrm{i}\pi^2}\frac{1}{(0)(q)((p_2+k)^2-m^2)}\frac{16}{t}\,\frac{1}{4}\mathrm{Tr}\,(\hat{p}_1'B^{\chi_1}\hat{p}_1O_{11'})\times \\ &\times\ \frac{1}{4}\mathrm{Tr}\,(\hat{p}_2\gamma_\sigma(-\hat{p}_2-\hat{k})\gamma_\lambda\hat{p}_2'\gamma_\rho), \\ I_{29}^{\chi_1} &= \int\frac{\mathrm{d}^4k}{\mathrm{i}\pi^2}\frac{1}{(0)(q)((p_2+k)^2-m^2)}\frac{16}{t_1}\,\frac{1}{4}\mathrm{Tr}\,(\hat{p}_1'B^{\chi_1}\hat{p}_1\gamma_\rho)\times \\ &\times\ \frac{1}{4}\mathrm{Tr}\,(\hat{p}_2\gamma_\sigma(-\hat{p}_2-\hat{k})\gamma_\lambda\hat{p}_2'O_{22'}), \end{aligned} \tag{1.107}$$

$$
\begin{aligned}
I &= \int \frac{\mathrm{d}^4k}{\mathrm{i}\pi^2}\frac{1}{(0)(q)}\biggl\{\frac{4}{s_1}\frac{1}{4}\mathrm{Tr}\,(\hat{p}_2'\gamma_\rho\hat{p}_1'B^{\chi_1}\hat{p}_1O^{12}\hat{p}_2(\hat{A}+\hat{B}))+\\
&+ \frac{4}{s_1}\frac{1}{4}\mathrm{Tr}\,(\hat{p}_2'O_{1'2'}\hat{p}_1B^{\chi_1}\hat{p}_1\gamma_\rho\hat{p}_2(\hat{A}+\hat{B}))\biggr\},\\
&\hat{A}=\frac{\gamma_\sigma(-\hat{p}_2-\hat{k})\gamma_\lambda}{(p_2+k)^2-m^2}, \quad \hat{B}=\frac{\gamma_\lambda(-\hat{p}_2'+\hat{k})\gamma_\sigma}{(-p_2'+k)^2-m^2}.
\end{aligned}
$$

Here

$$
\begin{aligned}
B^{\chi_1} &= \frac{\gamma_\lambda(\hat{p}_1-\hat{k}_1-\hat{k})\gamma_\sigma(\hat{p}_1-\hat{k}_1)\gamma_\mu}{-\chi_1(d)}+\frac{\gamma_\lambda(\hat{p}_1-\hat{k}_1-\hat{k})\gamma_\mu(\hat{p}_1-\hat{k})\gamma_\sigma}{(d)(1)}+\\
&+ \frac{\gamma_\mu(\hat{p}_1'+\hat{k}_1)\gamma_\lambda(\hat{p}_1-\hat{k})\gamma_\sigma}{\chi_1'(1)}, \quad (q)=(p_2-p_2'+k)^2-\lambda^2, \qquad (1.108)\\
(d) &= (p_1-k_1-k)^2-m^2, \quad (1)=(p_1-k)^2-m^2, \quad (0)=k^2-\lambda^2.
\end{aligned}
$$

Analytic evaluations divulge a lack of both double logarithmic ($\sim L_s^2$) and infrared logarithmic ($\sim \ln(\lambda/m)L$) terms in the box contribution.

In spite of the explicit proportionality of the individual contributions to the structures E_0, O_0, and I_0, the overall expression turns out to be somewhat convoluted, despite its having a factorized form in each gauge-invariant subset of diagrams. We parametrize the correction coming from the B-type FD as follows:

$$
\mathrm{d}\sigma_B=\mathrm{d}\sigma_0\frac{\alpha}{\pi}L_s\Delta_B, \qquad \Delta_B=2\ln\frac{ss_1}{uu_1}+\frac{2}{F}(\Phi_Q+\Phi_R)\ln\frac{tt_1}{ss_1}. \quad (1.109)
$$

The total virtual correction to the cross section has the form

$$
\begin{aligned}
\mathrm{d}\sigma^{\mathrm{virt}} &= \mathrm{d}\sigma_G+\mathrm{d}\sigma_{\Gamma\Pi}+\mathrm{d}\sigma_B=\\
=\frac{\alpha}{\pi}\biggl[-L_s^2 &+ L_s\biggl(\frac{11}{3}+4\ln\frac{\lambda}{m}+\Delta_G+\Delta_{\Gamma\Pi}+\Delta_B\biggr)+\mathcal{O}(1)\biggr], \quad (1.110)\\
\Delta_G+\Delta_{\Gamma\Pi} &= \frac{1}{F}\biggl(\Phi\ln\frac{s^2}{tt_1}+\Phi_R\ln\frac{t^2}{ss_1}+\Phi_Q\ln\frac{t_1^2}{ss_1}+\Phi_P\ln\frac{s_1^2}{tt_1}\biggr),
\end{aligned}
$$

where $\Phi_P=\hat{P}\Phi$, $\Phi_Q=\hat{Q}\Phi$, and $\Phi_R=\hat{R}\Phi$.

1.3.4. Contribution from Additional Soft Photon Emission. Consider now radiative Bhabha scattering accompanied by emission of an additional soft photon in the centre-of-mass reference frame. By *soft* we mean that its energy does not exceed some small quantity $\Delta\varepsilon$, compared to the energy ε of the initial beams. The corresponding cross section has the form

$$
\begin{aligned}
&\mathrm{d}\sigma^{\mathrm{soft}}=\mathrm{d}\sigma_0\delta^{\mathrm{soft}},\\
&\delta^{\mathrm{soft}}=-\frac{4\pi\alpha}{16\pi^3}\int\frac{\mathrm{d}^3k_2}{\omega_2}\biggl(-\frac{p_1}{p_1k_2}+\frac{p_1'}{p_1'k_2}+\frac{p_2}{p_2k_2}-\frac{p_2'}{p_2'k_2}\biggr)^2\biggr|_{\omega_2<\Delta\varepsilon}. \qquad (1.111)
\end{aligned}
$$

The soft photon energy does not exceed $\Delta\varepsilon \ll \varepsilon_1 = \varepsilon_2 \equiv \varepsilon \sim \varepsilon_1^{'} \sim \varepsilon_2^{'}$. In order to calculate the right-hand side of Eq. (1.111), we use the master equation [31]:

$$
\begin{aligned}
&-\frac{4\pi\alpha}{16\pi^3}\int\frac{\mathrm{d}^3k}{\omega}\frac{(q_i)^2}{(q_ik)^2}\bigg|_{\omega<\Delta\varepsilon} = -\frac{\alpha}{\pi}\ln\left(\frac{\Delta\varepsilon m}{\lambda\varepsilon_i}\right), \quad \omega=\sqrt{k^2+\lambda^2}\,,\\
&\frac{4\pi\alpha}{16\pi^3}\int\frac{\mathrm{d}^3k}{\omega}\frac{2q_1q_2}{(kq_1)(kq_2)}\bigg|_{\omega<\Delta\varepsilon} = \frac{\alpha}{\pi}\left[L_q\ln\left(\frac{m^2(\Delta\varepsilon)^2}{\lambda^2\varepsilon_1\varepsilon_2}\right)+\frac{1}{2}L_q^2-\right.\\
&\qquad\left.-\frac{1}{2}\ln^2\left(\frac{\varepsilon_1}{\varepsilon_2}\right)-\frac{\pi^2}{3}+\mathrm{Li}_2\left(\cos^2\frac{\theta}{2}\right)\right].
\end{aligned}
\tag{1.112}
$$

Here we used the notation

$$
\begin{aligned}
&L_q=\ln\frac{-q^2}{m^2}\,, \quad q_1^2=q_2^2=m^2, \quad -q^2=-(q_1-q_2)^2\gg m^2,\\
&q_{1,2}=(\varepsilon_{1,2},\mathbf{q}_{1,2}), \qquad \theta=\widehat{\mathbf{q}_1\mathbf{q}_2},
\end{aligned}
\tag{1.113}
$$

where ε_1, ε_2, and θ are the energies and angle between the 3-momenta $\mathbf{q}_1, \mathbf{q}_2$, respectively; and λ is the fictitious photon mass (all defined in the centre-of-mass system).

The contributions of each possible term on rhs of Eq. (1.111) are

$$
\begin{aligned}
&\frac{\pi}{\alpha}\delta^{\mathrm{soft}} = -\Delta_1-\Delta_2-\Delta_1'-\Delta_2'+\Delta_{12}+\Delta_{1'2'}+\Delta_{11'}+\Delta_{22'}-\Delta_{12'}-\Delta_{1'2},\\
&\Delta_1=\Delta_2=\ln\frac{m\Delta\varepsilon}{\varepsilon\lambda}, \quad \Delta_1'=\ln\frac{m\Delta\varepsilon}{\varepsilon_1^{'}\lambda}, \quad \Delta_2'=\ln\frac{m\Delta\varepsilon}{\varepsilon_2^{'}\lambda},\\
&\Delta_{12}=2L_s\ln\frac{m\Delta\varepsilon}{\varepsilon\lambda}+\frac{1}{2}L_s^2-\frac{\pi^2}{3},\\
&\Delta_{1'2'}=L_{s_1}\ln\left(\frac{(m\Delta\varepsilon)^2}{\varepsilon_1^{'}\varepsilon_2^{'}\lambda^2}\right)+\frac{1}{2}L_{s_1}^2-\frac{1}{2}\ln^2\left(\frac{\varepsilon_1^{'}}{\varepsilon_2^{'}}\right)-\frac{\pi^2}{3}+\mathrm{Li}_2\left(\cos^2\frac{\theta_{1'2'}}{2}\right),\\
&\Delta_{11'}=L_{t_1}\ln\left(\frac{(m\Delta\varepsilon)^2}{\varepsilon_1^{'}\varepsilon\lambda^2}\right)+\frac{1}{2}L_{t_1}^2-\frac{1}{2}\ln^2\left(\frac{\varepsilon_1^{'}}{\varepsilon}\right)-\frac{\pi^2}{3}+\mathrm{Li}_2\left(\cos^2\frac{\theta_{1'}}{2}\right),\\
&\Delta_{22'}=L_t\ln\left(\frac{(m\Delta\varepsilon)^2}{\varepsilon\varepsilon_2^{'}\lambda^2}\right)+\frac{1}{2}L_t^2-\frac{1}{2}\ln^2\left(\frac{\varepsilon_2^{'}}{\varepsilon}\right)-\frac{\pi^2}{3}+\mathrm{Li}_2\left(\sin^2\frac{\theta_{2'}}{2}\right),\\
&\Delta_{1'2}=L_{u_1}\ln\left(\frac{(m\Delta\varepsilon)^2}{\varepsilon\varepsilon_1^{'}\lambda^2}\right)+\frac{1}{2}L_{u_1}^2-\frac{1}{2}\ln^2\left(\frac{\varepsilon_1^{'}}{\varepsilon}\right)-\frac{\pi^2}{3}+\mathrm{Li}_2\left(\sin^2\frac{\theta_{1'}}{2}\right),\\
&\Delta_{12'}=L_u\ln\left(\frac{(m\Delta\varepsilon)^2}{\varepsilon\varepsilon_2^{'}\lambda^2}\right)+\frac{1}{2}L_u^2-\frac{1}{2}\ln^2\left(\frac{\varepsilon}{\varepsilon_2^{'}}\right)-\frac{\pi^2}{3}+\mathrm{Li}_2\left(\cos^2\frac{\theta_{2'}}{2}\right),
\end{aligned}
\tag{1.114}
$$

$$L_u = \ln\frac{-u}{m^2}\,, \quad L_{u_1} = \ln\frac{-u_1}{m^2}\,, \quad \mathrm{Li}_2(z) \equiv -\int\limits_0^z \frac{\mathrm{d}x}{x}\ln(1-x),$$

where $\varepsilon_1^{'}, \varepsilon_2^{'}$ are the centre-of-mass energies of the scattered electron and positron, respectively; $\theta_{1'}, \theta_{2'}$ are their scattering angles (measured from the initial electron momentum direction); and $\theta_{1'2'}$ is the angle between the scattered electron and positron momenta.

Separating out large logarithms, we obtain

$$\delta^{\mathrm{soft}} = \frac{\alpha}{\pi}\left\{4(L_s-1)\ln\frac{m\Delta\varepsilon}{\lambda\varepsilon} + L_s^2 + L_s\ln\frac{tt_1}{uu_1} + L_s\ln\frac{1-c_{1'2'}}{2} + \mathcal{O}(1)\right\},$$
$$c_{1'2'} = \cos\theta_{1'2'}. \tag{1.115}$$

This can be written in another form, using experimentally measurable quantities, the relative energies of the scattered leptons and the scattering angles:

$$\begin{aligned} y_i &= \frac{\varepsilon_i'}{\varepsilon}\,, \quad c_i = \cos\theta_i'\,, \quad \frac{1}{2}(1-c_{1'2'}) = \frac{y_1+y_2-1}{y_1y_2}\,, \\ -\frac{t}{s} &= y_2\frac{1+c_2}{2}\,, \ -\frac{u}{s} = y_2\frac{1-c_2}{2}\,, \ -\frac{t_1}{s} = y_1\frac{1-c_1}{2}\,, \\ \frac{s_1}{s} &= y_1+y_2-1\,, \ -\frac{u_1}{s} = y_1\frac{1+c_1}{2}. \end{aligned} \tag{1.116}$$

1.3.5. Conclusions. The double logarithmic terms of type L_s^2 and those proportional to $L_s\ln(\lambda/m)$ cancel in the overall sum with the corresponding terms from the soft photon contribution (1.115). Omitting vacuum polarization, we obtain in the logarithmic approximation

$$\begin{aligned} \mathrm{d}\sigma^{\mathrm{soft+virt}} &= \mathrm{d}\sigma_0\frac{\alpha}{\pi}\left[L_s\left(4\ln\frac{\Delta\varepsilon}{\varepsilon} + \Delta_L\right) + \Delta(y_1,y_2,c_1,c_2)\right], \\ \Delta_L &= 3 + \ln\frac{(1-c_1)(1-c_2)}{(1+c_1)(1+c_2)} + \ln\frac{y_1+y_2-1}{y_1y_2} + \\ &+ \frac{1}{F}\left[\Phi\ln\frac{s^2}{tt_1} + \Phi_P\ln\frac{s_1^2}{tt_1} + \Phi_Q\ln\frac{t_1^2}{ss_1} + \Phi_R\ln\frac{t^2}{ss_1}\right] + \\ &+ 2\ln\frac{ss_1}{uu_1} + \frac{2}{F}(\Phi_Q+\Phi_R)\ln\frac{tt_1}{ss_1}. \end{aligned} \tag{1.117}$$

The function $\Delta(y_1,y_2,c_1,c_2)$ is quite complicated. To compare it with Δ_L, we give their numerical values (omitting vacuum polarization) for a certain set of points from physical regions (1.118) and $y_1+y_2>1$, $D>0$ (see Table 2). Considering the kinematics typical of large angle inelastic Bhabha scattering, we

Table 2. **Numeric estimates of Δ_L and Δ versus y_1, y_2, c_1, c_2**

No.	y_1	y_2	c_1	c_2	Δ_L	Δ
1	0.36	0.89	−0.70	−0.10	10.70	−24.53
2	0.59	0.66	0.29	−0.06	4.86	−11.41
3	0.67	0.67	0.50	0.30	5.82	−35.58
4	0.68	0.65	0.60	−0.50	4.10	−10.45

show the lowest-order contribution previously obtained [32] and the radiative corrections calculated in this work.

After performing loop integration and shifting logarithms ($L_i = L_s + L_{is}$), one can see that the terms containing infrared singularities and double logarithmic terms $\sim L_s^2$, are associated with a factor equal to the corresponding Born contribution. This is true of all types of contributions.

The phase volume

$$\mathrm{d}\Gamma = \frac{\mathrm{d}^3p_1'\mathrm{d}^3p_2'\mathrm{d}^3k_1}{\varepsilon_1'\varepsilon_2'\omega_1}\delta^{(4)}(p_1+p_2-p_1'-p_2'-k_1)$$

can be transformed in various ways [32]. We introduce the variables (see Eq. (1.116))

$$y_i = \frac{\varepsilon_i'}{\varepsilon}, \quad c_i = \cos\theta_i', \quad \theta_i' = \widehat{\mathbf{p}_1, \mathbf{p}_i}', \quad 0 < y_i < 1, \quad -1 < c_{1,2} < 1, \quad (1.118)$$

which parametrize the kinematics of the outgoing particles (these do not include a common degree of freedom, a rotation about the beam axis). The phase volume then takes the form

$$\begin{aligned}
&\mathrm{d}\Gamma = \frac{\pi s\mathrm{d}y_1\mathrm{d}y_2\mathrm{d}c_1\mathrm{d}c_2}{2\sqrt{D(y_1,y_2,c_1,c_2)}}\Theta(y_1+y_2-1)\Theta(D(y_1,y_2,c_1,c_2)),\\
&D(y_1,y_2,c_1,c_2) = \rho^2 - c_1^2 - c_2^2 - 2c_{1'2'}c_1c_2, \qquad (1.119)\\
&\rho^2 = 2(1-c_{1'2'})\frac{(1-y_1)(1-y_2)}{y_1y_2}.
\end{aligned}$$

The allowed region of integration is a triangle in the y_1, y_2 plane and the interior of the ellipse $D > 0$ in the c_1, c_2 plane.

We now discuss the relation of our result to the renormalization group approach. The dependence on $\Delta\varepsilon/\varepsilon$ in (1.117) disappears when one takes into account hard two-photon emission. The leading contribution arises from the kinematics when the second hard photon is emitted close to the direction of

motion of one of the incoming or outgoing particles:

$$\begin{aligned}
\mathrm{d}\sigma^{\mathrm{hard}} &= \frac{\alpha}{2\pi}L_s\left[\frac{1+z^2}{1-z}\left(\mathrm{d}\sigma_0(zp_1,p_2,p_1',p_2')+\mathrm{d}\sigma_0(p_1,zp_2,p_1',p_2')\right)\mathrm{d}z+\right.\\
&+ \left.\frac{1+z_1^2}{1-z_1}\mathrm{d}\sigma_0\left(p_1,p_2,\frac{p_1'}{z_1},p_2'\right)\mathrm{d}z_1+\frac{1+z_2^2}{1-z_2}\mathrm{d}\sigma_0\left(p_1,p_2,p_1',\frac{p_2'}{z_2}\right)\mathrm{d}z_2\right],\\
&\quad z=1-x_2,\quad z_i=\frac{y_i}{y_i+x_2},\quad x_2=\frac{\omega_2}{\varepsilon}. \qquad (1.120)
\end{aligned}$$

The fractional energy of the additional photon varies within the limits $\Delta\varepsilon/\varepsilon < x_2 = \omega_2/\varepsilon < 1$. This formula agrees with the Drell–Yan form of radiative Bhabha scattering (with switched-off vacuum polarization)

$$\begin{aligned}
\mathrm{d}\sigma(p_1,p_2,p_1',p_2') &= \int \mathrm{d}x_1\,\mathrm{d}x_2\,\mathcal{D}(x_1)\mathcal{D}(x_2)\,\mathrm{d}\sigma_0\left(x_1p_1,x_2p_2,\frac{p_1'}{z_1},\frac{p_2'}{z_2}\right)\times\\
&\times\ \mathcal{D}(z_1)\mathcal{D}(z_2)\mathrm{d}z_1\mathrm{d}z_2, \qquad (1.121)
\end{aligned}$$

where the nonsinglet structure functions $\mathcal{D}$ are [33]

$$\begin{aligned}
\mathcal{D}(z) &= \delta(1-z)+\frac{\alpha}{2\pi}L\mathcal{P}^{(1)}(z)+\left(\frac{\alpha}{2\pi}L\right)^2\frac{1}{2!}\mathcal{P}^{(2)}(z)+\ldots,\\
\mathcal{P}^{(1)}(z) &= \lim_{\Delta\to 0}\left[\frac{1+z^2}{1-z}\Theta(1-z-\Delta)+\delta(1-z)\left(2\ln\Delta+\frac{3}{2}\right)\right]. \qquad (1.122)
\end{aligned}$$

In our calculations we see explicitly a factorization of the terms containing double logarithmic contributions and infrared single logarithmic ones, which arise from G- and $\Gamma\Pi$-type FD. To be precise, the corresponding contributions to the cross section have the structure of the Born cross section (1.94). But the above claim fails to be true for terms containing single logarithms. Hence, the Drell–Yan form (1.121) is not valid in this case, and the factorization theorem breaks down, because the mass singularities (large logarithms) do not factorize before the Born structure. That is because of plenty of different type amplitudes and kinematic variables, which describe our process. The reason for the violation of a naive usage of factorization in the Drell–Yan form has presumably the same origin with that found in Ref. 34, where the authors claimed that it is necessary to study independently the renormalization group behavior of leading logarithms before different amplitudes of the same process. Note that in the $e\mu \to e\mu\gamma$ reaction, which can easily be extracted from our results, factorization does take place. We also see from (1.117) that factorization will take place if all the logarithmic terms become equal, i. e., $\ln(s_1/m^2) = \ln(s/m^2) = \ldots$. The source for the violation of the factorization theorem, we found, might have a relation to some of those found in other problems [35].

Numerical estimates (see Table 2) for the Φ factory energy range ($\sqrt{s} \simeq 1$ GeV) show that the contribution of the nonleading terms coming from virtual and soft real photon emission might reach $35\,\%$. Additional hard photon emission will also contribute to Δ_L and Δ. To get an explicit form of that correction, one has to take into account a definite experimental set-up.

Obviously, an analogous phenomenon of the factorization theorem violation takes place in QCD in the processes like $q\bar{q} \to q\bar{q}g$ and $q\bar{q} \to q\bar{q}\gamma$. A consistent investigation of the latter processes, taking into account the phenomenon found, can give a certain correction to predictions for large angle jet production and direct hard photon emission at proton-antiproton colliders.

1.4. Radiative Large Angle Bhabha Scattering in Collinear Kinematics. Here we are going to consider the complementary specific kinematics, in which the photon moves within a narrow cone of small opening angle $\theta_0 \ll 1$ together with one of the incoming or outgoing charged particles. Thus, the result obtained here may be used in experiments with the tagging of scattered electron (positron) in detectors of small aperture $\theta_0 \ll 1$.

This part is organized as follows. In Sect. 1.4.1 the Born level cross section of radiative Bhabha scattering is revised in the collinear kinematics of photon emission along initial (scattered) electron. We introduce here the physical gauge of real photon that is extensively used in the next sections. In Sect. 1.4.2 a set of crossing transformations which enables us to consider in some detail only the scattering type amplitudes of loop corrections to the process is described. Besides, we restrict ourselves to the kinematics of hard photon emission along initial electron. In Sect. 1.4.3 the corrections due to virtual and soft real photon emission in the case $\mathbf{k}_1 \parallel \mathbf{p}_1$ are considered. The general expression for correction in the case of hard photon emission along scattered electron is given in Sect. 1.4.4. In Sect. 1.4.5 we consider a contribution (in LLA) coming from two hard photon emission and derive a general expression for radiative correction. In conclusion we discuss the relation with structure function approach and the accuracy of the results obtained. Some useful expressions for loop integrals are given in Appendix II and the results of numeric estimates are given in graphs.

1.4.1. Born Expressions in Collinear Kinematics. Let us begin revising the radiative Bhabha scattering process

$$e^-(p_1) \;+\; e^+(p_2) \;\to\; e^-(p_1') \;+\; e^+(p_2') \;+\; \gamma(k_1) \tag{1.123}$$

at the tree level. We define the collinear kinematical domains as those in which the hard photon is emitted close (within a narrow cone with opening angle $\theta_0 \ll 1$) to the incident ($\theta_{1(2)} = \widehat{\mathbf{p}_{1(2)}\mathbf{k}_1} < \theta_0$) or the outgoing electron (positron) ($\theta'_{1(2)} = \widehat{\mathbf{p}'_{1(2)}\mathbf{k}_1} < \theta_0$) direction of motion. Because of the symmetry between electron and positron we may restrict ourselves to a consideration of only two collinear regions, which correspond to the emission of the photon along the electron momenta. The

two remaining contributions to the differential cross section of the process (1.123) can be obtained by the substitution $\mathcal{Q}$

$$\mathrm{d}\sigma_{\mathrm{coll}} = \left[1 + \mathcal{Q}\left(\begin{array}{c} p_1 \leftrightarrow p_2 \\ p_1' \leftrightarrow p_2' \end{array}\right)\right]\left\{\mathrm{d}\sigma^{\gamma}(\mathbf{k}_1 \parallel \mathbf{p}_1) + \mathrm{d}\sigma^{\gamma}(\mathbf{k}_1 \parallel \mathbf{p}_1')\right\}. \quad (1.124)$$

To begin with, let us recall the known expression [6] in Born approximation for the general kinematics, i. e., assuming all the squares of the momenta transferred among fermions to be large compared to the electron mass squared:

$$\mathrm{d}\sigma_0^{\gamma} = \frac{\alpha^3}{8\pi^2 s} T \mathrm{d}\Gamma, \qquad \mathrm{d}\Gamma = \frac{\mathrm{d}^3\mathbf{p}_1'\mathrm{d}^3\mathbf{p}_2'\mathrm{d}^3\mathbf{k}_1}{\varepsilon_1'\varepsilon_2'\omega_1}\delta^4(p_1 + p_2 - p_1' - p_2' - k_1),$$

$$T = \frac{S}{tt_1ss_1}\left[ss_1(s^2 + s_1^2) + tt_1(t^2 + t_1^2) + uu_1(u^2 + u_1^2)\right] -$$

$$- \frac{16m^2}{\chi_2'^2}\left(\frac{s}{t_1} + \frac{t_1}{s} + 1\right)^2 - \frac{16m^2}{\chi_1'^2}\left(\frac{s}{t} + \frac{t}{s} + 1\right)^2 - \frac{16m^2}{\chi_2^2}\left(\frac{s_1}{t_1} + \frac{t_1}{s_1} + 1\right)^2 -$$

$$- \frac{16m^2}{\chi_1^2}\left(\frac{s_1}{t} + \frac{t}{s_1} + 1\right)^2, \quad (1.125)$$

$$\begin{aligned} S &= 4\left[\frac{s}{\chi_1\chi_2} + \frac{s_1}{\chi_1'\chi_2'} - \frac{t_1}{\chi_1\chi_1'} - \frac{t}{\chi_2\chi_2'} + \frac{u_1}{\chi_2\chi_1'} + \frac{u}{\chi_1\chi_2'}\right], \\ s &= (p_1 + p_2)^2, \quad s_1 = (p_1' + p_2')^2, \quad t = (p_2 - p_2')^2, \quad t_1 = (p_1 - p_1')^2, \\ u &= (p_1 - p_2')^2, \quad u_1 = (p_2 - p_1')^2, \quad \chi_i = 2p_ik_1, \quad \chi_{1,2}' = 2p_{1,2}'k_1. \end{aligned}$$

In the collinear kinematical domain in which $\mathbf{k}_1 \parallel \mathbf{p}_1$, the above formula takes the form

$$\begin{aligned} \mathrm{d}\sigma_0^{\gamma}(\mathbf{k}_1 \parallel \mathbf{p}_1) &= \frac{\alpha^3}{\pi^2 s}\frac{\mathrm{d}^3\mathbf{k}_1}{\omega_1}\frac{1}{\chi_1}\Upsilon F\frac{\mathrm{d}^3\mathbf{p}_1'\mathrm{d}^3\mathbf{p}_2'}{\varepsilon_1'\varepsilon_2'}\delta^4((1-x)p_1 + p_2 - p_1' - p_2') = \\ &= \mathrm{d}W_{p_1}\mathrm{d}\sigma_0((1-x)p_1, p_2), \quad (1.126) \\ \Upsilon &= \frac{1 + (1-x)^2}{x(1-x)} - \frac{2m^2}{\chi_1}, \qquad F = \left(\frac{s_1}{t} + \frac{t}{s_1} + 1\right)^2, \end{aligned}$$

where

$$\begin{aligned} & s_1 = s(1-x),\ y_1 = \frac{\varepsilon_1'}{\varepsilon} = 2\frac{1-x}{a},\ y_2 = \frac{\varepsilon_2'}{\varepsilon} = \frac{2 - 2x + x^2 + cx(2-x)}{a}, \\ & a = 2 - x + cx, \quad \omega_1 = \varepsilon x, \quad s = 4\varepsilon^2, \quad \chi_1 = \frac{s}{2}x(1 - c_1\beta), \quad (1.127) \\ & t = t_1(1-x) = -s\frac{(1-x)^2(1-c)}{a}, \quad c = \cos(\widehat{\mathbf{p}_1\mathbf{p}_1'}), \quad c_1 = \cos(\widehat{\mathbf{p}_1\mathbf{k}_1}), \\ & \beta = \sqrt{1 - \frac{m^2}{\varepsilon^2}}, \qquad \mathrm{d}W_{p_1} = \frac{\alpha}{2\pi^2}\frac{1-x}{\chi_1}\Upsilon\frac{\mathrm{d}^3\mathbf{k}_1}{\omega_1}. \end{aligned}$$

Here y_i are the energy fractions of the scattered leptons and $\mathrm{d}\sigma_0(p_1(1-x),p_2)$ is the cross section of the elastic Bhabha scattering process.

Throughout the chapter we use the following relations among invariants

$$s_1+t+u_1=4m^2-\chi_1\approx 0,\qquad s+t_1+u=4m^2+\chi_1\approx 0.$$

In the case $\mathbf{k}_1\parallel\mathbf{p}_1'$ we have

$$\begin{gathered}\mathrm{d}\sigma_0^\gamma(\mathbf{k}_1\parallel\mathbf{p}_1')=\frac{\alpha}{2\pi^2}\frac{1}{\chi_1'}\tilde{\Upsilon}\frac{\mathrm{d}^3\mathbf{k}_1}{\omega_1}(1-x)\mathrm{d}\sigma_0(p_1,p_2),\\ \tilde{\Upsilon}=\frac{1+(1-x)^2}{x}-\frac{2m^2}{\chi_1'}.\end{gathered}\tag{1.128}$$

These expressions could also be inferred by using the method of quasi-real electrons [21] and starting from the nonradiative Bhabha cross section.

After integration over a hard collinear ($\mathbf{k}_1\parallel\mathbf{p}_1$) photon angular phase space, the cross section of radiative Bhabha scattering in the Born approximation is found to be

$$\begin{aligned}\left.\frac{\mathrm{d}\sigma_0^\gamma}{\mathrm{d}x\mathrm{d}c}\right|_{\mathbf{k}_1\parallel\mathbf{p}_1}&=\frac{4\alpha^3}{s}\left[\frac{1+(1-x)^2}{x}L_0-2\frac{1-x}{x}\right]\times\\ &\times\left(\frac{3-3x+x^2+2cx(2-x)+c^2(1-x(1-x))}{(1-x)(1-c)a^2}\right)^2(1+\mathcal{O}(\theta_0^2)),\end{aligned}\tag{1.129}$$

where $L_0=\ln\left(\varepsilon\theta_0/m\right)^2$. And in the case $\mathbf{k}_1\parallel\mathbf{p}_1'$ it reads

$$\begin{gathered}\left.\frac{\mathrm{d}\sigma_0^\gamma}{\mathrm{d}x\mathrm{d}c}\right|_{\mathbf{k}_1\parallel\mathbf{p}_1'}=\frac{\alpha^3}{4s}\left[\frac{1+(1-x)^2}{x}L_0'-2\frac{1-x}{x}\right]\left(\frac{3+c^2}{1-c}\right)^2(1+\mathcal{O}(\theta_0^2)),\\ L_0'=\ln\left(\frac{\varepsilon_1'\theta_0}{m}\right)^2,\qquad \varepsilon_1'=\varepsilon(1-x).\end{gathered}\tag{1.130}$$

The simplest way to reproduce these results is to use the physical gauge for the real photon which in the beam c.m.s. sets the photon polarization vector to be a space-like 3-vector $\mathbf{e}_\lambda$ having density matrix

$$\sum_\lambda e_\mu^\lambda e_\nu^{\lambda *}=\begin{cases}0, & \text{if } \mu \text{ or } \nu=0\\ \delta_{\mu\nu}-n_\mu n_\nu, & \mu=\nu=1,2,3,\end{cases}\qquad \mathbf{n}=\frac{\mathbf{k}_1}{\omega_1},$$

with the properties

$$\begin{gathered}\sum_\lambda|e_\lambda|^2=-2,\quad \sum_\lambda|p_1e_\lambda|^2=\varepsilon^2(1-c_1^2),\\ \sum_\lambda|p_1'e_\lambda|^2=\frac{t_1u_1}{s},\quad \sum_\lambda(p_1e_\lambda)(p_1'e_\lambda)^*\overset{\theta\to 0}{\sim}\theta.\end{gathered}\tag{1.131}$$

These properties enable us to omit mass terms in the calculations of traces and, besides, to restrict ourselves to the consideration of *singular* terms (see Eq. (1.132)) only, both at the Born and one-loop level. As shown in [36], this gauge is proved useful for a description of jet production in quantum chromodynamics; it is also very well suited to our case because it allows one to simplify a lot the calculation with respect, for instance, to the Feynman gauge. What is more, it possesses another very attractive feature related with the structure of the correction to be mentioned below (see Appendix II).

With these tools at our disposal let us turn now to the main point. The contributions, which survive the limit $\theta_0 \to 0$, arise from the terms containing

$$\frac{(p_1 e)^2}{\chi_1^2}, \quad \frac{e^2}{\chi_1}, \quad \frac{(p_1' e)^2}{\chi_1}. \tag{1.132}$$

Other omitted terms (in particular those which do not contain a factor χ_1^{-1}) can be safely neglected since they give a contribution of the order of θ_0^2 which determines the accuracy of our calculations

$$1 + \mathcal{O}\left(\frac{\alpha}{\pi}\theta_0^2 L_s\right), \qquad \frac{m}{\varepsilon} \ll \theta_0 \ll 1. \tag{1.133}$$

In the realistic case this corresponds to an accuracy of the order of per mille.

1.4.2. Crossing Relations. In this and the next section we shall consider the case $\mathbf{k}_1 \parallel \mathbf{p}_1$. In the case of photon emission along p_1' one can get the desired expression by using the *left-to-right* permutation

$$|M|^2_{\mathbf{k}_1 \parallel \mathbf{p}_1'} = \mathcal{Q}\begin{pmatrix} p_1 \leftrightarrow -p_1' \\ p_2 \leftrightarrow -p_2' \end{pmatrix} |M|^2_{\mathbf{k}_1 \parallel \mathbf{p}_1}. \tag{1.134}$$

From now on we deal with scattering type amplitudes (FD) with the emission of hard photon by initial electron. This is possible due to the properties of the physical gauge. The contribution of annihilation type amplitudes may be derived by applying the momenta replacement operation as follows:

$$\Delta|M|^2_{\text{annih}} = \{\mathcal{Q}(p_1' \leftrightarrow -p_2)\}\, \Delta|M|^2_{\text{scatt}} \equiv \{Q_1\}\, \Delta|M|^2_{\text{scatt}}. \tag{1.135}$$

In considering FD with two photons in the scattering channel (box FD) one may examine only those with uncrossed photons because a contribution of the others may be obtained by the permutation $p_2 \leftrightarrow -p_2'$. Thus the general answer becomes

$$|M|^2_{\mathbf{k}_1 \parallel \mathbf{p}_1} = \Re e \left\{ (1+Q_1)[G+L] + \frac{1}{s_1 t}(1+Q_1)(1+Q_2)[s_1 t(B+P)] \right\}, \tag{1.136}$$

with the permutation operators acting as

$$Q_1F(s_1,t_1,s,t)=F(t,s,t_1,s_1),\quad Q_2F(s,u,s_1,u_1)=F(u,s,u_1,s_1).$$

1.4.3. Virtual and Soft Photon Emission in $\mathbf{k}_1 \parallel \mathbf{p}_1$ *Kinematics.* One-loop QED RC (which are described by seventy-two Feynman diagrams) can be classified out into the two gauge invariant subsets (see Fig. 6):

- single photon exchange between electron and positron lines (G-, L-type);
- double photon exchange between electron and positron lines (B-, P-type).

For L-type FD (see Fig. 6 ((3), (4))) the initial spinor $u(p_1)$ is replaced by

$$\frac{\alpha}{2\pi}A_2\hat{k}_1\hat{e}u(p_1),$$

with

$$A_2=\frac{1}{\chi_1}\left\{-\frac{\rho}{2(\rho-1)}+\frac{2\rho^2-3\rho+2}{2(\rho-1)^2}L_\rho+\frac{1}{\rho}\left[-\mathrm{Li}_2(1-\rho)+\frac{\pi^2}{6}\right]\right\},$$
$$L_\rho=\ln\rho,\qquad \rho=\frac{\chi_1}{m^2}.$$

The relevant contribution to the matrix element squared and summed over spin states reads

$$\begin{aligned}\Delta|M|^2_L&=2^9\pi^2\alpha^4\frac{A_2}{\chi_1}\frac{s_1^3-u_1^3}{s_1t^2}\left[Y-\frac{2(2-x)}{1-x}W\right],\\ Y&=4(p_1e)^2-\frac{x}{1-x}e^2\chi_1,\qquad W=(p_1e)^2.\end{aligned}\tag{1.137}$$

The contribution of vertex insertion, vacuum polarization* and G_1-type FD (see Fig. 6 ((1), (2), (5))) has the following form

$$\begin{aligned}\Delta|M|^2_{\Pi,\Gamma,\Gamma_a}&=2^{10}\pi^2\alpha^4\left[\Pi_t+\Gamma_t+\frac{1}{4}\Gamma_a\right]\frac{s_1^3-u_1^3}{t^2s_1\chi_1^2}Y,\\ \Pi_t&=\frac{1}{3}L_t-\frac{5}{9},\quad \Gamma_t=(L_\lambda-1)(1-L_t)-\frac{1}{4}L_t-\frac{1}{4}L_t^2+\frac{\pi^2}{12},\\ \Gamma_a&=-3L_t^2+4L_tL_\rho+3L_t+4L_\lambda-2\ln(1-\rho)-\frac{\pi^2}{3}+2\mathrm{Li}_2(1-\rho)-4,\\ L_\lambda&=\ln\frac{m}{\lambda},\quad L_t=\ln\frac{-t}{m^2},\quad \mathrm{Li}_2(z)=-\int\limits_0^z\frac{\mathrm{d}x}{x}\ln(1-x).\end{aligned}\tag{1.138}$$

*For realistic applications one should also add to Π the contributions due to μ and τ leptons and hadrons.

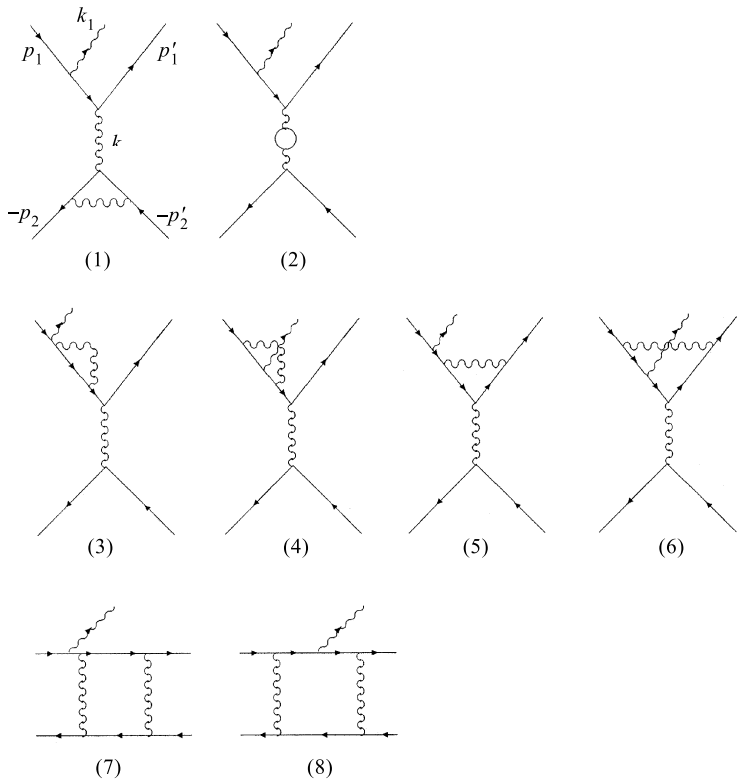

Fig. 6. Some representatives of FD for radiative Bhabha scattering up to second order: (1) is the vertex insertion; (2) is the vacuum polarization insertion; graphs denoted by (3); (4) are of the L-type; (5) is of G_1-type; (6) is of G_2-type; (7) is of B-type and (8) is of P-type

Here λ is as usual the IR cut-off parameter to be cancelled at the end of calculus against a soft photon contribution.

For the contribution of G_2-type FD (see Fig. 6 (6)) with four denominators we obtain

$$\Delta|M|^2_G = 2^9\alpha^4\pi^2\frac{s_1^3-u_1^3}{ts_1\chi_1(1-x)}\Bigg[(J-J_1)Y + \\ + \frac{2(2-x)}{1-x}W(J_{11}-J_1+xJ_{1k}-xJ_k)\Bigg]. \quad (1.139)$$

It turns out that only the scalar integral and the coefficients before p_1, k_1 in the vector and tensor integrals give nonvanishing contribution in the limit $\theta_0 \to 0$

$$\int \frac{\mathrm{d}^4k}{\mathrm{i}\pi^2}\frac{(1,k^\mu,k^\mu k^\nu)}{(0)(1)(2)(q)} = (J, J_1 p_1^\mu + J_k k_1^\mu, J_{11} p_1^\mu p_1^\nu + J_{kk} k_1^\mu k_1^\nu + J_{1k}(p_1 k_1)^{\mu\nu}),$$
$$(0) = k^2 - \lambda^2,\ (1) = k^2 - 2p_1 k,\ (2) = k^2 - 2p_1' k,$$
$$(q) = k^2 - 2k(p_1 - k_1) - \chi_1, \quad (ab)^{\mu\nu} = a^\mu b^\nu + a^\nu b^\mu,$$

and the terms having no p_1 or k_1 momentum in the decomposition have been omitted for their unimportance.

The B-type FD shown in Fig. 6 (7) with uncrossed legs gives

$$\Delta|M|_B^2 = 2^9\pi^2\alpha^4 Y \frac{1}{s_1 t \chi_1^2}\Bigg[(u_1^3 - s_1^3)s_1(B + a - b) - \\ - u_1^3 s_1\left(c + a_{1'2'} + a_{1'2} + \frac{2}{s_1}a_g\right) + s_1^3(c[t - u_1] + 2J_0)\Bigg], \quad (1.140)$$

where the coefficients are associated with scalar, vector and tensor integrals over loop momentum

$$\int \frac{\mathrm{d}^4k}{\mathrm{i}\pi^2}\frac{(1,k^\mu,k^\mu k^\nu)}{b_0 b_1 b_2 b_3} = (B, B^\mu, B^{\mu\nu}), \qquad J_0 = \int \frac{\mathrm{d}^4k}{\mathrm{i}\pi^2}\frac{1}{b_1 b_2 b_3},$$
$$b_0 = k^2 - \lambda^2, \qquad b_1 = k^2 + 2p_1' k, \qquad b_2 = k^2 - 2p_2' k,$$
$$b_3 = k^2 - 2qk + t, \qquad q = p_2' - p_2,$$
$$B^\mu = (ap_1' + bp_2' + cp_2)^\mu,$$
$$B^{\mu\nu} = a_g g^{\mu\nu} + a_{1'1'} p_1^{'\mu} p_1^{'\nu} + a_{22} p_2^\mu p_2^\nu + a_{2'2'} p_2^{'\mu} p_2^{'\nu} + a_{1'2}(p_1' p_2)^{\mu\nu} + \\ + a_{1'2'}(p_1' p_2')^{\mu\nu} + a_{22'}(p_2 p_2')^{\mu\nu}.$$

For P-type FD (see Fig. 6 (8)) with uncrossed photon legs we have

$$\Delta|M|_P^2 = 2^9\pi^2\alpha^4\frac{s_1^3 - u_1^3}{t\chi_1(1-x)}\Bigg[Y(E - E_1) + \\ + \frac{2(2-x)}{1-x}W(E_{11} - E_1 + xE_{1k} - xE_k)\Bigg]. \quad (1.141)$$

Here we are using the definition (with tensor structures giving no contributions in the limit $\theta_0 \to 0$ dropped)

$$\int \frac{\mathrm{d}^4k}{\mathrm{i}\pi^2}\frac{(1,k^\mu,k^\mu k^\nu)}{a_0 a_1 a_2 a_3 a_4} = (E, E_1 p_1^\mu + E_k k_1^\mu, E_{11} p_1^\mu p_1^\nu + E_{kk} k_1^\mu k_1^\nu + \\ + E_{1k}(p_1^\mu k_1^\nu + p_1^\nu k_1^\mu)),$$

$$a_0 = k^2 - \lambda^2, \quad a_1 = k^2 - 2p_1k, \quad a_2 = k^2 - 2k(p_1 - k_1) - \chi_1,$$

$$a_3 = k^2 + 2p_2k, \qquad a_4 = k^2 - 2qk + t.$$

Note that in the evaluating of P-type FD we are allowed to put $k_1 = xp_1$, thus keeping only p_1 momentum containing terms in the decomposition.

Collecting all the contributions (for the explicit expressions of all the coefficients see Appendix II) given above we arrive at the general expression for the virtual corrections with $\rho = x[1 + (\varepsilon\theta/m)^2] \ll s/m^2$

$$\begin{aligned}
&2\,\Re e\sum(M_0^*M)_{\mathbf{k}_1\|\mathbf{p}_1} = \\
&= \frac{2^{11}\alpha^4\pi^2}{\chi_1}F\Upsilon\left\{\frac{2-x}{1-x}\frac{w}{\Upsilon}\Phi + 2L_\lambda(2 - L_t - L_{t_1} - L_s - \right. \\
&-L_{s_1} + L_u + L_{u_1}) + \frac{\pi^2}{3} + \mathrm{Li}_2(x) - \frac{101}{18} + \ln\left|\frac{\rho}{1-\rho}\right| + L_{u_1}^2 - L_t^2 - \\
&-L_{s_1}^2 + L_\rho\ln(1-x) + \frac{11}{3}L_t - \vartheta + \ln^2\frac{s_1}{t} + \frac{1}{F}\left[\Pi + 3\frac{t^3 - u_1^3}{s_1^2 t}\ln\frac{s_1}{t} + \right. \\
&+\frac{2u_1(u_1^2+s_1^2) - ts_1^2}{4t^2s_1}\ln^2\frac{u_1}{t} + \frac{2u_1(u_1^2+t^2) - t^2s_1}{4ts_1^2}\ln^2\frac{u_1}{s_1} + \\
&\left.\left.+\frac{s_1}{2t}\ln\frac{u_1}{t} + \frac{t}{2s_1}\ln\frac{u_1}{s_1} - \frac{3}{4}\pi^2\left(\frac{s_1}{t} + \frac{t}{s_1}\right)\right]\right\},
\end{aligned} \tag{1.142}$$

where we have used the following definitions

$$\begin{aligned}
\vartheta &= \frac{x}{\rho - x}\left[\mathrm{Li}_2(1-\rho) - \frac{\pi^2}{6} + \mathrm{Li}_2(x) + L_\rho\ln(1-x)\right], \\
\Pi &= \frac{s_1^3 - u_1^3}{s_1 t^2}\left[\frac{\pi}{\alpha}\left(\frac{1}{1-\Pi_t} - 1\right) - \frac{1}{3}L_t + \frac{5}{9}\right] + \\
&+ \frac{t^3 - u_1^3}{s_1^2 t}\left[\frac{\pi}{\alpha}\Re e\left(\frac{1}{1-\Pi_{s_1}} - 1\right) - \frac{1}{3}L_{s_1} + \frac{5}{9}\right], \\
\Pi_{s_1} &= \frac{1}{3}(L_{s_1} - \mathrm{i}\pi) - \frac{5}{9}, \quad \Phi = \chi_1 A_2 + t_1\chi_1(J_{11} - J_1 + xJ_{1k} - xJ_k), \\
w &= \frac{1}{x} - \frac{1}{\rho}, \quad L_{s_1} = \ln\frac{s_1}{m^2}, \quad L_u = \ln\frac{-u}{m^2}, \quad L_{u_1} = \ln\frac{-u_1}{m^2}, \\
L_t &= \ln\frac{-t}{m^2}, \quad L_{t_1} = \ln\frac{-t_1}{m^2}.
\end{aligned}$$

After integration over χ_1 one gets additional large logs of the form $L_0 = L_s + \ln(\theta_0^2/4)$. Terms containing the last factor have to be cancelled against

a contribution coming from the emission of hard photon outside a narrow cone $\theta < \theta_0 \ll 1$ (and supplied by the same set of virtual and soft corrections), which was considered in [16]. In the case of two hard photon emission it is necessary to consider four kinematical regions, namely when both are emitted inside/outside a cone and one inside/another outside.

Fortunately enough, the w structure, which obviously violates factorization feature, does not contribute in LLA due to a cancellation of large logs in Φ. What for a correction to the above structure coming from P-type graph it vanishes in the sum of FD with crossed and uncrossed photon legs (for a more comprehensive account see Appendix II).

The total expression can be obtained by summing virtual photon emission corrections and those arising from the emission of additional soft photon with energy not exceeding $\Delta\varepsilon \ll \varepsilon$.

The emission of a soft photon is seen as a process factored out of a hard subprocess (in our case the latter is exactly a hard collinear photon emission) so this is seemingly come into an evident conflict with a hard collinear emission. Nevertheless, arguments similar to those given in the paper devoted to the problem of DIS with tagged photon [37] may be applied in the present chapter: the factorization of the two in the *differential* cross section is present and we are, hence, allowed to consider a soft photon emission restricted as usual by

$$\frac{\Delta\varepsilon}{\varepsilon} \ll 1. \tag{1.143}$$

Thus the soft correction can be written as

$$\begin{aligned}
\sum |M|^2_{\text{hard+soft}} &= \sum |M|^2_B w_{\text{soft}}(\mathbf{k}_1 \parallel \mathbf{p}_1), && (1.144)\\
w_{\text{soft}}(\mathbf{k}_1 \parallel \mathbf{p}_1) &= -\frac{\alpha}{4\pi^2} \int\limits_{\omega<\Delta\varepsilon} \frac{\mathrm{d}^3\mathbf{k}}{\sqrt{\mathbf{k}^2+\lambda^2}} \left(-\frac{p_1}{p_1 k} + \frac{p_1'}{p_1' k} + \frac{p_2}{p_2 k} - \frac{p_2'}{p_2' k} \right)^2,
\end{aligned}$$

where M_B denotes the matrix element of the hard photon emission at the Born level and in the kinematics $\mathbf{k}_1 \parallel \mathbf{p}_1$ it reads

$$\sum |M|^2_B = \frac{2^{11}\alpha^3\pi^3}{\chi_1} \Upsilon F. \tag{1.145}$$

Now let us check the cancellation of the terms containing L_λ. Indeed it takes place in the sum of contributions arising from emission of virtual and soft real

photons. To show that we bring the soft correction into the form

$$
\begin{aligned}
&w_{\text{soft}}(\mathbf{k}_1 \parallel \mathbf{p}_1) = \\
&= \frac{\alpha}{\pi}\Bigg\{2\left(\ln\frac{\Delta\varepsilon}{\varepsilon}+L_\lambda\right)(-2+L_s+L_{s_1}+L_t+L_{t_1}-L_u-L_{u_1})+\frac{1}{2}(L_s^2+L_{s_1}^2+ \\
&+L_t^2+L_{t_1}^2-L_u^2-L_{u_1}^2)+\ln y_1(L_{u_1}-L_{s_1}-L_{t_1})+\ln y_2(L_u-L_t-L_{s_1})+ \\
&+\ln(y_1y_2)-\frac{2\pi^2}{3}-\frac{1}{2}\ln^2\frac{y_1}{y_2}+\mathrm{Li}_2\left(\frac{1+c_{1'2'}}{2}\right)+\mathrm{Li}_2\left(\frac{1+c_{1'}}{2}\right)+ \\
&+\mathrm{Li}_2\left(\frac{1-c_{2'}}{2}\right)-\mathrm{Li}_2\left(\frac{1-c_{1'}}{2}\right)-\mathrm{Li}_2\left(\frac{1+c_{2'}}{2}\right)\Bigg\}, \quad (1.146)
\end{aligned}
$$

where c_i are the cosines of emission angles of ith particle with respect to the beam direction ($\mathbf{p}_1$ in c.m.s.), $c_{1'2'}$ is the cosine of the angle between scattered fermions in c.m.s. of the colliding particles and y_i are their energy fractions and in the case $\mathbf{k}_1 \parallel \mathbf{p}_1$ we have

$$
c_1' = c, \quad \frac{1+c_{1'2'}}{2} = 1-\frac{1-x}{y_1y_2}, \quad \frac{1-c_2'}{2} = \frac{y_1(1+c)}{2y_2(1-x)}. \quad (1.147)
$$

Then the cancellation of infrared singularities in the sum is evident from comparison of Eqs. (1.142), (1.146). The terms with $\ln(\Delta\varepsilon/\varepsilon)$ should be cancelled when adding a contribution of a second hard photon having energy above the registration threshold $\Delta\varepsilon$.

The complete expression for the correction in the case $\mathbf{k}_1 \parallel \mathbf{p}_1$ reads

$$
\begin{aligned}
&R = 2\,\Re e\sum(M_0^*M)+|M|^2_{\text{soft}} = \\
&= \frac{2^{11}\alpha^4\pi^2}{\chi_1}F\Upsilon\Bigg\{\frac{2-x}{1-x}\frac{w}{\Upsilon}\Phi+4\ln\left(\frac{\Delta\varepsilon}{\varepsilon}\right)\Bigg[-1+L_{t_1}+\frac{1}{2}\Bigg(-\ln(1-x)+ \\
&+2\ln\frac{s}{-u}\Bigg)\Bigg]+\frac{11}{3}L_t+(L_\rho-L_t)\ln(1-x)-L_t\ln(y_1y_2)+\ln^2\frac{s_1}{-t}+ \\
&+\ln y_1\ln(1-x)+\ln(y_1y_2)\left(1+\ln\frac{-u}{s}\right)-\frac{\pi^2}{3}+\mathrm{Li}_2(x)-\frac{101}{18}-\vartheta+ \\
&+\ln\left|\frac{\rho}{1-\rho}\right|-\frac{1}{2}\ln^2\frac{y_1}{y_2}+\ln(1-x)\ln\frac{-u}{s}+\mathrm{Li}_2\left(\frac{1+c_{1'2'}}{2}\right)+\mathrm{Li}_2\left(\frac{1+c_{1'}}{2}\right)+ \\
&+\mathrm{Li}_2\left(\frac{1-c_{2'}}{2}\right)-\mathrm{Li}_2\left(\frac{1-c_{1'}}{2}\right)-\mathrm{Li}_2\left(\frac{1+c_{2'}}{2}\right)+\frac{1}{F}\Bigg[\Pi+3\frac{t^3-u_1^3}{s_1^2t}\ln\frac{s_1}{-t}+
\end{aligned}
$$

$$+\frac{2u_1(u_1^2+s_1^2)-ts_1^2}{4t^2s_1}\ln^2\frac{u_1}{t}+\frac{2u_1(u_1^2+t^2)-t^2s_1}{4ts_1^2}\ln^2\frac{-u}{s}+\frac{s_1}{2t}\ln\frac{u_1}{t}+$$
$$+\frac{t}{2s_1}\ln\frac{-u}{s}-\frac{3}{4}\pi^2\left(\frac{s_1}{t}+\frac{t}{s_1}\right)\Bigg]\Bigg\},$$
$$\mathrm{d}\sigma(\mathbf{k}_1\parallel\mathbf{p}_1)=\frac{1}{2^{11}\pi^5 s}R\mathrm{d}\Gamma. \tag{1.148}$$

1.4.4. Kinematics $\mathbf{k}_1\parallel\mathbf{p}_1'$. We put here a set of replacements one can use in order to obtain the modulus of matrix element squared and summed over spin states for the case $\mathbf{k}_1\parallel\mathbf{p}_1'$, starting from the analogous expression for $\mathbf{k}_1\parallel\mathbf{p}_1$ (Eq. (1.136)) and using the replacement of momenta $p_1\leftrightarrow-p_1', p_2\leftrightarrow-p_2'$. The last operation results in the following substitutions:

$$\begin{gathered}x\to-\frac{x}{1-x},\quad \chi_1\to-\chi_1',\\ s\leftrightarrow s_1,\quad u\leftrightarrow u_1,\quad t\to t,\quad t_1\to t_1.\end{gathered} \tag{1.149}$$

Then under these permutations the expression for virtual corrections given in Eq. (1.142) gets transformed yielding the following result for the collinear domain $\mathbf{k}_1\parallel\mathbf{p}_1'$

$$2\Re e\sum(M_0^*M)_{\mathbf{k}_1\parallel\mathbf{p}_1'}=\frac{2^{11}\alpha^4\pi^2}{\chi_1'}\tilde{F}\tilde{\Upsilon}\Bigg\{\frac{2-x}{1-x}\frac{\tilde{w}}{\tilde{\Upsilon}}\tilde{\Phi}+2L_\lambda(2-L_t-L_{t_1}-L_s-$$
$$-L_{s_1}+L_u+L_{u_1})+\frac{\pi^2}{3}+\mathrm{Li}_2\left(\frac{-x}{1-x}\right)-\frac{101}{18}+\ln\left(\frac{\xi}{\xi+1}\right)+L_u^2-$$
$$-L_t^2-L_s^2-L_\xi\ln(1-x)+\frac{11}{3}L_t+\ln^2\frac{s}{-t}+\frac{1}{\tilde{F}}\Bigg[\tilde{\Pi}+3\frac{t^3-u^3}{s^2t}\ln\frac{s}{-t}+$$
$$+\frac{2u(u^2+s^2)-ts^2}{4t^2s}\ln^2\frac{u}{t}+\frac{2u(u^2+t^2)-t^2s}{4ts^2}\ln^2\frac{-u}{s}+\frac{s}{2t}\ln\frac{u}{t}-\tilde{\vartheta}+$$
$$+\frac{t}{2s}\ln\frac{-u}{s}-\frac{3}{4}\pi^2\left(\frac{s}{t}+\frac{t}{s}\right)\Bigg]\Bigg\}, \tag{1.150}$$

with

$$\begin{aligned}\tilde{\Pi}&=\frac{s^3-u^3}{st^2}\left[\frac{\pi}{\alpha}\left(\frac{1}{1-\Pi_t}-1\right)-\frac{1}{3}L_t+\frac{5}{9}\right]+\\&+\frac{t^3-u^3}{s^2t}\left[\frac{\pi}{\alpha}\Re e\left(\frac{1}{1-\Pi_s}-1\right)-\frac{1}{3}L_s+\frac{5}{9}\right],\\ \tilde{F}&=\left(\frac{s}{t}+\frac{t}{s}+1\right)^2,\qquad \tilde{w}=-\frac{1-x}{x}+\frac{1}{\xi},\qquad \xi=\frac{\chi_1'}{m^2}\end{aligned}$$

and $\tilde{\Phi}, \tilde{\vartheta}$ derived upon applying a set of replacements from Eq. (1.149) on the quantities Φ, ϑ.

The contribution from the soft photon emission is described by

$$w_{\rm soft}(\mathbf{k}_1 \parallel \mathbf{p}_1') = \frac{\alpha}{\pi}\left[4\left(\ln\frac{\Delta\varepsilon}{\varepsilon} + L_\lambda\right)\left(-1 + L_s + \ln\frac{1-c}{1+c} + \frac{1}{2}\ln(1-x)\right) + \right.$$
$$+ L_s^2 + 2L_s\ln\frac{1-c}{1+c} - \frac{1}{2}\ln^2(1-x) + \ln(1-x) + \ln^2\frac{1-c}{2} -$$
$$\left. - \ln^2\frac{1+c}{2} - \frac{2\pi^2}{3} + 2{\rm Li}_2\left(\frac{1+c}{2}\right) - 2{\rm Li}_2\left(\frac{1-c}{2}\right)\right]. \quad (1.151)$$

The total correction for the case $\mathbf{k}_1 \parallel \mathbf{p}_1'$ has the following form

$$\tilde{R} = 2\,\Re e\sum(M_0^* M) + |M|^2_{\rm soft} =$$
$$= \frac{2^{11}\alpha^4\pi^2}{\chi_1'}\tilde{F}\tilde{\Upsilon}\left\{\frac{2-x}{1-x}\frac{\tilde{w}}{\tilde{\Upsilon}}\tilde{\Phi} + 4\ln\left(\frac{\Delta\varepsilon}{\varepsilon}\right)\left(-1 + L_s + \frac{1}{2}\ln(1-x) + \right.\right.$$
$$\left. + \ln\frac{1-c}{1+c}\right) + \frac{\pi^2}{3} + {\rm Li}_2\left(\frac{-x}{1-x}\right) - \frac{101}{18} + \ln\left(\frac{\xi}{\xi+1}\right) - 2\ln^2(1-x) +$$
$$+ \frac{11}{3}L_t - L_\xi\ln(1-x) + \ln^2\frac{s}{-t} - \frac{2}{3}\pi^2 + \ln(1-x) - \tilde{\vartheta} + 2{\rm Li}_2\left(\frac{1+c}{2}\right) -$$
$$- 2{\rm Li}_2\left(\frac{1-c}{2}\right) + \frac{1}{\tilde{F}}\left[\tilde{\Pi} + 3\frac{t^3-u^3}{s^2 t}\ln\frac{s}{-t} + \frac{1}{4t^2 s}\ln^2\left(\frac{u}{t}\right)(2u(u^2+s^2) - \right.$$
$$\left. - ts^2) + \frac{1}{4ts^2}\ln^2\left(\frac{-u}{s}\right)(2u(u^2+t^2) - t^2 s) + \frac{s}{2t}\ln\frac{u}{t} + \frac{t}{2s}\ln\frac{-u}{s} - \right.$$
$$\left.\left. - \frac{3}{4}\pi^2\left(\frac{s}{t} + \frac{t}{s}\right)\right]\right\},$$
$$\mathrm{d}\sigma(\mathbf{k}_1 \parallel \mathbf{p}_1') = \frac{1}{2^{11}\pi^5 s}\tilde{R}\mathrm{d}\Gamma. \quad (1.152)$$

Performing the integration over a hard-photon angular phase space (inside a narrow cones) we put the RC to the cross section coming from virtual and soft real additional photons valid to a logarithmic accuracy in the form

$$\frac{\mathrm{d}\sigma^{\gamma(V+S)}}{\mathrm{d}x\mathrm{d}c} = \frac{\mathrm{d}\sigma_0^\gamma}{\mathrm{d}x\mathrm{d}c}\frac{\alpha}{\pi}\left[C\frac{\Delta\varepsilon}{\varepsilon} + L_t\Xi_L + \Xi\right]. \quad (1.153)$$

In Fig. 7, *a,b* given are the ratio of $\Xi/(L_t\Xi_L)$ versus x for the collinear kinematics considered above.

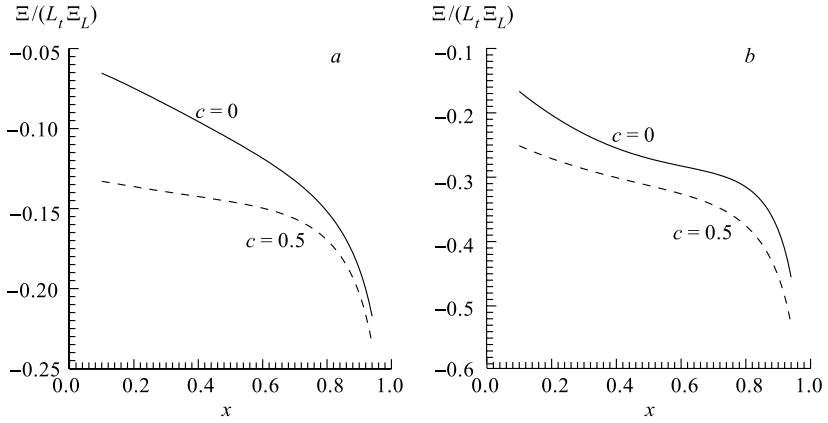

Fig. 7. The ratio $\dfrac{\Xi}{L_t \Xi_L}$ (see Eq. (1.153)) versus $x = \dfrac{\omega_1}{\varepsilon}$ for the case: *a*) $\mathbf{k}_1 \parallel \mathbf{p}_1$; *b*) $\mathbf{k}_1 \parallel \mathbf{p}_1'$

1.4.5. Two Hard Photons Emission and Results in LLA. Turning to the structure of the result obtained, it should be noted that all the terms quadratic in *large* logarithms $L_{t_1} \sim L_{s_1} \sim L_u \gg L_\rho$ are mutually cancelled out as expected.

From the formula (1.148) it immediately follows that (upon doing an integration over a hard photon angular (within a narrow cone) phase space) the w term that is not proportional to Υ, which is in fact the kernel of the nonsinglet electron structure function, is not dangerous in the sense of a feasible violation of the expected Drell–Yan form of the cross section, because it does contribute only at next-to-leading order.

Performing the above-mentioned integration and confining ourselves to LLA we get for the sum of virtual and soft photons

$$\frac{\mathrm{d}\sigma^{\gamma(S+V)}}{\mathrm{d}x\mathrm{d}c} = \frac{\mathrm{d}\sigma_0^\gamma}{\mathrm{d}x\mathrm{d}c}\frac{\alpha}{\pi}L\left[4\ln\frac{\Delta\varepsilon}{\varepsilon} + \frac{11}{3} - \frac{1}{2}\ln(1-x) - \ln(y_1 y_2)\right]. \quad (1.154)$$

The LLA contribution coming from the emission of second hard photon with total energy exceeding $\Delta\varepsilon$ consists of a part corresponding to the case in which both hard photons (with total energy εx) are emitted by initial electron [13]

$$\begin{aligned}\frac{\mathrm{d}\sigma^{2\gamma}}{\mathrm{d}x\mathrm{d}c} &= \frac{\mathrm{d}\sigma_0^\gamma}{\mathrm{d}x\mathrm{d}c}\frac{\alpha}{\pi}L\left[\frac{x\mathcal{P}_\Theta^{(2)}(1-x)}{4(1+(1-x)^2)} + \frac{1}{2}\ln(1-x) - \ln\frac{\Delta\varepsilon}{\varepsilon} - \frac{3}{4}\right],\\ P_\Theta^{(2)}(z) &= 2\left[\frac{1+z^2}{1-z}\left(2\ln(1-z) - \ln z + \frac{3}{2}\right) + \frac{1+z}{2}\ln z - 1 + z\right],\end{aligned} \quad (1.155)$$

and the remaining part which describes the emission of second hard photon along scattered electron and positrons. The latter, upon combining with the part of

contributions of soft and virtual photons to our process

$$\frac{\mathrm{d}\sigma_0^\gamma}{\mathrm{d}x\mathrm{d}c}\frac{3\alpha}{\pi}L\left[\ln\frac{\Delta\varepsilon}{\varepsilon}+\frac{3}{4}\right],$$

may be represented via electron structure function in the spirit of the Drell–Yan approach

$$\begin{aligned}\langle\frac{\mathrm{d}\sigma_0^\gamma}{\mathrm{d}x\mathrm{d}c}\rangle\Big|_{\mathbf{k}_1\|\mathbf{p}_1} &= \frac{\alpha}{2\pi}\frac{1+(1-x)^2}{x}L_0\int \mathrm{d}z_2\mathrm{d}z_3\mathrm{d}z_4\mathcal{D}(z_2)\mathcal{D}(z_3)\mathcal{D}(z_4)\times\\ &\times \frac{\mathrm{d}\sigma_0(p_1(1-x),z_2p_2;q_1,q_2)}{\mathrm{d}c},\end{aligned}\tag{1.156}$$

with the nonsinglet structure function $\mathcal{D}(z)$ [33]

$$\begin{aligned}\mathcal{D}(z) &= \delta(1-z)+\frac{\alpha}{2\pi}L\mathcal{P}^{(1)}(z)+\left(\frac{\alpha}{2\pi}L\right)^2\frac{1}{2!}\mathcal{P}^{(2)}(z)+\dots,\\ P^{(1,2)}(z) &= \lim_{\Delta\to 0}\left\{\delta(1-z)P_\Delta^{(1,2)}+\Theta(1-\Delta-z)P_\Theta^{(1,2)}(z)\right\},\\ P_\Delta^{(1)} &= 2\ln\Delta+\frac{3}{2},\quad P_\Theta^{(1)}(z)=\frac{1+z^2}{1-z},\\ P_\Delta^{(2)} &= \left(2\ln\Delta+\frac{3}{2}\right)^2-\frac{2\pi^2}{3},\dots\end{aligned}\tag{1.157}$$

These functions describe the emission of (real and virtual) photons both by final electron and by positrons. The multiplier before the integral stands for the emission of a hard photon by the initial electron. Thus Eq. (1.156) actually represents the partially integrated Drell–Yan form of the cross section. Quite the same arguments are applicable to the second case in which a hard photon is emitted by the final electron.

The cross section of the hard subprocess $e(p_1z_1)+\bar{e}(p_2z_2)\to e(q_1)+\bar{e}(q_2)$ entering Eq. (1.156) has the form

$$\begin{aligned}&\frac{\mathrm{d}\sigma_0(z_1p_1,z_2p_2;q_1,q_2)}{\mathrm{d}c}=\\ &=\frac{8\pi\alpha^2}{s}\left[\frac{z_1^2+z_2^2+z_1z_2+2c(z_2^2-z_1^2)+c^2(z_1^2+z_2^2-z_1z_2)}{z_1(1-c)(z_1+z_2+c(z_2-z_1))^2}\right]^2.\end{aligned}\tag{1.158}$$

The momenta of scattered electron q_1 and positron q_2 are completely determined by the energy-momentum conservation law

$$q_1^0 = \varepsilon\frac{2z_1z_2}{z_1+z_2+c(z_2-z_1)}, \qquad q_1^0+q_2^0=\varepsilon(z_1+z_2),$$
$$c=\cos\widehat{\mathbf{q}_1,\mathbf{p}}_1, \qquad z_1\sin\widehat{\mathbf{q}_1,\mathbf{p}}_1 = z_2\sin\widehat{\mathbf{q}_2,\mathbf{p}}_1.$$

In general their energies differ from those detected in experiment $\varepsilon_1', \varepsilon_2'$, namely

$$\varepsilon_1' = q_1^0 z_3, \qquad \varepsilon_2' = q_2^0 z_4,$$

whereas the emission angles are the same in LLA.

Collecting the two expressions presented in Eqs. (1.154), (1.155) one can rewrite the result in LLA as

$$\left.\frac{\mathrm{d}\sigma^\gamma}{\mathrm{d}x\mathrm{d}c}\right|_{\mathbf{k}_1\parallel\mathbf{p}_1} = \left(\frac{\mathrm{d}\sigma_0^\gamma}{\mathrm{d}x\mathrm{d}c}\right)_{\mathbf{k}_1\parallel\mathbf{p}_1}\{1+\delta_1\}, \tag{1.159}$$
$$\delta_1 = \left(\frac{\langle\frac{\mathrm{d}\sigma_0^\gamma}{\mathrm{d}x\mathrm{d}c}\rangle}{\frac{\mathrm{d}\sigma_0^\gamma}{\mathrm{d}x\mathrm{d}c}}\right)_{\mathbf{k}_1\parallel\mathbf{p}_1} - 1 + \frac{\alpha}{\pi}L\left[\frac{2}{3}-\ln(y_1y_2)+\frac{x\mathcal{P}_\Theta^{(2)}(1-x)}{4(1+(1-x)^2)}\right].$$

For the case $\mathbf{k}_1 \parallel \mathbf{p}_1'$ the correction is found to be

$$\left.\frac{\mathrm{d}\sigma^\gamma}{\mathrm{d}x\mathrm{d}c}\right|_{\mathbf{k}_1\parallel\mathbf{p}_1'} = \left(\frac{\mathrm{d}\sigma_0^\gamma}{\mathrm{d}x\mathrm{d}c}\right)_{\mathbf{k}_1\parallel\mathbf{p}_1'}\{1+\delta_{1'}\},$$
$$\delta_{1'} = \left(\frac{\langle\frac{\mathrm{d}\sigma_0^\gamma}{\mathrm{d}x\mathrm{d}c}\rangle}{\frac{\mathrm{d}\sigma_0^\gamma}{\mathrm{d}x\mathrm{d}c}}\right)_{\mathbf{k}_1\parallel\mathbf{p}_1'} - 1 + \frac{\alpha}{\pi}L\left[\frac{2}{3}+\frac{x\mathcal{P}_\Theta^{(2)}(1-x)}{4(1+(1-x)^2)}\right],$$
$$\left\langle\frac{\mathrm{d}\sigma_0^\gamma}{\mathrm{d}x\mathrm{d}c}\right\rangle\Bigg|_{\mathbf{k}_1\parallel\mathbf{p}_1'} = \frac{\alpha}{2\pi}\frac{1+(1-x)^2}{x}L_0'\int \mathrm{d}z_1\mathrm{d}z_2\mathrm{d}z_4\mathcal{D}(z_1)\mathcal{D}(z_2)\mathcal{D}(z_4)\times$$
$$\times \frac{\mathrm{d}\sigma_0(z_1p_1,z_2p_2;q_1,q_2)}{\mathrm{d}c}, \tag{1.160}$$

with $L_0' = L_0 + 2\ln(1-x)$.

For the case when the energies of scattered fermions are not detected the expressions (1.156), (1.160) may be simplified due to $\int \mathrm{d}z\mathcal{D}(z)=1$ and z_3, z_4 independence of the integrand in $\mathbf{k}_1 \parallel \mathbf{p}_1$ kinematics (z_4 independence in $\mathbf{k}_1 \parallel \mathbf{p}_1'$ case).

The x dependence of δ_1 is shown in the Fig. 8 for different values of the cosine of scattering angle c. For a hard photon emission by final particles the correction δ_1' strongly depends on the experimental conditions of particles detection: the energy thresholds of detection of scattered fermions. This dependence for δ_1 is much more weaker, namely about $1\,\%$.

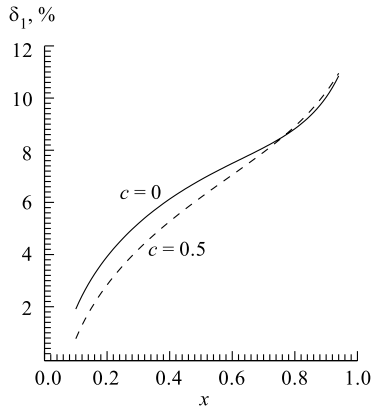

Fig. 8. The x dependence of δ_1 (see Eq. (1.159)) for different values of the cosine of scattering angle c. Other parameters chosen are: $\theta_0 = 0.1,\ \varepsilon = 1$ GeV

In conclusion let us recapitulate the results given in Eqs. (1.159), (1.160). They both respect the Drell–Yan form for a cross section in LLA. Nevertheless, a certain deviation away from RG structure function representation at a second order of PT in $\mathbf{k}_1 \parallel \mathbf{p}_1$ kinematics is observed. The term destroying expectations based on RG approach comes from definite contribution of a soft photon emission, the term with $\ln(y_1 y_2)$ in Eq. (1.159) which cannot be included into the structure function approach. Its appearance is presumably a mere consequence of a complicate kinematics of $2 \to 3$ type hard subprocess (see [16]); for such a kind of processes the validity of the Drell–Yan form for a cross section was not proved so far. Another possible way out is a careful analysis of a *conflict* between a soft and hard collinear photon emission. We have used the factorized form of a soft photon emission (1.144) under the condition (1.143). But, to the moment, this representation in the peculiar case at hand is not rigorously proved as well.

The accuracy of our calculations of virtual and soft photon corrections is determined by the omitted terms of the order of

$$1 + \mathcal{O}\left(\theta_0^2 \frac{\alpha}{\pi} L_s, \frac{m^2}{s} \frac{\alpha}{\pi} L_s\right), \tag{1.161}$$

which corresponds to a per mille level. The accuracy of the correction coming from two hard photon emission is determined by $\mathcal{O}((\alpha/\pi)\ln(4/\theta_0^2))$ and at $1\,\%$ level.

1.5. Large-Angle Bhabha Scattering at LEP2. Electron-positron scattering at large angles is one of the processes studied at LEP2 collider. The small-angle Bhabha is used there for luminosity measurements in the same manner as at LEP1 [38], whereas the large-angle kinematics provides information for the precise verification of the Standard Model and searches for a new physics [39–43].

Few years ago the precision of LABS description at LEP energies had been of about 2 percent [11]. That was before the commencement of data taking by

LEP2. And such a precision was assumed to be appropriate for experimental data analysis. At present the experimental community requirements became more rigorous fixing the precision to be achieved by theory at level of 0.13–0.21 %. This precision tag is one third of the experimental accuracy itself. It was derived to make the theoretical contribution to the resulting systematic uncertainty reasonably small. This way one can guarantee, that a large theoretical error would not eat up the small experimental one. That was due to the efforts of extremely large and expensive collaborations. During the second Monte Carlo LEP2 workshop [44] a considerable improvement in the theoretical description of the process is reached. Several groups were working on detailed comparisons of their calculations and estimation of uncertainties.

In this chapter we present our point of view upon the theoretical accuracy, which could now be achieved and the one realized in event generator LABSMC [44–46].

1.5.1. LABSMC Event Generator. Initially the LABSMC event generator was developed to simulate large-angle Bhabha scattering at energies of about a few GeV's at electron-positron colliders like VEPP-2M and DAΦNE. The code included the Born level matrix element, a complete set of $\mathcal{O}(\alpha)$ QED RC, and a higher order leading logarithmic RC by means of the electron structure functions. The relevant set of formulae can be found in Ref. 12. The generation of events is performed using an original algorithm, which combines advantages of semianalytical programs and Monte Carlo generators.

The structure of our event generator was described in paper [46]. An extension of the code to higher energies is done by introducing electroweak (EW) contributions, such as Z exchange, into the matrix elements. The third [47] and fourth [48] order leading logarithmic photonic corrections were also included in the new version (see the write-up in Ref. 44).

The LABSMC program contains:

- tree level electroweak Born cross section;
- complete set of $\mathcal{O}(\alpha)$ QED radiative corrections (RC);
- vacuum polarization corrections by leptons, hadrons [49], and W bosons;
- one-loop electroweak RC and effective EW couplings according to [50] by means of DIZET [51] package;
- higher order leading log photonic corrections accounted via the electron structure functions [33, 47, 48];
- matrix element for radiative Bhabha scattering with both γ and Z exchange [52, 53], vacuum polarization RC, and optionally ISR leading log RC (with exponentiation according to Ref. 33);

- light pair corrections in the $\mathcal{O}(\alpha^2 L^2)$ leading logarithmic approximation [14], including (optionally) the two-photon mechanism.

An independent Monte Carlo has been created to scrutinize the pair corrections. It was found that the leading log contributions, which are factorized before the Compton scattering and $e\bar{e} \to \gamma\gamma$ processes, are negligibly small at LEP2 energies, that is, because of the features of the corresponding kernel cross sections. Therefore these contributions were omitted in LABSMC. Another source of corrections which appears just at LEP2 energies, is double resonant processes, where both the primary electron pair and the secondary pair are produced via resonating Z-boson propagators. Such a contribution is assumed by the experimental community as a background to Bhabha scattering. And the corresponding contribution is subtracted from the experimental data in a preliminary step of analysis.

The inclusion of the third and fourth order LLA photonic corrections allows not to use exponentiation. A simple estimate [48] shows that the difference between the two treatments at LEP2 is negligible, meanwhile the exponentiation requires a specific event generation procedure.

LABSMC is a FORTRAN program. It works as follows. First, the code makes initialization and reads flags and parameters from a list provided by user. It performs integration of different contributions to matrix element over the ordered phase space in the semianalytical branch. Then it generates events. The 4-momenta of generated particles are to be analyzed in a user subroutine to perform a concrete event selection. A certain control of technical precision is provided by comparison of the results from the semianalytical branch and the Monte Carlo one. Note, that for a case of complicated cuts, which cannot be done in the semianalytical branch, one has to increase the number of generated events to reach the required precision.

A number of flags, to be set by user, allows one to switch between different options and perform specific comparisons and investigations. In particular one can switch to generation of only radiative events with visible photons. That allows one to avoid technical problems due to low statistics in this case.

A detailed comparison with Monte Carlo program BHWIDE [54] has been performed [44] for a large set of different event selection procedures.

A reasonably good agreement was seen for the Born cross section (with adjusted EW parameters), supplied with the pure QED photonic radiative corrections. For the bulk of event selections the difference between the results of the two codes was less than 0.1 %. But for some specific observables (with the so-called BARE event selections) LABSMC was about 0.4 % higher than BHWIDE. Therefore, one can suppose, that the difference in BARE observables is not due to the different approaches to photonic corrections themselves, but rather a consequence of different treatment (realization) of conditions for particle registration in the BARE case. An agreement between these programs in the pure QED part

is not a big surprise. Actually they take into account the same set of photonic radiative corrections: the Born and the first order are complete, the higher orders contain the same leading logs. In both cases, starting from the second order, the subleading corrections (like $\alpha^2 L$) are incomplete, they are one of the most important sources of uncertainties.

After *switching on* the electroweak contributions we received a considerably larger discrepancy: 1.4–2.4 % for barrel angular acceptance ($|\cos\theta| \lesssim 0.72$), and 0.1–0.6 % for a more wide region with end-caps included ($|\cos\theta| \lesssim 0.95$). The dependence on the angular acceptance is clear. For the wide angular region the pure QED contribution (mainly the t-channel photon exchange) gives about 95 % of the observed cross section. While for the barrel region one has much more important EW contribution of about 25 % (s-channel Z-boson exchange, Z-γ interference, etc.). Therefore at present the most important problem in the comparisons is the treatment of electroweak effects.

1.5.2. Electroweak Contributions. The set of electroweak effects was included into LABSMC according to Ref. 50 by means of DIZET [51] package. The program BHWIDE calls the EW parameters and corrections from the code ALIBABA [5]. Starting from the Born level the programs have different values of the EW coupling constants. In other words, they are using different schemes for EW running constants and loop corrections.

A comparison of the Bhabha cross section integrated over photons is in a fair agreement (see Table 3, error-bars are dropped) with a number of other codes published in [55]. But the level of agreement (disagreement) is not satisfactory for the recent precise experimental results come from LEP2 collaborations.

Table 3. **Comparison with Fig. 21 from Ref. 55, cross sections in pb**

E_{CM}, GeV	BHWIDE	TOPAZ0	BHAGENE3	UNIBAB	SABSPV	BHAGEN95	LABSMC
	$\vartheta_{\mathrm{acol}} = 10^\circ$						
175	35.257	35.455	34.690	34.498	35.740	35.847	35.337
190	29.899	30.024	28.780	29.189	30.270	30.352	29.941
205	25.593	25.738	24.690	25.976	25.960	26.007	25.687
	$\vartheta_{\mathrm{acol}} = 25^\circ$						
175	39.741	40.487	39.170	39.521	40.240	40.505	40.029
190	33.698	34.336	32.400	33.512	34.100	34.331	33.954
205	28.929	29.460	27.840	28.710	29.280	29.437	29.178

The most important contribution under consideration is now the s-channel Z exchange. In the LABSMC code it can be computed separately (there are options to choose channels and exchange bosons). This way we compared this contribution with the corresponding result got by ZFITTER program [50], that describes only the s-channel electron-positron annihilation. A perfect agreement

has been observed for the cross section of the process $e^+e^- \to Z^* \to e^+e^-$ with all available EW corrections included (while the photonic corrections were *switched off*). From the other hand, the realization of EW stuff in ZFITTER is in a perfect agreement [56] with an alternative approach applied in TOPAZ0 [57]. Moreover, the package DIZET is continuously supported by the authors to include the most recent theoretical calculation in the EW sector. It is used by many other groups for different applications, such as KKMC [58] Monte Carlo for high-energy electron-positron annihilation, or HECTOR [59] semianalytical code for deep inelastic scattering. The EW sector in ALIBABA had been tuned many years ago for the Z-peak region. Since that time it was not updated, as far as we know. Our first attempt to incorporate the EW corrections into LABSMC was just to call them from ALIBABA, as it is done in BHWIDE. Test runs of the program showed unrealistic quantities for the running electroweak constants (from the M_Z scale to the LEP2 one). To produce the numbers in Ref. 45, an adjustment of the initialization values of EW parameters was done in certain subroutines of the ALIBABA code. Nevertheless, the results did not seem satisfactory in the context of the high precision, required. That is why the invoking of ALIBABA was substituted in LABSMC by the one of DIZET.

1.5.3. Radiative Return with a Visible Photon. At LEP2 the radiative return to the Z peak due to photon or pair radiation gives a sizable contribution to the cross section. This process is used itself in particular to look for anomalous gauge boson couplings.

The pure tree level matrix element [53] for radiative process

$$e^+ + e^- \longrightarrow e^+ + e^- + \gamma + (n\gamma) \tag{1.162}$$

was supplemented in LABSMC by radiative corrections due to initial state soft and hard collinear radiation by means of the electron structure function approach [33]. The electron-positron pair production was taken into account quite the same way. We took the t-channel momentum transfer to be an energy scale for the structure functions. That's owing to the dominance of the corresponding amplitudes. The vacuum polarization correction to the photon propagators is applied as well.

Table 4. **The cross section in pb of radiative Bhabha scattering with a visible photon in different approximations**

	Total		Without Z peak	
E_{CM}, GeV	183	189	183	189
Tree-level	0.9817	0.9146	0.8251	0.7727
Vacuum polarization	1.1022	1.0342	0.9630	0.8853
Vac. pol. + ISR LLA	1.0842	1.0088	0.9346	0.8770

In Table 4 we give the result got under the following conditions:

1. $E_{\rm CM} = 183$, 189 GeV;
2. $|\cos\theta_{e^\pm}| < 0.95$;
3. At least one electron has $|\cos\theta_e| < 0.7$;
4. Electrons should have transverse momenta above 1 GeV;
5. The final particles are to be isolated by at least 20° from each other;
6. The total observed energy $> 0.8\ E_{\rm CM}$; $|\cos\theta_\gamma| < 0.7$.

In the columns *without Z peak* we excluded the events with the invariant mass of the electron-positron pair in the range $85 < M_{e\bar{e}} < 95$ GeV. As could be seen from the numbers, the ISR LLA corrections are in this case of the order 2 %. The additional nonstandard LLA corrections, which were found in Ref. 16, make a small shift of the correction (an independent verification of this investigation is required).

The complete set of $\mathcal{O}(\alpha)$ radiative corrections to the process (1.162) is unknown. To estimate the uncertainty of our result we look at the relative size of the known leading and subleading $\mathcal{O}(\alpha)$ RC to the Bhabha process itself. For an analogous set of cuts for Bhabha scattering, the difference of the correction values is found to be $\delta_{\rm tot} - \delta_{\rm LLA} \approx 1\,\%^*$. This way we estimate the precision of our results for the radiative process (1.162) to be of the order 1.5 %.

1.5.4. Numerical Illustrations. Let us consider the Bhabha cross section under the following conditions:

1. The centre-of-mass energy is 206 GeV;
2. The energy threshold for an electron registration is 5.15 GeV;
3. The angular acceptance for the registered e^+e^- pair is 44–136° degree;
4. The angle between the outgoing electron and positron should exceed 0.1 rad.

The corresponding numerical results are presented in Table 5. One can see that the pure t-channel QED Born (the first line) still dominates, but not as much as in the case of small angle Bhabha. The difference between the third and second lines gives us an idea about the size of the contribution due to Z-boson exchange and its interference with QED amplitudes. The effect is rather large: about $-25\,\%$ in our case.

*The special cut on the scattering angle of «at least one electron has $|\cos\theta_e| < 0.7$» is similar to the narrow-wide event selection in small angle Bhabha at LEP1. In both cases we see a considerable reduction of the RC size. If we apply this cut, the difference $\delta_{\rm tot} - \delta_{\rm LLA}$ is well below the 1 % level.

Table 5. **The large angle Bhabha cross section in different approximations**

No.	Approximation	σ, pb
1	t-chan. QED Born	27.692
2	QED Born	24.482
3	EW Born	18.496
4	Improved EW Born	18.505
5	EW Born with vac. pol.	21.277
6	Corr. w/o pairs	20.970
7	Corr. with pairs	20.952

In the fourth line the so-called improved electroweak Born approximation is presented. EW corrections, which can be factorized before the Born level functions are taken into account there. One can see that because of the choice of the scheme applied we have a small effect of EW corrections. In fact, the main effect of running EW constants has been already taken into account in the EW Born (line 3), where the values of the EW parameters (M_Z, $\cos\theta_W$) were taken at the proper energy scale.

The size of the vacuum polarization effect in the virtual photon propagators (compare lines 3 and 5) is considerable. That is why the uncertainty in the vacuum polarization by hadrons will propagate to the resulting error of Bhabha description.

The radiative corrections (except for those induced by a pair production) are taken into account in the 6th line. The effect due to pair corrections (see the last line) is rather small in our case. Numerical results for many other different event selection criteria can be found in Ref. 44.

1.5.5. Estimate of the Theoretical Uncertainty of Bhabha Description at LEP2 Energies. The theoretical uncertainty of LABSMC Monte Carlo event generator is estimated by the analysis of the following sources of errors.

- A considerably large amount of about 0.10 % is coming from the hadronic contribution into vacuum polarization.

- The $\mathcal{O}(\alpha^2 L)$ photonic corrections, which are not implemented in the program, can give as large as 0.20 %. Note, that for small angle Bhabha at LEP1 we had the corresponding contribution of the order of 0.15 % [60], and so we can estimate the uncertainty, taking into account that the large logarithm L in the large angle kinematics is greater.

- The approximate treatment of hadronic pair corrections contributes at the level no more than 0.03 %, depending on the concrete event selection.

- Photonic corrections in high orders $\mathcal{O}(\alpha^3 L^2, \alpha^5 L^5, ...)$ are not calculated in the code. Actually they are small (0.02 %) enough to be safely neglected.

- Uncertainties in the electroweak coupling constants and loop corrections can give rise to about 0.03 %.

Taking into account the limited technical precision, we derive the resulting uncertainty of the code for description of large angle Bhabha scattering at LEP2 to be of the order of 0.3 %.

The authors of event generator BHWIDE [54] have a bit higher estimate of the uncertainty of their code: 0.5 %. In fact, they do not take into account radiative corrections due to pair production, and exploit an old version of electroweak corrections implemented in the code ALIBABA [5]. A program of detailed comparisons between the two codes is in progress. A good agreement was found for the Bhabha cross section within the pure QED (without electroweak contributions).

By comparing a semianalytical and pure Monte Carlo patches of the code we have a good control over such parameters as the precision of numerical integration and the number of events to be generated. That allows one to reach a required level of the uncertainty in numerical evaluations.

2. OUTLOOK

Let's summarize what has been given above and outline the problems to be considered in the subject in future. First of all a few words on the overview of the problem are in order. As has been quoted in the introduction, LABS is heavily exploited for the monitoring and calibration at e^+e^- colliders of moderately high energies. Therefore one must know the cross section for this process as better as possible. To reach the one per mille accuracy it is required to take into account RC up to a third order in LLA and up to a second order in NLA. Above we gave the detailed account of RC NLA (and of course LLA) calculation to LABS in various settings. Considered are a two-hard-photon emission and a hard-lepton pair production for collinear and semicollinear regions of additional particles' emission, as well as a radiative LABS in two complementary kinematics. For the first two options results obtained agree in LLA with RG expectations whereas in the last two cases we observe certain deviation from the Drell–Yan picture.

It has to be mentioned that the theoretical treatment of Bhabha scattering to a per mille accuracy requires accounting for the gauge invariant sets of genuine two-loop box amplitudes. This means that the consideration of two-loop level diagrams presented here is not complete. To the moment those classes (the so-called decorated and eikonal type diagrams) are not consistently worked out though it should be noted that there is some progress in the analytical evaluation

of these classes of amplitudes [61–63]. Their book-keeping in NLA gives a contribution proportional to the terms of the order $\mathcal{O}(\alpha^2 L/\pi^2)$, that is at the level of $0.1\,\%$. A complete knowledge of nonleading terms will give rise to corrections of the order $0.05\,\%$.

Appendix I. We present here the list of integrals (see Eqs. (1.19)–(1.22)):

$$\begin{aligned}
&\overline{\frac{A_2}{A^2A_1}} = \frac{L_0}{x_1x_2r_1^2}\left[\frac{1}{2}L_0 + \ln\frac{x_2r_1^2}{x_1y} - 1 + \frac{x_1x_2}{y}\right],\\
&\overline{\frac{1}{AA_1}} = \frac{L_0}{x_1x_2r_1}\left[\frac{1}{2}L_0 + \ln\frac{x_2r_1^2}{x_1y}\right], \qquad \overline{\frac{m^2}{AA_1^2}} = -\frac{L_0}{x_1^2x_2r_1}\,, \qquad \text{(I.1)}\\
&\overline{\frac{1}{A_1A_2}} = \frac{L_0^2}{x_1x_2}, \qquad \overline{\frac{1}{A_1B_2}} = -\frac{L_0}{y_1x_1x_2}(L_0 + 2\ln y_1),\\
&L_0 = \ln z_0 \equiv L + l, \qquad l = \ln\left(\frac{\theta_0^2}{4}\right), \qquad L = \ln\left(\frac{4\varepsilon^2}{m^2}\right).
\end{aligned}$$

The remaining integrals could be obtained by simple substitutions defined in Eqs. (1.19)–(1.22).

Appendix II. Here we give the expressions for the quantities associated with G-type integrals:

$$\begin{aligned}
J &= -\frac{1}{\chi_1 t_1}\left[-2L_\lambda L_{t_1} + 2L_{t_1}L_\rho - L_t^2 - 2\mathrm{Li}_2(x) - \frac{\pi^2}{6}\right],\\
J_1 &= \frac{1}{t_1\chi_1}\int\limits_0^\rho \frac{\mathrm{d}z}{1-z}\frac{\ln z}{1-\lambda z} = \frac{A}{t_1\chi_1}\left(1 + \frac{x}{\rho - x}\right) = \frac{A+\vartheta}{t_1\chi_1},\\
J_k &= -\frac{1}{t_1\chi_1\rho}\int\limits_0^\rho \frac{\mathrm{d}z}{1-z}\frac{z\ln z}{1-\lambda z},\\
J_{11} &= -\frac{1}{t_1\chi_1}\int\limits_0^\rho \frac{\mathrm{d}z}{(1-z)(1-\lambda z)}\left(1 + \frac{z\ln z}{1-z}\right), \qquad \text{(II.1)}\\
J_{1k} &= \frac{1}{t_1\chi_1\rho}\int\limits_0^\rho \frac{z\mathrm{d}z}{(1-z)(1-\lambda z)}\left(1 + \frac{z\ln z}{1-z}\right),\\
A &= \mathrm{Li}_2(1-\rho) - \frac{\pi^2}{6} + \mathrm{Li}_2(x) + L_\rho\ln(1-x), \quad \lambda = \frac{x}{\rho}, \quad \rho = \frac{\chi_1}{m^2}.
\end{aligned}$$

In the limit $\rho \gg 1$ we have

$$\Phi = \chi_1 A_2 + t_1\chi_1(J_{11} - J_1 + xJ_{1k} - xJ_k) = -\frac{1}{2} + \mathcal{O}(\rho^{-1})$$

and that is the reason why w structure does contribute only to the next-to-leading terms.

In general the expression for 5-denominator one-loop scalar, vector and tensor integrals are some complicate functions of five independent kinematical invariants (in the derivation we extensively use the technique developed in [64]). In the limit $m^2 \ll \chi_1 \ll s \sim -t$ they may be considerably simplified because of singular $1/\chi_1$ terms only kept:

$$\begin{aligned}
E &= \frac{1}{s_1}D_{0124} + \frac{1}{t}D_{0123},\\
E_1 &= -xE_k = \frac{1}{2\chi_1}\left(D_{0134} - (1-x)D_{0234} - xD_{1234} + \chi_1 E\right),\\
D_{0124} &= \frac{1}{xt_1\chi_1}\left[L_\rho^2 + 2L_\rho \ln\frac{x}{1-x} - \ln^2\frac{x}{1-x} - \frac{2\pi^2}{3}\right],\\
\Re e D_{0123} &= \frac{1}{s\chi_1}\left[L_{s_1}^2 - 2L_{s_1}L_\rho - 2L_sL_\lambda + \frac{\pi^2}{6} + 2\mathrm{Li}_2(x)\right], \qquad \text{(II.2)}\\
\Re e D_{0234} &= \frac{1}{s_1 t}\left[L_{s_1}^2 + 2L_{s_1}L_\lambda - 2L_\rho L_{s_1} + 2L_{s_1}L_t - \frac{5\pi^2}{6}\right],\\
\Re e D_{0134} &= \frac{1}{st}\left[L_s^2 + 2L_sL_\lambda - 2(L_{t_1} + \ln(x))L_s + 2L_sL_t + \frac{7\pi^2}{6}\right],\\
\Re e D_{1234} &= -\frac{1}{s_1xt_1}\left[-L_s^2 + 2L_s(L_{t_1} + \ln(x)) + 2L_{s_1}L_\lambda - \frac{7\pi^2}{6}\right].
\end{aligned}$$

The structure $E_{11} + xE_{1k}$ has the form $1/(s\chi_1)f(x,\chi_1)$ and will vanish after performing the operation $(1+Q_2)s_1tP$ given in (1.136) which yields a contribution of P-type graphs with crossed and uncrossed photon legs.

The following coefficient for the scalar integral is obtained in the calculation of B-type FD:

$$B = \frac{1}{s_1 t}\left[L_{s_1}^2 + 2L_{s_1}L_\lambda - 2L_{s_1}L_\rho + 2L_{s_1}L_t + \frac{\pi^2}{6}\right]. \qquad \text{(II.3)}$$

For the vector integral coefficients we get

$$\begin{aligned}
a &= -\frac{1}{2s_1u_1t}\left[-\pi^2 s_1 + 2u_1\,\mathrm{Li}_2(1-\rho) - s_1L_t^2 + tL_{s_1}^2 - 2tL_{s_1}L_t\right],\\
b &= -\frac{1}{2s_1t}\left[\frac{2\pi^2}{3} + 2\,\mathrm{Li}_2(1-\rho) - 2L_{s_1}^2 + 4L_{s_1}L_\rho - 2L_{s_1}L_t\right],
\end{aligned}$$

$$c = \frac{1}{2s_1u_1t}\Bigg[2u_1\,\mathrm{Li}_2(1-\rho) + \frac{\pi^2}{6}(4u_1+6t) + (t-2u_1)L_{s_1}^2 - s_1L_t^2 + \\ + 4u_1L_{s_1}L_\rho + 2s_1L_{s_1}L_t\Bigg]. \quad \text{(II.4)}$$

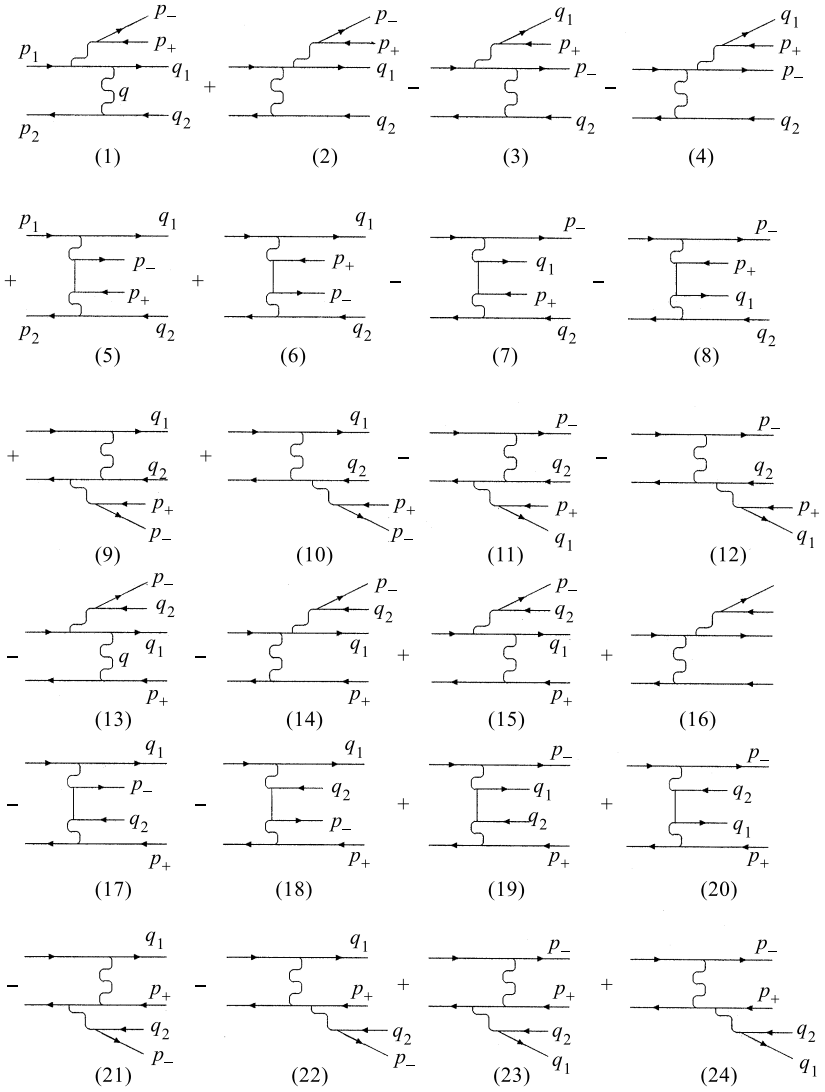

Fig. 9. *a*) Feynman diagrams for real pair production ((1)–(24))

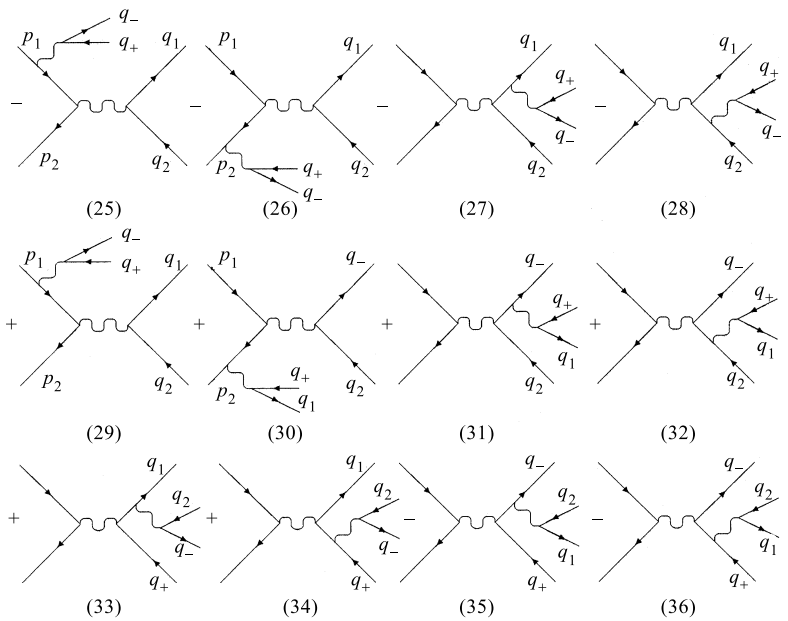

Fig. 9. *b*) Feynman diagrams for real pair production ((25)–(36))

The relevant quantities for tensor B-type integrals are:

$$\begin{aligned}
a_{1'2'} &= \frac{1}{s_1 t}\left(\frac{\rho}{\rho-1}L_\rho - L_t\right), \qquad a_g = -\frac{1}{4u_1}[(L_{s_1}-L_t)^2+\pi^2],\\
a_{1'2} &= -\frac{1}{2u_1^2}[(L_t-L_{s_1})^2+\pi^2] + \frac{1}{tu_1}(L_{s_1}-L_t) -\\
&- \frac{1}{s_1 t}\left(\frac{\rho}{\rho-1}L_\rho - L_{s_1}\right), \qquad \text{(II.5)}\\
J_0 &= \frac{1}{s_1}\left[\frac{3}{2}L_{s_1}^2 - 2L_{s_1}L_\rho - \mathrm{Li}_2(1-\rho) - \frac{4\pi^2}{3}\right].
\end{aligned}$$

As has been mentioned in the text, the physical gauge exploited provides a direct extraction of the kernel of the structure function out of the traces both in the tree- and loop-level amplitudes. The pattern emerging

$$\begin{aligned}
(\hat{p}_1-\hat{k}_1+m)\hat{e}(\hat{p}_1+m)\hat{e}(\hat{p}_1-\hat{k}_1+m) &= 4(p_1e)^2(\hat{p}_1-\hat{k}_1) - e^2\chi_1\hat{k}_1 \approx\\
&\approx (1-x)Y\hat{p}_1, \qquad \text{(II.6)}\\
\hat{k}_1\hat{e}(\hat{p}_1+m)\hat{e}(\hat{p}_1-\hat{k}_1+m) &\approx (1-x)\left(2\frac{2-x}{1-x}W - Y\right)\hat{p}_1
\end{aligned}$$

shows this clearly.

Appendix III. Above we present the full set of 36 Feynman diagrams (Fig. 9) describing the real e^+e^- pair production in a large angle Bhabha scattering process.

Acknowledgements. Its a pleasure to thank N. Merenkov, H. Anlauf, V. Antonelli, L. Trentadue, V. Astakhov and E. Zemlyanaya for fruitful collaboration. The work of EK and BS was supported in part by RFBR 01-02-17437 and HLP 2001-02.

REFERENCES

1. *Arbuzov A. B. et al.* // Phys. Lett. B. 1996. V.383. P.238.
2. *Ward B. F. L. et al.* // Phys. Lett. B. 1999. V.450. P.262;
   Montagna G. et al. // Nucl. Phys. B. 1999. V.547. P.39.
3. *Dolinsky S. I. et al.* // Phys. Rep. 1991. V.202. P.91.
4. *Aloisio A. et al.* The DAΦNE Physics Handbook. 1993. V.2;
   Drago E., Venanzoni G. KLOE MEMO 59/96;
   Franzini P. The Second DAΦNE Physics Handbook. 1995. V.2. P.471.
5. *Beenakker W. et al.* // Nucl. Phys. B. 1991. V.349. P.323.
6. *Berends F. A. et al.* // Phys. Lett. B. 1981. V.103. P.124;
   Berends F. A. et al. // Nucl. Phys. B. 1982. V.206. P.61.
7. *Montagna G. et al.* // Nucl. Phys. B. 1993. V.401. P.3.
8. *Placzek W. et al.* Preprint CERN-TH/99-07. 1997; hep-ph/9903381.
9. *Caffo M., Gatto R., Remiddi E.* // Nucl. Phys. B. 1985. V.252. P.378.
10. *Arbuzov A., Fadin V., Kuraev E. et al.* // CERN Yellow Report. CERN 95–03. 1995. P.369;
    Arbuzov A., Fadin V., Kuraev E. et al. Preprints CERN-TH/95-313, UPRF-95-438.
11. *Jadach S., Nicrosini O. (conv.)* Event generators for Bhabha scattering // CERN Yellow Report. CERN 96-01. 1996. V.2.
12. *Arbuzov A. B. et al.* // JHEP. 1997. V.10. P.001.
13. *Arbuzov A. B. et al.* // Nucl. Phys. B. 1997. V.483. P.83.
14. *Arbuzov A. B. et al.* // Nucl. Phys. B. 1996. V.474. P.271;
    Arbuzov A. B. et al. // Phys. Atom. Nucl. 1997. V.60. P.591.
15. *Arbuzov A. B., Kuraev E. A., Shaikhatdenov B. G.* // Mod. Phys. Lett. A. 1998. V.13. P.2305.
16. *Arbuzov A. B., Kuraev E. A., Shaikhatdenov B. G.* // JETP. 1999. V.88. P.213.
17. *Antonelli V., Kuraev E. A., Shaikhatdenov B. G.* // JETP Lett. 1999. V.69. P.900;
    Antonelli V., Kuraev E. A., Shaikhatdenov B. G. // Nucl. Phys. B. 2000. V.568. P.39.
18. *Budny R.* // Phys. Lett. B. 1975. V.55. P.227;
    Redhead M. L. C. // Proc. Roy. Soc. 1953. V.220. P.219;
    Половин Р. В. // ЖЭТФ. 1956. Т.31. С.449;
    Berends F. A. et al. // Nucl. Phys. B. 1974. V.68. P.541.
19. *Berends F. A., Kleiss R.* // Nucl. Phys. B. 1983. V.228. P.537.
20. *Berends F. A. et al.* // Nucl. Phys. B. 1986. V.264. P.243.
21. *Baier V. N., Fadin V. S., Khoze V. A.* // Nucl. Phys. B. 1973. V.65. P.381.

22. *Merenkov N. P.* // Sov. J. Nucl. Phys. 1988. V.48. P.1073.
23. *Кураев Е. А., Перышкин А. Н.* // ЯФ. 1985. Т.42. С.1195.
24. *Kuraev E. A., Pyoryshkin A. N., Fadin V. S.* INP Preprint 89-91. Novosibirsk, 1991.
25. *Merenkov N. P.* // Sov. J. Nucl. Phys. 1989. V.50. P.469.
26. *Арбузов А. Б. и др.* // ЖЭТФ. 1995. Т.108. С.1164.
27. *Akhiezer A. I., Berestetski V. B.* Quantum Electrodynamics. M.: Nauka, 1981.
28. *Судаков В. В.* // ЖЭТФ. 1974. Т.30. С.87.
29. *Кураев Е. А., Меренков Н. П., Фадин В. С.* // ЯФ. 1987. Т.45. С.782.
30. *Arbuzov A. B., Kuraev E. A., Shaikhatdenov B. G.* hep–ph/9805308.
31. *t'Hooft G., Veltman M.* // Nucl. Phys. B. 1979. V.153. P.365.
32. *Eidelman S., Kuraev E., Panin V.* // Nucl. Phys. B. 1979. V.148. P.245.
33. *Kuraev E. A., Fadin V. S.* // Sov. J. Nucl. Phys. 1985. V.41. P.466.
34. *Гинзбург И. Ф., Ширков Д. В.* // ЖЭТФ. 1965. Т.49. С.335.
35. *Collins J., Frankfurt L., Strikman M.* // Phys. Lett. B. 1993. V.307. P.161;
Gotsman E., Levin E., Maor V. // Phys. Lett. B. 1997. V.406. P.89;
Berger E. L., Guo X., Qiu J. // Phys. Rev. Lett. 1996. V.76. P.2234;
Duncan A., Mueller A. H. // Phys. Rev. D. 1980. V.21. P.1636;
Duncan A., Mueller A. H. // Phys. Lett. B. 1980. V.90. P.159;
Милштейн А., Фадин В. С. // ЯФ. 1981. Т.33. С.1391.
36. *Bassetto A., Ciafaloni M., Marchesini G.* // Phys. Rep. 1983. V.100. P.201.
37. *Anlauf H. et al.* // JHEP. 1998. V.10. P.013; Phys. Rev. D. 1999. V.59. P.014003.
38. *Арбузов А. Б., Кураев Е. А.* // ЭЧАЯ. 1996. Т.27. С.1247.
39. *Bourilkov D.* // JHEP. 1999. V.8. P.006.
40. *Bourilkov D.* hep-ph/0002172.
41. *Acciarri M. (for L3 Collaboration)* // Phys. Lett. B. 1998. V.439. P.183.
42. *Beccaria M. et al.* hep-ph/0002101.
43. *Kawamoto T.* // Acta Phys. Polon. B. 1997. V.28. P.683.
44. *Kobel M. (for Two Fermion Working Group Collaboration)* hep-ph/0007180.
45. *Arbuzov A. B.* hep-ph/9910280.
46. *Arbuzov A. B.* hep-ph/9907298.
47. *Skrzypek M.* // Acta Phys. Polon. B. 1992. V.23. P.135.
48. *Arbuzov A. B.* // Phys. Lett. B. 1999. V.470. P.252.
49. *Eidelman S., Jegerlehner F.* // Z. Phys. C. 1995. V.67. P.585.
50. *Bardin D. et al.* hep-ph/9908433.
51. *Bardin D. Y. et al.* // Comput. Phys. Commun. 1990. V.59. P.303.
52. *Bohm M., Denner A., Hollik W.* // Nucl. Phys. B. 1988. V.304. P.687.
53. *Berends F. A., Kleiss R., Hollik W.* // Nucl. Phys. B. 1988. V.304. P.712.
54. *Jadach S., Placzek W., Ward B. F.* // Phys. Lett. B. 1997. V.390. P.298.
55. *Anlauf H. et al.* // CERN Yellow Report 96-01. 1996. V.2. P.229.

56. *Bardin D., Grunewald M., Passarino G.* hep-ph/9902452.

57. *Montagna G. et al.* // Comput. Phys. Commun. 1999. V.117. P.278.

58. *Jadach S., Ward B.F., Was Z.* // Comput. Phys. Commun. 2000. V.130. P.260.

59. *Arbuzov A. et al.* // Comput. Phys. Commun. 1996. V.94. P.128.

60. *Arbuzov A. B. et al.* // Nucl. Phys. B. 1997. V.485. P.457.

61. *Faldt G., Osland P.* // Nucl. Phys. B. 1994. V.413. P.16, 64;
Erratum — ibid. 1994. V.419. P.404.

62. *Smirnov V. A., Veretin O. L.* // Nucl. Phys. B. 2000. V.566. P.469.

63. *Bern Z., Dixon L., Ghinculov A.* // Phys. Rev. D. 2001. V.63. P.053007.

64. *Van Neerven W. L., Vermaseren J. A. M.* // Phys. Lett. B. 1984. V.137. P.241.